

ACTIVE RESISTOR-CAPACITOR
BODE-TYPE EQUALISERS

BY

Mohammed ZYOUTE

A Thesis submitted for the Degree of
DOCTOR OF PHILOSOPHY
of the
UNIVERSITY OF LONDON

Department of Electrical engineering,
Imperial College of Science and Technology,
University of London.

July, 1981

ABSTRACT

New designs for active RC Bode-type variable equalisers (VEs) are presented in this thesis. A distinction is made between the equalisers satisfying Bode's transfer function and those satisfying only its squared-modulus. The latter are referred to as quasi Bode-type VEs; they are derived from symmetrical lattice networks and, apart from some constraints on their shaping impedances, they can be very useful in applications where phase characteristics are of less importance. On the other hand the VEs satisfying Bode's transfer function are widely investigated. Some have been also derived from symmetrical lattice networks and others from a new basic structure. This new structure constitutes a major contribution to the design of active RC VEs. It has the advantage of being very simple and extremely flexible. This flexibility is illustrated by a variety of examples. Moreover, the usual variable range $[0, \infty]$, which is covered by an adjustable resistor, is shown that it can be reduced to any prescribed range $[0, m]$ without disturbing the properties of the transfer function. A final feature of the new structure is that it can lend itself to the grounding of both the shaping impedance and the adjustable resistor. The various practical examples show that nearly ideal performance characteristics can be obtained.

A C K N O W L E D G E M E N T S

I wish to express my deepest gratitude to my supervisor Dr. A.G. Constantinides for his guidance, help and advice given during the course of this work, particularly at its most critical stages. Working with Dr. A.G. Constantinides has been a privilege and a great experience.

The work reported here has been suggested by the late Dr. W. Saraga who has supervised it with warm encouragement and enthusiasm; his death was a great loss to all those who were benefiting from his valuable experience.

I am very grateful to the many who have contributed directly and indirectly to this work. Particularly thanks are due to Mr. B. Singh for his many helpful suggestions and comments. My thanks are also due to Dr. D.G. Haigh and all my colleagues and friends of the old Communication Section and the new Signal Processing Section.

I would like to express my gratitude to Professor M. Najim for his guidance and stimulation for research. Many thanks are due to my friends Dr. A. El Hassouni and A. Rachdi for their support.

Finally, I would like to thank Mrs. Mavis Moriarty for her skilful typing of the manuscript.

The work reported in this thesis was done while the author was on leave from Faculté des Sciences, Rabat.

TABLE OF CONTENTS

	<u>Page</u>
TITLE	1
ABSTRACT	2
ACKNOWLEDGEMENTS.	3
TABLE OF CONTENTS.	4
LIST OF TABLES AND FIGURES.	7
<u>CHAPTER I.</u>	<u>THE EQUALISATION PROBLEM</u>
	11
1.1	Introduction.
	12
1.2	A Bode-type variable equaliser.
	13
1.3	Aims and organisation of the thesis.
	18
<u>CHAPTER II.</u>	<u>REVIEW OF PREVIOUS WORK.</u>
	23
2.1	Brglez's approach.
	24
2.1.1.	Transformation of the original transfer function.
	24
2.1.2.	Active realisations.
	26
2.2	Other approaches.
	29
2.2.1.	VE with differential amplifiers.
	29
2.2.2.	VE using feedback and feedforward.
	31
2.3	An example of non-Bode-type VE.
	34
2.4	Conclusions.
	36

		<u>Page</u>
<u>CHAPTER III</u>	<u>SOME QUASI-BODE-TYPE VARIABLE EQUALISERS.</u>	42
3.1	Introduction.	43
3.2	Transformation of Bode's transfer function for VEs.	45
3.3	Lattice circuits and transformations.	47
	3.3.1. Passive unsymmetrical lattice circuits.	47
	3.3.2. Passive symmetrical lattice circuits.	48
3.4	Active realisations.	50
	3.4.1. Example I: fan equaliser.	51
	3.4.2. Example II: bump equaliser.	52
3.5	Phase considerations and effects of the amplifier finite gain bandwidth product.	56
	3.5.1. Phase considerations.	56
	3.5.2. Effects of the amplifier finite gain bandwidth product.	58
3.6	Conclusions.	61
<u>CHAPTER IV</u>	<u>A BODE EQUALISER USING A SINGLE OP-AMP.</u>	75
4.1	Introduction.	76
4.2	The new circuit.	76
4.3	Practical examples.	80
	4.3.1. Fan equaliser.	80
	4.3.2. Bump equaliser.	81
4.4	Discussion.	89

<u>CHAPTER V</u>	<u>A NEW BASIC DESIGN FOR BODE EQUALISERS.</u>	96
5.1	Introduction.	97
5.2	The basic network.	97
5.3	Some active network transformations by terminal interchange.	100
	5.3.1. Transformation A.	101
	5.3.2. Transformation B.	102
5.4	VEs derived from the basic network by terminal interchange.	103
5.5	VE with a prescribed maximum range of variation of the variable resistor.	106
5.6	A design with a grounded variable resistor.	109
5.7	Some practical results.	114
5.8	Conclusion.	115
<u>CHAPTER VI</u>	<u>EFFECTS OF THE AMPLIFIER FINITE GAIN BANDWIDTH PRODUCT.</u>	131
6.1	Introduction.	132
6.2	The comparison method.	132
	6.2.1. Fan equalisers.	132
	6.2.2. Bump equalisers.	134
6.3	The optimisation method.	142
6.4	Some computed results.	148
<u>CHAPTER VII</u>	<u>GENERAL CONCLUSIONS AND SUGGESTIONS FOR FUTURE WORK.</u>	166
REFERENCES.		169

LIST OF TABLES AND FIGURES.

	<u>Page</u>
<u>CHAPTER I.</u>	
Figure 1.1	21
1.2	21
1.3	22
<u>CHAPTER II.</u>	
Figure 2.1	37
2.2	37
2.3	37
2.4	38
2.5	38
2.6	38
2.7	38
2.8	38
2.9	39
2.10a	39
2.10b	39
2.11	39
2.12	39
2.13	40
2.14	40
2.15	40
2.16	41
<u>CHAPTER III</u>	
Table 3.1	58
Figure 3.1	62
3.2	62
3.3	62
3.4	62
3.5	62
3.6	62
3.7	63
3.8	63
3.9	63
3.10	63

	<u>Page</u>
 <u>CHAPTER III</u>	
Figure 3.11	63
3.12	64
3.13	64
3.14	64
3.15	64
3.16	65
3.17	66
3.18a	66
3.18b	66
3.19	66
3.20	67
3.21	68
3.22	69
3.23	69
3.24	69
3.25	70
3.26	71
3.27	71
3.28	72
3.29	73
3.30	73
3.31a	73
3.31b	73
3.32a	74
3.32b	74
 <u>CHAPTER IV</u>	
Figure 4.1	90
4.2	90
4.3	90
4.4	90
4.5	90
4.6	91
4.7	91
4.8	92
4.9	93

	<u>Page</u>
<u>CHAPTER IV</u>	
Figure 4.10	93
4.11	93
4.12	94
4.13	95
4.14	95
 <u>CHAPTER V</u>	
TABLES 5.1	100
5.2	105
Figure 5.1	116
5.2	116
5.3	117
5.4	117
5.5	118
5.6	118
5.7	119
5.8	120
5.9	121
5.10	121
5.11	121
5.12	122
5.13	122
5.14	122
5.15	123
5.16	123
5.17	124
5.18	125
5.19	126
5.20	127
5.21	127
5.22a	128
5.22b	129
5.23a	128
5.23b	130

LIST OF TABLES AND FIGURES

continued

<u>CHAPTER VI</u>	<u>Page</u>
TABLES 6.1	135, 136, 137
6.2	138, 139, 140
6.3	145
6.4	149, 150
6.5	153
Figures 6.1	154
6.2	154
6.3	155
6.4	155
6.5	156
6.6	156
6.7	157
6.8	157
6.9	158
6.10	158
6.11	159
6.12	159
6.13	160
6.14	160
6.15	161
6.16	161
6.17	162
6.18	162
6.19	163
6.20	163
6.21	164
6.22	164
6.23	165

CHAPTER I

THE EQUALISATION PROBLEM

- 1.1 Introduction.
- 1.2 A Bode-type variable equaliser.
- 1.3 Aims and organisation of the thesis.

1.1 Introduction.

The use of equalisers to compensate for the distortions in the phase and amplitude characteristics of transmission lines and other signal processing systems is well known in communication, where high quality lines are required. It is therefore required that an equaliser should have a defined characteristic fixed by the system with which it is associated. However, very often, the characteristics of the equaliser cannot be prescribed in advance; this is either due to the fact that the characteristics of the system are not known with sufficient precision or that they vary with time. A typical example is a communication cable for which the loss frequency characteristics vary with temperature and other weather conditions. To compensate for these distortions it is necessary to use not only the ordinary fixed equaliser but also a variable equaliser.

It is relevant to make a distinction between the terms "variable" and "adjustable". For example the electrical properties of a transmission line are variable; they are a function of its environment over which we have little or no control. Whereas the electrical properties of the equaliser are adjustable as they can be set to any value, within a range, to compensate for the variability of the transmission line. Although the term "adjustable equaliser" seems more appropriate than the conventionally used term "variable equaliser", we shall conform here with normal usage and use variable instead of adjustable.

The basic design theory of variable equalisers (VEs) was developed by Bode [1,2] , some 40 years ago, and his principles are still

widely applicable. His circuit realisation aimed at LRC circuits, and later improvements and refinements contributed by other circuit designers[3,4,5] require, in the present era of microelectronic inductorless active RC circuits, at least revision and supplementation. This need for active RC filters during the last ten years has been motivated primarily by the availability of good, inexpensive integrated circuit (IC) operational amplifiers. This permits the realisation of filters which are cheaper, smaller, and more easily manufactured. This is very important in the case of equalisers because they are used in large numbers.

In this work, we are mainly interested in amplitude equalisation and our aim will be the realisation of RC Bode-type VEs. What is a Bode-type VE? What are its properties? The answer to these questions are dealt with in the following section.

1.2 A Bode-type variable equaliser.

In 1937, Bode invented VEs in response to the need of the maintenance of high quality transmission in long telephone circuits. In those lines the distortions are mainly due to temperature variations and, in some cases, to humidity changes. In some of these carrier systems the maximum change in attenuation is around 1dB per mile; it is therefore important, if a reasonable standard is to be maintained, to compensate with great accuracy for those changes. Since a large number of compensating elements are needed in the overall carrier frequency system, this compensating element should be made as simple as possible, preferably of a kind that lends itself readily to automatic control.

The idealised loss frequency characteristic of a Bode-type

VE is of the following form [2]

$$\alpha(w,k) = \alpha_o(w) + k(R_v) \alpha_1(w) \quad (1.1)$$

where $k(R_v)$ is a frequency-independent real adjustment parameter whose value, as a function of an adjustable resistor R_v , can be varied from -1 to +1. $\alpha_1(w)$ is a frequency dependent response under our control (to Bode this function corresponds to the temperature characteristic, and $k(R_v)$ expresses the calibration of the controlling element with respect to temperature). $\alpha_o(w)$ represents a reference response (or a fixed loss), it could be either dependent or independent of the frequency.

Equation (1.1) describes a family of curves (Fig.1.1) symmetrically arranged around the mean curve:

$$\alpha(w,0) = \alpha_o(w) \quad (1.2a)$$

the outer curves are given by

$$\alpha(w,\pm 1) = \alpha_o(w) \pm \alpha_1(w) \quad (1.2b)$$

for any $k(-1 \leq k \leq +1)$ the family of curves satisfies the symmetry condition :

$$\alpha(w,+k) + \alpha(w,-k) = 2 \alpha_o(w) \quad (1.2c)$$

furthermore, at all w_i for which $\alpha_1(w_i) = 0$, all curves go through one or more common points given by

$$\alpha(w_i,k) = \alpha_o(w_i), \text{ for any } k (-1 \leq k \leq +1) \quad (1.2d)$$

Since the transfer function $T_1(s)$ of a VE containing an adjustment resistor R_v must be of the bilinear form [35]:

$$T_1(s) = \frac{A(s) R_v + B(s)}{C(s) R_v + D(s)} \quad (s=j\omega) \quad (1.3)$$

with a corresponding loss-frequency characteristic

$$\alpha_1(\omega) = -10 \log_{10} |T_1(s)|^2 \quad (1.4)$$

we can see that equation (1.1) can never be fully satisfied by a physical circuit.

In order to illustrate how unsuitable a circuit satisfying (1.3) (but not (1.1)) can be, let us investigate the circuit in Fig. 1.2 which produces the family of curves shown in Fig. 1.3. Although these curves have a common point of confluence at zero frequency and behave acceptably at high frequencies; at an intermediate frequency range however, the various curves intersect each other in a way which very strongly violates (1.1). This can be easily investigated for any positive couple (R_{vx}, R_{vy}) . The intersection point of the curves corresponding to R_{vx} and R_{vy} (apart from the common point of confluence at $\omega=0$) is given by :

$$\omega_{xy} = \frac{1}{C_0} \left(\frac{2}{2R_{vx} R_{vy} + R_0(R_{vx} + R_{vy})} \right)^{\frac{1}{2}} \quad (1.5)$$

An alternative form of the transfer function $T_1(s)$ in (1.3) is therefore required and which satisfies, at least approximately, the ideal equation in (1.1).

An acceptable approximation to (1.1), given by Bode, can be obtained by a transfer function $T(s)$ of the form

$$T(s, \gamma) = T_0(s) \frac{1 + \gamma H(s)}{\gamma + H(s)} \quad (1.6)$$

The parameter γ is chosen to be equal to R_v/R_0 , where R_0 is a suitable reference resistance and R_v is a variable resistance; ideally γ varies from 0 via 1 to ∞ (this range $[0, \infty]$ will be referred to as the 'whole range' of variation of the variable element). $H(s)$ is a normalised driving point impedance function which, we shall see, is a function of a shaping impedance $Z_0(s)$. The transfer function $T_0(s)$ is of less importance and it could be realised by means of a separate non-variable equaliser circuit. For further discussions and for all the design methods with which we are dealing here, $T_0(s)$ is a constant M (i.e. independent of the frequency) which, within limits, can be freely chosen. Thus (1.6) becomes

$$T(s, \gamma) = M \frac{1 + \gamma H(s)}{\gamma + H(s)} \quad (1.7)$$

This transfer function represents a family of curves; the mean curve is given by

$$T(s, 1) = M \quad (1.8a)$$

and the outer curves by

$$T(s, 0) = M [H(s)]^{\pm 1} \quad (1.8b)$$

for any γ , the symmetry condition is

$$T(s, \gamma) \cdot T(s, \gamma^{-1}) = M^2 \quad (1.8c)$$

and for any γ , at all w_i for which $H(jw_i) = 1$, the common points are given by

$$T(jw_i, \gamma) = M \quad (1.8d)$$

The family of curves obtained from (1.7) satisfy similar conditions to those obtained from (1.1). The approximation made in choosing (1.7) instead of (1.1) can be justified. Let us first write (1.7) in a slightly different form.

$$e^{-\alpha} = e^{-\alpha_0} \frac{1 + \gamma e^{-\phi}}{\gamma + e^{-\phi}} \quad (1.9)$$

If (1.9) represents a transfer function, the loss (in nepers) is given by

$$\alpha = \alpha_0 - \ln \frac{1 + \gamma e^{-\phi}}{\gamma + e^{-\phi}} \quad (1.10)$$

let $y = \frac{1 + \gamma e^{-\phi}}{\gamma + e^{-\phi}} \quad (1.11)$

and $W = \frac{y-1}{y+1} = \frac{\gamma-1}{\gamma+1} \cdot \frac{1-e^{-\phi}}{1+e^{-\phi}} \quad (1.12)$

then if we write y in terms of W we have

$$y = \frac{1+W}{1-W} \quad (1.13)$$

developing $\ln y$ as a power series of W we get

$$\ln y = 2 \left[W + \frac{W^3}{3} + \frac{W^5}{5} + \dots \right] \quad (1.14)$$

which gives

$$\ln y = - \frac{\gamma-1}{\gamma+1} \phi - \frac{1}{12} \frac{\gamma-1}{\gamma+1} \left[\left(\frac{\gamma-1}{\gamma+1} \right)^2 - 1 \right] \phi^3 + \dots \quad (1.15)$$

Inserting (1.15) in (1.10) yields

$$\alpha = \alpha_0 + \frac{\gamma-1}{\gamma+1} \phi + \frac{1}{12} \frac{\gamma-1}{\gamma+1} \left[\left(\frac{\gamma-1}{\gamma+1} \right)^2 - 1 \right] \phi^3 + f(\gamma)\phi^5 + \dots \quad (1.16)$$

The first two terms in (1.16) can be identified with the quantities appearing on the right hand side of equation (1.1). The remaining terms represent the departure from the ideal case. Bode [1] has estimated that the loss deviation is about 0.1 dB when the maximum value of ϕ is 1 neper, corresponding to a total variation in attenuation of about 18 dB.

Although passive realisations of (1.7) performed quite well in the past, they have however some disadvantages such as the requirement for dual impedances (which makes the use of inductors compulsory) and non-constant input and output impedances in most practical realisations.

1.3 Aims and organisation of the thesis.

Bode's transfer function for VEs and the properties of its loss-frequency characteristics have been defined above. This project is mainly concerned with active RC realisations of this transfer function.

The designs could include either transistors or op-amps. Transistors are only suitable when a very wide frequency range is required because their finite gain bandwidth product f_T can be far higher than that of op-amps. However, within the voice frequency band, where in signal processing systems the demand for VEs may be considerable, it is useful to concentrate on active RC designs using op-amps. On the other hand, the variable element by which the amplitude of the frequency-response is varied is chosen to be a single two-terminal adjustable resistor. Compared with capacitors, resistors are easily adjustable and make the structures suitable for automatic control. The designs using three-terminal variable resistors [6,7] are not considered. In this thesis a significant number of new designs of active RC VEs, which are believed to be original, are presented. They are very attractive and can be useful to active RC designers; in some cases nearly ideal performance characteristics can be obtained. Although most of the structures are built with discrete components, they can conceivably be implemented microelectronically.

The structure of the thesis is as follows: In chapter 2 a review of the work related to the design of active RC Bode VEs is presented, it includes methods using either Op-amps or transistors. An example of a non-Bode VE is also given. To overcome some of the disadvantages of those designs, a new kind of equaliser is developed in chapter 3; we referred to them as 'quasi Bode-type' VEs because they do not satisfy the transfer function (1.7) itself but only its squared-modulus. They have, therefore, identical loss-frequency characteristics with those of the corresponding Bode-type VEs; nevertheless, they introduce an extra positive phase shift. In Chapter 4, advantage is taken of the use of symmetrical lattice networks, in developing the equalisers in Chapter 3, to design a Bode equaliser free of the restrictions inherent to quasi Bode-type equalisers. These two

chapters are made independent because of the particular behaviour of the phase-frequency characteristics of the networks in chapter 3.

In chapter 5, a new basic design for Bode VEs is introduced. It is believed to be, so far, the best structure. It is less sensitive to the amplifier finite gain bandwidth product and it is very flexible. This flexibility is illustrated by the use of terminal interchange transformations [21, 29, 30,31] which lead to the design of a wide range of alternative Bode equalisers. An attempt is made, in chapter 6, to minimise the effect of the f_T and a comparison method of the sensitivities to this effect is presented. The final conclusions concerning the usefulness and the practicality of the new equalisers are discussed in Chapter 7.

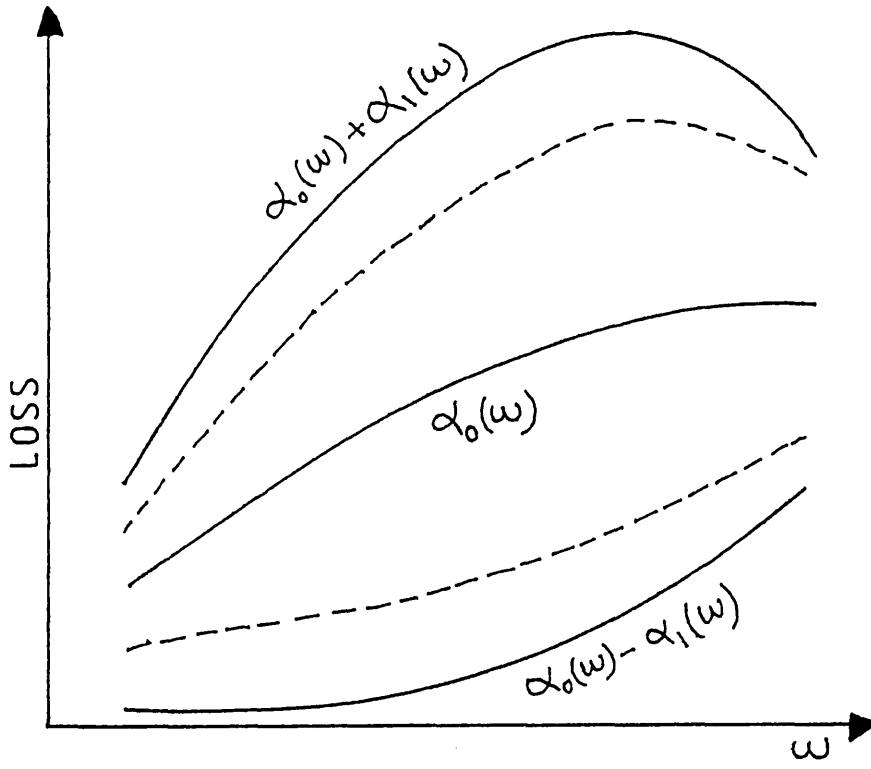


Fig. 1.1 symmetrical characteristics obtained from a Bode-type VE.

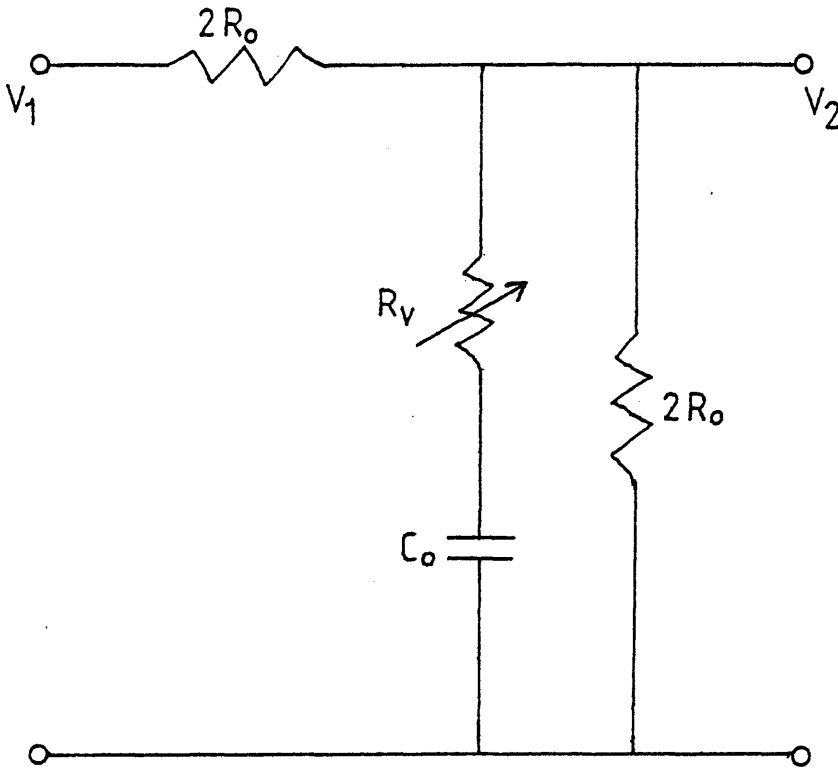


Fig. 1.2 unsuitable VE circuit.

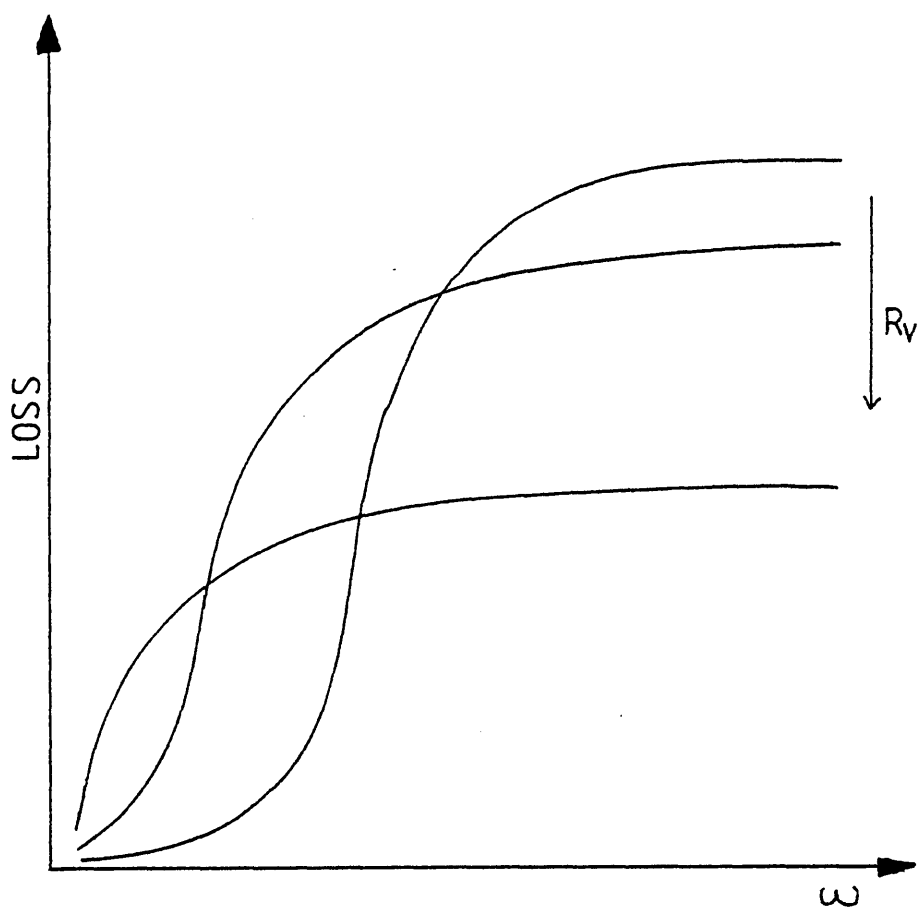


Fig. 1.3 characteristics obtained from the circuit in Fig. 1.2

CHAPTER II

REVIEW OF PREVIOUS WORK

- 2.1 Brglez's approach.
 - 2.1.1 Transformation of the original transfer function.
 - 2.1.2. Active realisations.

- 2.2 Other approaches.
 - 2.2.1 VE with differential amplifiers.
 - 2.2.2 VE using feedback and feedforward.

- 2.3 An example of non-Bode-type VE.

- 2.4 Conclusion.

CHAPTER II REVIEW OF PREVIOUS WORK

In this chapter we shall discuss some of the work which has been achieved in the field of active RC VEs and especially active RC Bode-type VEs.

2.1 Brglez's approach.

In 1974, Brglez was the first to publish a work on active RC Bode-type VEs [8,9]. His approach is based on the transformation of Bode's original transfer function (1.7); and he showed that by mapping the range of the variable element from $[0, \infty]$ to $[-R_0, +R_0]$, one arrives at a different formulation of the equaliser transfer function.

2.1.1. Transformation of the original transfer function.

Let us first rewrite equation (1.7)

$$T(s, \gamma) = M \frac{1 + \gamma H(s)}{\gamma + H(s)} \quad (1.7)$$

The new parameters in the new transfer function to be found are related to (1.7) via the bilinear transformation, namely

$$H(s) = \frac{1 - H_0(s)}{1 + H_0(s)} \quad (2.1)$$

$$\gamma = \frac{1 + \rho}{1 - \rho} \quad (\text{i.e. } \rho = \frac{1 - \gamma}{1 + \gamma}) \quad (2.2)$$

Inserting (2.1) and (2.2) into (1.7) produces a new transfer function

$T_o(s, \rho)$

$$T_o(s, \rho) = M \frac{1 - \rho H_o(s)}{1 + \rho H_o(s)} \quad (2.3)$$

From (2.2) we see that if γ in (1.7) varies from 0 to ∞ , then ρ varies from +1 to -1. If we set $\rho = R_v/R_o$, where R_o is a suitable reference resistance and R_v the variable resistance; we can cover the whole range of variation by varying R_v between $+R_o$ and $-R_o$.

The convergence property of (2.3) is identical with that of (1.7) and both approximate the ideal equaliser equation (1.1). The basic contribution of Brglez is to identify ρ in (2.3) as the variable element and $H_o(s)$ the shaping immittance; and the realisation of the new transfer function with unsymmetrical passive lattice network containing a single shaping impedance $Z_o(s)$ (Fig. 2.1). Comparing the transfer function of this circuit and (2.3) we get

$$\begin{aligned} M &= \frac{1}{2} \\ \rho &= R_v / R_o \\ H_o(s) &= \frac{R_o}{R_o + Z_o(s)} \end{aligned} \quad (2.4)$$

The resistance R_o in series with $Z_o(s)$ is essential in this case otherwise the circuit will not behave as a VE and will be reduced to the familiar lattice form.

The advantage of this structure is that it does not require dual impedances but it has the disadvantage to halve the range of the variable element (ρ varies only from 0 to 1), and does not permit

simultaneous grounding of the input and the output ports. Moreover, the reference flat loss is not 0dB but 6dB.

2.1.2 Active realisations.

The simplest active realisation of (2.3) is the circuit shown in Fig. 2.2 which corresponds to the passive lattice network in Fig.2.1. Its voltage transfer function is given by

$$T(s, R_v) = \frac{R_o - R_v + Z_o(s)}{R_o + R_v + Z_o(s)} \quad (2.5)$$

Comparing (2.5) and (2.3) we get

$$M = 1$$

$$\rho = R_v/R_o \quad (2.6)$$

$$H_o(s) = \frac{R_o}{R_o + Z_o(s)}$$

At the cost of using a single transistor, the reference flat loss is shifted to 0dB and a common ground to the input and output ports is made available; but the whole range of variation cannot be covered by using this structure because R_v varies only between 0 and $+R_o$.

The solution to this problem is a realisation which takes advantage of active all-pass network structures [10]. By inserting a negative impedance converter (NIC) into this structure, Brglez [8] presented his first active RC ~~VE~~ which covers the whole range of variation. The circuit is shown in Fig. 2.3 where the physical variable resistor

R_x varies from 0 to $+ 2 R_o$ which makes $R_v = R_x - R_o$ vary from $-R_o$ to $+ R_o$. This equaliser represents a valuable alternative to passive designs because it does not require dual impedances; its reference flat loss is 0dB and since its output terminal occurs at the output terminal of an operational amplifier (op-amp) it can be used as basic building block for direct cascading into multiple sections.

In order to remove the need for a NIC and the associated op-amp, an alternative design containing a circuit-modifying switch has been proposed [9]. The transfer function of this circuit (Fig. 2.4) is given by

$$T_o(s,p) = - \frac{1-\rho H_o(s)}{1+\rho H_o(s)} , \text{ switch connected to 1}$$

$$T'_o(s,p) = - \frac{1 + \rho H_o(s)}{1 - \rho H_o(s)} , \text{ switch connected to 2} \tag{2.7}$$

with $\rho = R_v/R_o$; $0 \leq R_v \leq R_o$

and

$$H_o(s) = \frac{R_o}{R_o + Z_o(s)}$$

This structure does not need an extra op-amp to cover the whole range of variation but its main disadvantage is the necessity to vary R_v in different directions, depending on the switch position. This is not desirable if automatic regulation is required (i.e. at a fixed frequency R_v should be increased not only to increase the positive loss but also to decrease the negative loss).

It can be verified that interchanging R_v and $Z_o(s) + R_o$ will also result in (2.7); however the resulting network would be unstable if the switch is connected to position 2 when the shaping impedance $Z_o(s)$ is a simple capacitor.

Another structure which has the transfer function in (2.7) is shown in Fig. 2.5; in this case we have

$$\rho = G_v/G_o \quad 0 \leq G_v \leq G_o$$

$$H_o(s) = \frac{G_o}{G_o + Y_o(s)}$$

where $Y_o(s)$ is the shaping admittance, $G_o = 1/R_o$ and $G_v = 1/R_v$. This configuration has been used by Brglez to equalise the lower bandedge frequency response over an amplitude range of ± 10 dB ($Y_o(s)$ is a capacitor, see Fig. 2.6). But the main attractive feature of the configuration is the design of a 'bump' equaliser shown in Fig. 2.7 which has the transfer function

$$T_o(s) = - \frac{s^2 + (hw_o/Q)s + w_o^2}{s^2 + (w_o/Q)s + w_o^2}, \quad \text{SW connected to 2} \quad (2.8)$$

$$T'_o(s) = 1/T_o(s), \quad \text{SW connected to 1}$$

where

$$w_o^2 = \frac{1}{L_o C_o}$$

$$Q = \frac{w_o C_o}{G_q + G_o - G_v}$$

$$h = \frac{G_q + G_o + G_v}{G_q + G_o - G_v} \quad (2.9)$$

In practice the inductor L_o could be simulated by an active RC single or two amplifiers circuit. The kind of loss-frequency response obtained by this equaliser is shown in Fig. 2.8. It is worth pointing out that the resonant frequency $f_o = \omega_o/2\pi$ is adjusted by means of L_o (a resistor in active realisation) and the height h of the bump is adjusted by means of G_v ; from (2.9) we can see that these two adjustments are independent of each other. The variation in the sharpness of the bump (or its Q) can be achieved by varying G_q ; however, this would alter the height h . At a resonant frequency f_o , it is possible to maintain the constancy of the Q by ensuring a tracking between G_o and G_v which will result, of course, in height variations.

2.2 Other approaches.

2.2.1 VE with differential amplifiers.

In order to eliminate the need for a NIC or a circuit modifying switch in Brglez's circuits, Shida and Suzuki [11] proposed an alternative structure to realise a Bode-type VE. The starting point is the transformed Bode's transfer function in (2.3) which is broken down to the following form

$$T_o(s) = 2\left(\frac{1}{2} - T_1(s)\right)$$

$$T_1(s) = \frac{\rho H_o(s)}{1 + \rho H_o(s)} \quad (2.10)$$

For the time being, the multiplying coefficient M is assumed to be equal to 1. The signal flow graph in Fig. 2.9 shows this transformation. The voltage transfer function $T_1(s)$ can be realised, for example, by means of a shaping impedance, a variable resistor and a fixed resistor as shown in Fig. 2.10a. The whole range of variation can be covered by

varying $\rho = R_v/R_o$ between -1 and $+1$. But the aim of the authors is not to introduce a NIC in their design which provides the negative R_v range; they, instead, introduced balanced sources to the circuit in Fig. 2.10a which gives the equivalent circuit shown in Fig. 2.10b. This is the first step to get rid of the required NIC; the whole VE structure which contains the transformed circuit in Fig. 2.10b is shown in Fig. 2.11 where R_x is the physical variable resistor which replaces $R_o + 2R_v$ in the transformed circuit. The transfer function of the obtained VE is given by

$$T(s) = \frac{1}{2} \frac{1 - \rho H_o(s)}{1 + \rho H_o(s)} \quad (2.11)$$

where

$$H_o(s) = \frac{R_o}{R_o + Z_o(s)}$$

and

$$\rho = \frac{1}{2} \left(\frac{R_x}{R_o} - 1 \right)$$

It is easy to verify that if R_x varies from 0 to $+2R_o$, ρ is within the range $[-\frac{1}{2}; +\frac{1}{2}]$. At the outer limits of this range and when $Z_o(s)$ is purely reactive, the maximum loss that can be obtained with this configuration is about ± 1 Neper. For $\rho = 0$ (i.e. $R_x = R_o$) we get a reference flat loss of 6 dB.

Although this structure does not require a NIC or a switch; it uses nevertheless, two differential amplifiers and doubles the complexity of the shaping impedance. Moreover, the symmetrical amplitude variable range is restricted to ± 1 Neper and the reference flat loss is

no longer 0dB but 6dB.

An alternative design, which uses a single shaping admittance, has been proposed by the authors of reference [11] ; the circuit is shown in Fig. 2.12, its transfer function is given by

$$(2.11) \text{ with } H_o(s) = \frac{G_o}{G_o + Y_o(s)} \quad \text{and } \rho = \frac{1}{2} \left(\frac{G_x}{G_o} - 1 \right).$$

2.2.2. VE using feedback and feedforward.

The method has been proposed by Takasaki and al. [12] in 1976. Bode's transfer function (1.7) is simulated by signal flow graphs that have a forward, feedforward, and feedback paths as shown in Fig. 2.13. Both combinations (corresponding to solid or broken lines) have the same transfer function

$$T(s) = \frac{x + y_2(s)}{1 - xy_1(s)} \quad (2.12)$$

if we choose

$$y(s) = y_2(s) = -y_1(s)$$

we get

$$T(s) = \frac{x + y(s)}{1 + xy(s)} \quad (2.13)$$

which is the inverse of the transfer function in (1.7); therefore the

signal flow graphs in Fig. 2.13 can realise Bode-type variable equalisers in terms of variable gain element x and shaping network $y(s)$. An example, given by the authors, is the circuit in Fig. 2.14 which corresponds to the solid feedback and feedforward lines in Fig. 2.13.

Let us derive the transfer function $T(s) = V_2/V_1$ of this network where y_1 and y_2 are shaping networks and denote also the corresponding transfer admittances.

The current flowing into R_3 is

$$I_1 = \frac{V_1}{R_1} + y_1 V''$$

and the voltage across it is

$$V' = -R_3 \left\{ \frac{V_1}{R_1} + y_1 V'' \right\} \quad (2.14)$$

The current flowing into R_4 is

$$I_2 = \frac{V''}{R_2} + y_2 V'$$

and the output voltage is given by

$$V_2 = -R_4 \left\{ \frac{V''}{R_2} + y_2 V' \right\} \quad (2.15)$$

but V'' and V' are related by

$$V'' = k V' \quad (2.16)$$

where $k = \frac{R_v}{R_5 + R_v}$

Combining (2.14), (2.15) and (2.16) yields

$$T(s) = \frac{V_2}{V_1} = \frac{R_3 R_4}{R_1 R_2} \cdot \frac{k + R_2 Y_2}{1 + k R_3 y_1} \quad (2.17)$$

In order to give this transfer function the form of (2.13), let $x = ak$ (where a is an arbitrary positive number) and

$$y = aR_2 y_2 = R_3 y_1 / a$$

then we get

$$T(s) = \frac{R_3 R_4}{aR_1 R_2} \cdot \frac{x + y}{1 + xy} \quad (2.18)$$

Apart from a multiplying constant, equations (2.18) and (2.13) are identical. We have seen that for a Bode type VE x should vary between 0 and ∞ ; this is not the case because the upper limit of x is a (i.e. $0 \leq x \leq a$).

If $a=1$ and $R_1 = R_2 = R_3 = R_4 = R_0$; and if y_1 and y_2 are identical and represent the T-section in Fig. 2.15 we get the following transfer function

$$T(s) = \frac{x + y_0(s)}{1 + x y_0(s)} \quad (2.19)$$

where

$$y_0(s) = \frac{8 + sR_0 C_0}{8 + 3sR_0 C_0}$$

The corresponding loss-frequency characteristics are

symmetrical about a reference flat loss 0dB and correspond to those of a Bode-type fan equaliser.

The structure in Fig. 2.14 is suitable for high frequency equalisation because it uses transistors which could have very high f_T . In practice, the structure can only lend itself to discrete realisation or at most hybrid integration because it uses coupling capacitors of high values which are not available by microelectronic technology. Another disadvantage of the structure is that it uses two shaping networks.

2.3 An example of non-Bode-type VE.

In 1973, Fleischer [13] developed a variable amplitude equaliser which was used to improve the frequency response of data transmission lines (a variable delay equaliser which is not to be discussed here was also developed by the same author [13]).

The transfer function to be realised is of the form

$$T(s) = \frac{s^2 + hQs + \omega_o^2}{s^2 + Qs + \omega_o^2} \quad (2.20)$$

which corresponds to a bump equaliser where $\omega_o = 2\pi f_o$, f_o represents the resonant frequency, h is the bump height and Q describes the sharpness of the bump. It is required that each of these parameters should be freely adjusted.

In order to realise this biquadratic transfer function a biquad [14, 15] is used. Thus, the transfer function of the circuit shown in Fig. 2.16 is given by

$$T(s) = -\frac{R_8}{R_5} \cdot \frac{s^2 + \left\{ 1 + \frac{R_1}{R_4} \frac{R_5(R_6 - R_7)}{R_6 R_7} \right\} \frac{s}{R_1 C_1} + \frac{1}{R_2 R_3 C_1 C_2}}{s^2 + \frac{s}{R_1 C_1} + \frac{1}{R_2 R_3 C_1 C_2}} \quad (2.21)$$

If we set $R_5 = R_6 = R_8$ and $R_4 = R_1$, we get the desired transfer function

$$T(s) = -\frac{s^2 + \frac{R_5}{R_7} \frac{s}{R_1 C_1} + w_o^2}{s^2 + \frac{s}{R_1 C_1} + w_o^2} \quad (2.22)$$

where $w_o^2 = 1/R_2 R_3 C_1 C_2$.

The resonant frequency can, therefore, be adjusted by means of R_2 or R_3 , while the height $h = R_5/R_7$ is adjusted by means of R_7 , and the bandwidth is varied by changing R_1 but it is necessary that R_4 tracks R_1 .

Although the structure in Fig. 2.16 can provide a reference flat loss 0dB and a positive and a negative loss, it should not be regarded as a Bode-type bump VE because its transfer function can never be of the form of (1.7).

2.4 Conclusion.

Some of the work achieved in the design of active RC VEs has been briefly reviewed in this chapter. It is seen that most of the structures have many advantages when compared with their passive counterparts. They are very simple in their design, they are also very flexible because a single structure can produce different shapes of its frequency response depending on one or two shaping impedances. In order to illustrate a difference between a Bode-type and a non-Bode-type VE, an example of bump equaliser, which uses four op-amps, was given in section 2.3; another example of non-Bode bump equaliser can be found in reference [16] .

All the designs discussed in this chapter have their own advantages and also some disadvantages. In the following chapters we shall describe the significant number of circuits we have designed and compare them with the existing structures.

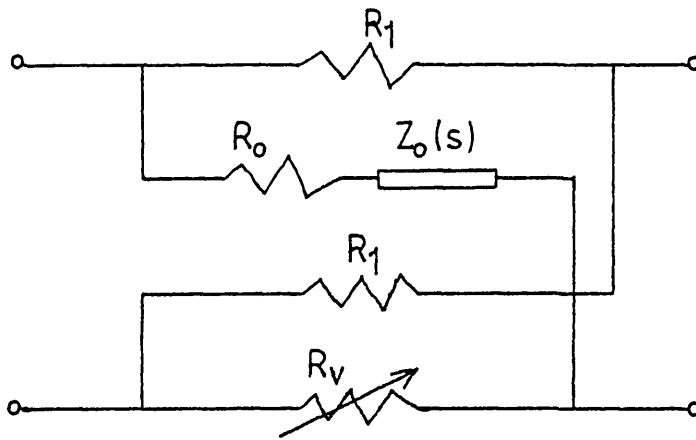


Fig. 2.1 passive VE using a single shaping impedance.

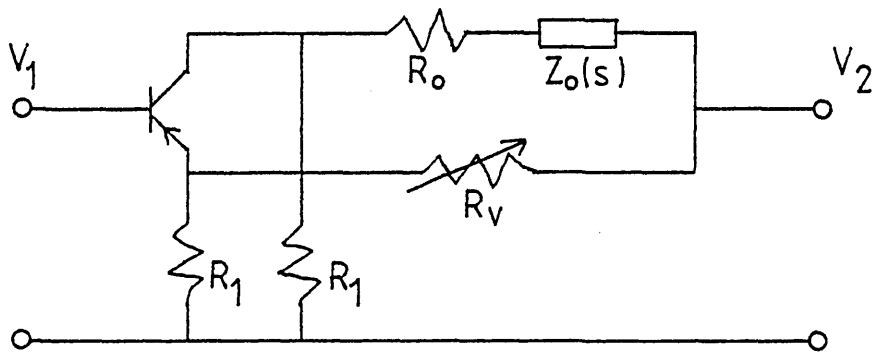


Fig. 2.2 active realisation of the circuit in Fig. 2.1

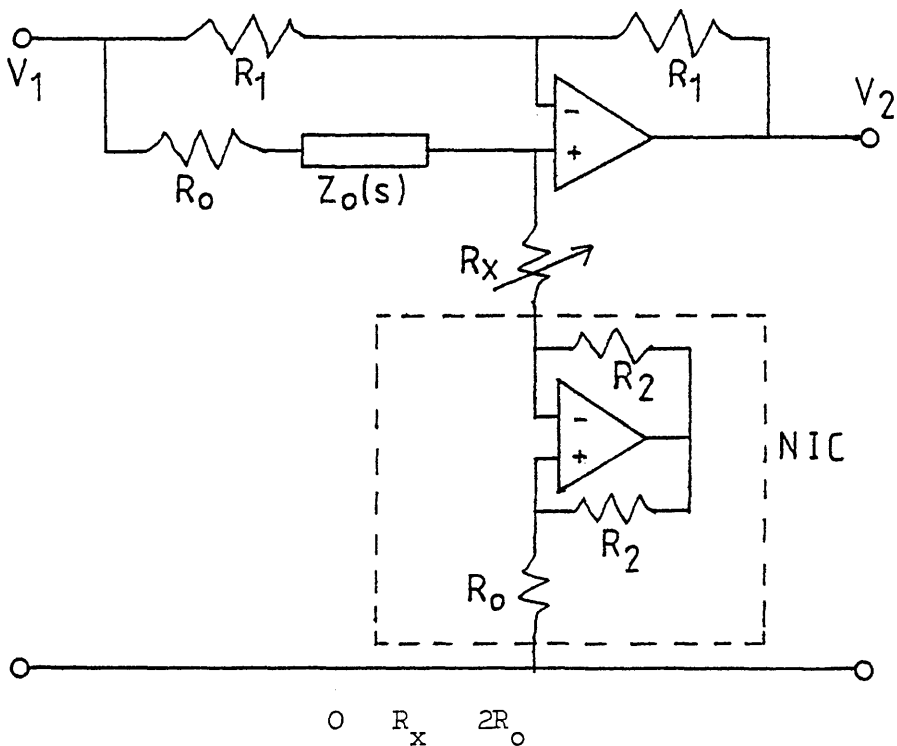


Fig. 2.3 inductorless VE using 2 op-amps.

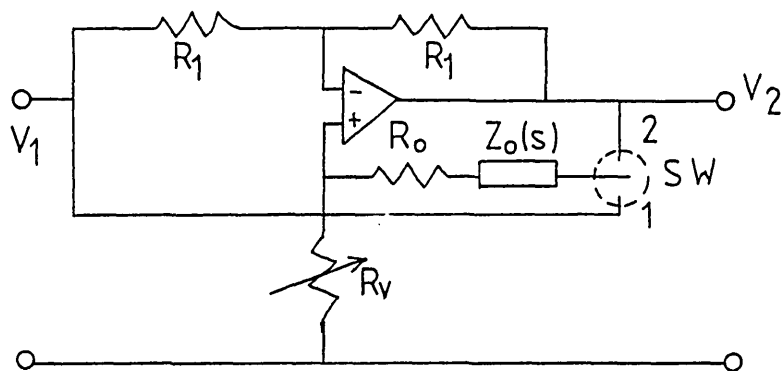


Fig. 2.4 VE using a switch.

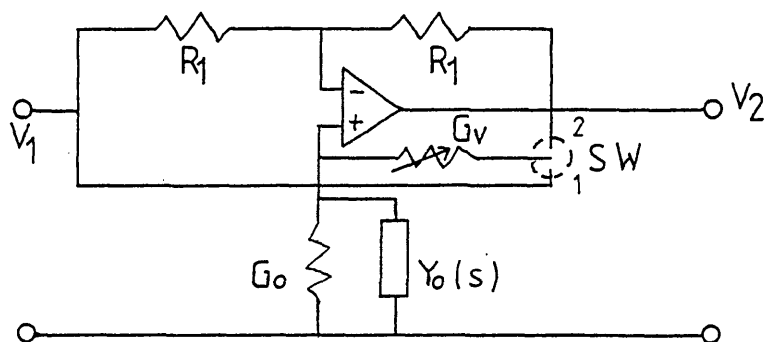


Fig. 2.5 alternative design to the VE in Fig. 2.4

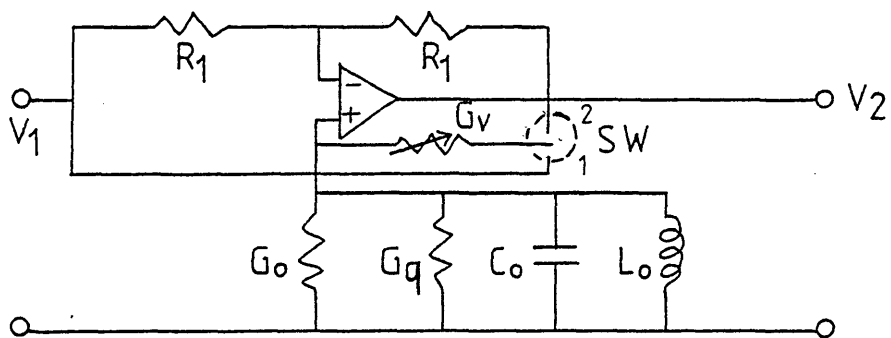


Fig. 2.7 Brglez's bump equaliser based on the circuit in Fig. 2.5

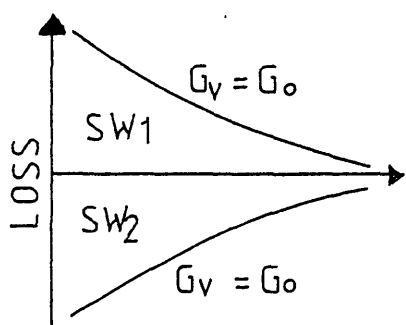


Fig. 2.6

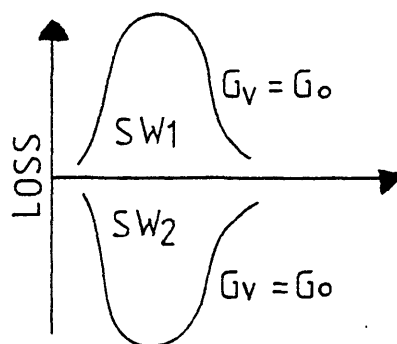


Fig. 2.8

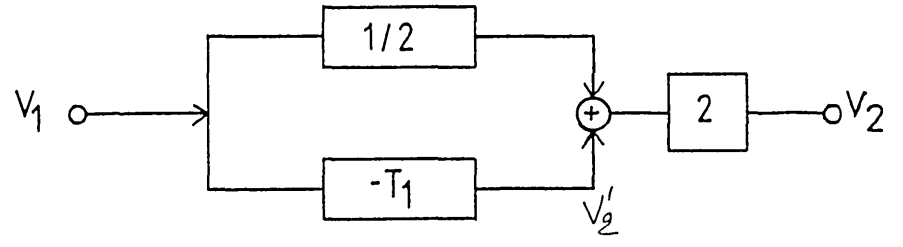


Fig. 2.9

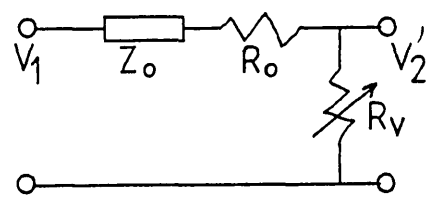


Fig. 2.10a

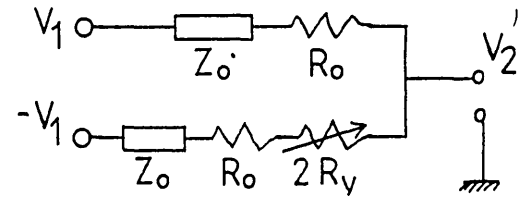


Fig. 2.10b

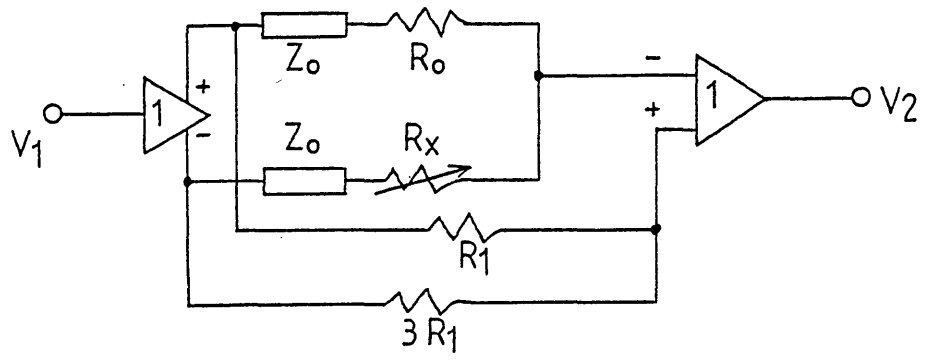


Fig. 2.11 VE with differential amplifiers.

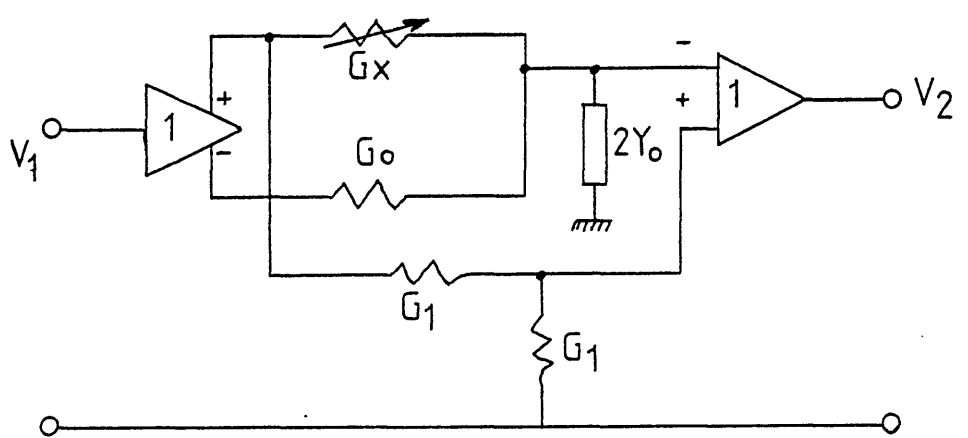


Fig. 2.12 alternative design using a single shaping impedance.

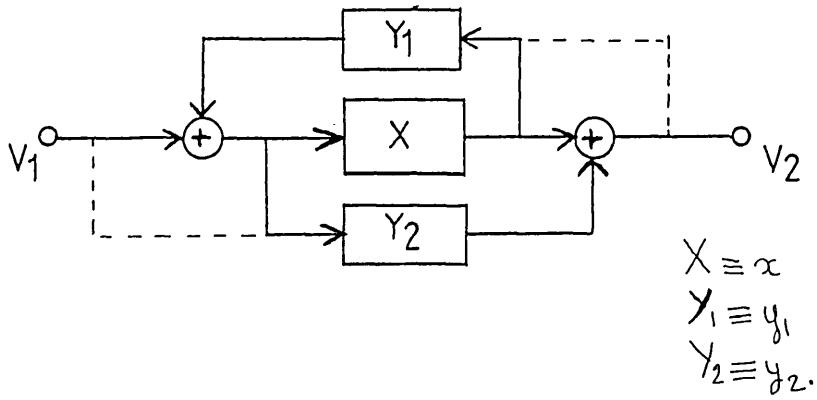


Fig. 2.13 signal flow-graph simulating Bode's transfer function.

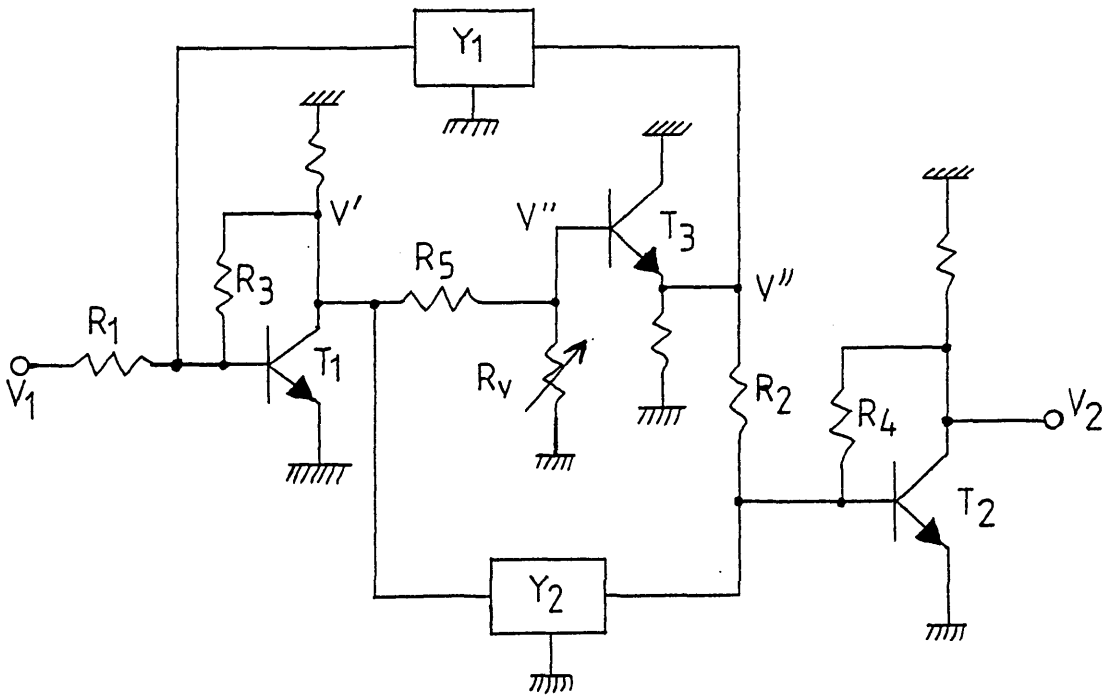


Fig. 2.14 example of realisation for signal flow-graph in Fig. 2.13

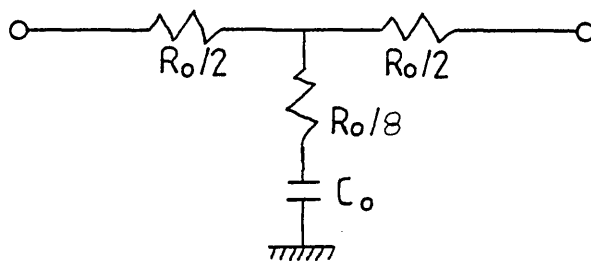


Fig. 2.15

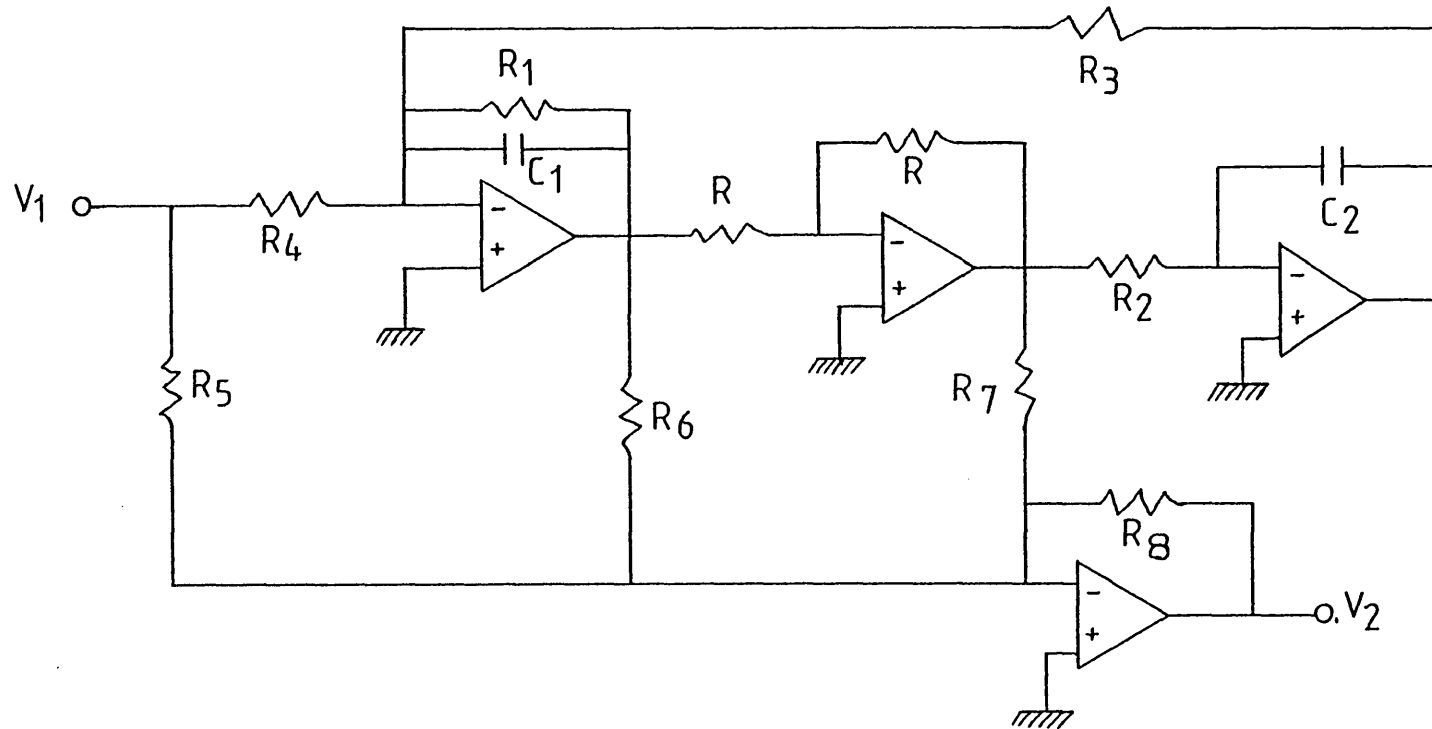


Fig. 2.16 example of non-Bode-type VE.

CHAPTER III

SOME QUASI-BODE-TYPE VARIABLE EQUALISERS

- 3.1 Introduction.
- 3.2 Transformation of Bode's transfer functions for VEs.
- 3.3 Lattice circuits and transformations.
 - 3.3.1 Passive unsymmetrical lattice circuits.
 - 3.3.2 Passive symmetrical lattice circuits.
- 3.4 Active realisations.
 - 3.4.1. Example I : fan equaliser.
 - 3.4.2. Example II: bump equaliser.
- 3.5 Phase considerations and effects of the amplifier finite gain bandwidth product.
 - 3.5.1. Phase considerations.
 - 3.5.2. Effects of the amplifier finite gain bandwidth product.
- 3.6 Conclusions.

CHAPTER III. SOME QUASI BODE-TYPE VARIABLE EQUALISERS.3.1 Introduction

The equalisers to be described in this chapter are based on Saraga's idea [17] whereby they do not satisfy the original transfer function (1.7) itself but only the corresponding modulus equation

$$|T(s, \gamma)| = \frac{|M [1 + \gamma H(s)]|}{|\gamma + H(s)|} \quad (3.1)$$

Therefore, we shall refer to the circuits satisfying (3.1) and not (1.7) as 'quasi Bode-type' VEs.

Since we are interested only in the loss-frequency characteristic (in dB) given by

$$\alpha(\omega, \gamma) = 10 \log |T(s, \gamma)|^2 \quad (3.2)$$

it is useful to write $H(s)$ (in (3.1)) in the form

$$H(s) = A + sB \quad (s = j\omega)$$

and to denote $20 \log |M|$ by M_0 ; then

$$|T(s, \gamma)|^2 = |M|^2 \frac{(1 + \gamma A)^2 + \omega^2 \gamma^2 B^2}{(\gamma + A)^2 + \omega^2 B^2} \quad (3.3)$$

The corresponding loss-frequency response is given by

$$\alpha(w, \gamma) = M_0 + 10 \log \frac{1 + 2\gamma A + \gamma^2 |H(s)|^2}{\gamma(\gamma + 2A) + |H(s)|^2} \quad (3.4)$$

let us investigate the property of this loss-frequency response which represents a family of curves:

the mean curve is given by

$$\alpha(w, 1) = M_0 \quad (3.5a)$$

and the outer curves are given by

$$\alpha(w, \infty) = M_0 \pm 20 \log |H(s)| \quad (3.5b)$$

for any γ , the symmetry condition is

$$\alpha(w, \gamma) + \alpha(w, \gamma^{-1}) = 2 M_0 \quad (3.5c)$$

and for all w_i for which $|H(jw_i)| = 1$, the common points are given by

$$\alpha(w_i, \gamma) = M_0 \quad (3.5d)$$

If we replace in (1.1) $\alpha_0(w)$ by M_0 - corresponding to the replacement of $T_0(s)$ in (1.6) by M in (1.7) - we note that equations (3.5) have a similar form to equations (1.2) and (1.8). This shows that the features, described by (1.2), of the ideally required VE characteristic $\alpha(w, k)$ defined by (1.1) are shared by $\alpha(w, \gamma)$ defined in (3.4), which

is based on $T(s,\gamma)$ defined by (1.7). However, as we have seen for (1.7), the exact proportionality relationship between $\alpha(w,k)$ and $\alpha_0(w)$ stipulated in (1.1) is not exactly satisfied by (3.4) but only approximated.

3.2 Transformation of Bode's transfer function for VEs.

In order to facilitate the investigation and the design of quasi Bode-type VEs, it is useful to derive a new equivalent relation to equation (3.1). To do this, we shall carry out a similar transformation, as the one used in Section 2.1.1, on equation (1.7). This equation is

$$T(s,\gamma) = M \frac{1 + \gamma H(s)}{\gamma + H(s)} \quad (3.6)$$

$$\text{let } H(s) = \frac{H_1(s) - 1}{H_1(s) + 1} \quad (3.7)$$

$$\text{and } \gamma = \frac{1+\rho}{1-\rho} \quad (3.8)$$

Inserting (3.7) and (3.8) into (3.6) yields

$$T(s,\rho) = M \frac{H_1(s) - \rho}{H_1(s) + \rho} \quad (3.9)$$

where ρ varies from -1 to +1, if in (3.6) γ varies from 0 to ∞ .

$H_1(s)$ is a normalised driving point impedance function which can be written under the form $H_1(s) = Z(s)/R_0$. If we set $\rho = R_v/R_0$ so that R_v varies over the range $-R_0 \dots 0 \dots +R_0$ then

$$T(s, R_v) = M \frac{Z(s) - R_v}{Z(s) + R_v} \quad (3.10)$$

$Z(s)$ in (3.10) can be written in the form $Z(s) = R(w) + jX(w)$; but we shall consider the special case where $R(w)$ is a constant resistance R_o and $jX(w)$ is the impedance of a pure reactance one-port so that

$$Z(s) = R_o + jX(w) \quad (3.11)$$

with this notation (3.10) becomes

$$T(s, R_v) = M \frac{R_o + jX(w) - R_v}{R_o + jX(w) + R_v} \quad (3.12)$$

the squared modulus of this function is :

$$|T(s, R_v)|^2 = M^2 \frac{(R_o - R_v)^2 + X^2(w)}{(R_o + R_v)^2 + X^2(w)} \quad (3.13)$$

It should be noted that if $Z(s)$ in (3.11) is a series combination of a variable resistor R_v and a purely reactive impedance $jX(w)$ and R_v is replaced by R_o , the transfer function (3.10) becomes:

$$T(s, R_v) = M \frac{R_v + jX(w) - R_o}{R_v + jX(w) + R_o} \quad (3.14)$$

The interchange of R_o and R_v in (3.12) and (3.14) does not affect the function (3.13). Thus, if in a network satisfying (3.13) we interchange R_o and R_v , the loss frequency characteristic of this network is not affected. This property of (3.13) will be used in the design of quasi Bode-type VEs and the phase shift introduced by this kind of equalisers will be discussed in section 3.5.

3.3 Lattice circuits and transformations.

3.3.1 Passive unsymmetrical lattice circuits.

The general form of an unsymmetrical lattice circuit is shown in Fig. 3.1. Its transfer function $T(s) = V_2/V_1$ is

$$T(s) = \frac{Z_2 Z_3 - Z_1 Z_4}{(Z_1 + Z_3)(Z_2 + Z_4)} \quad (3.15)$$

if we choose $Z_1 = Z_3 = R_1$, the transfer function (3.15)

becomes

$$T(s) = \frac{1}{2} \frac{Z_2 - Z_4}{Z_2 + Z_4} \quad (3.16)$$

If, as in the case of Brglez's circuit [8], we set $Z_2 = Z(s)$ and Z_4 the variable resistor R_v , we get the circuit shown in Fig. 3.2 with the transfer function

$$T(s, R_v) = \frac{1}{2} \frac{Z(s) - R_v}{Z(s) + R_v} \quad (3.17)$$

(3.17) is identical with (3.10) if $M = \frac{1}{2}$; furthermore if $Z(s)$ satisfies (3.11), the transfer function (3.17) agrees with (3.12) and the corresponding circuit is shown in Fig. 3.3.

The circuit in Fig. 3.3 can be modified by interchanging R_o and R_v . This modification leads to the circuit in Fig. 3.4. Its transfer function is the same as the one given in (3.14), therefore we can say that both the circuits in Figs. 3.3 and 3.4 have the same $|T(s, R_v)|^2$ of the form given in (3.13). We note that the lattice sections

we are dealing with are passive only when R_v lies in its positive half range. However, it is important to distinguish these passive circuits from the practical active realisations.

3.3.2. Passive symmetrical lattice circuits.

A symmetrical lattice section in its most general form, with terminating impedances Z_s and Z_L , is shown in Fig. 3.5. It can be obtained from the circuit in Fig. 3.1 by making $Z_4 = Z_1$ and $Z_3 = Z_2$. The transfer function $T(s) = V_2/V_1$ of this circuit is given by

$$T(s) = \frac{Z_L (Z_2 - Z_1)}{(Z_L + Z_s) (Z_1 + Z_2) + 2 (Z_L Z_s + Z_1 Z_2)} \quad (3.18)$$

In the following we examine some special cases

- a) $Z_s = \eta z_1$ and $Z_L = Z_1/\eta$, where η is an arbitrary real positive parameter. The corresponding transfer function is :

$$T(s) = \frac{Z_2 - Z_1}{(1+\eta)^2 (Z_2 + Z_1)} \quad (3.19)$$

- b) $Z_s = \eta Z_2$ and $Z_L = Z_2/\eta$

$$T(s) = \frac{Z_2 - Z_1}{(1+\eta)^2 (Z_2 + Z_1)} \quad (3.20)$$

If the terminations are equal (i.e. $\eta = 1$) we have for the case a

$Z_s = Z_L = Z_1$ and (3.19) becomes

$$T(s) = \frac{Z_2 - Z_1}{4(Z_2 + Z_1)} \quad (3.21)$$

For the case b: $Z_s = Z_L = Z_2$ and (3.20) becomes

$$T(s) = \frac{Z_2 - Z_1}{4(Z_2 + Z_1)} \quad (3.22)$$

The common sub-case of a and b is obtained for $\eta = 0$ (i.e. the transfer function $T(s)$ is the open circuit voltage ratio of the interminated section)

$$Z_s = 0, \quad Z_L \rightarrow \infty$$

$$T(s) = \frac{Z_2 - Z_1}{Z_2 + Z_1} \quad (3.23)$$

In the circuit in Fig. 3.5 the interchange of Z_1 and Z_2 leads to the transfer function in (3.18) multiplied by -1 which means that $|T(s)|$ remains unchanged. This is also valid for the T-sections equivalent to this circuit that we shall investigate and which are very attractive in the context of active realisations:

When Z_s and Z_L are chosen in accordance with (3.19); the T-section equivalent to the lattice circuit in Fig.3.5 is shown in Fig. 3.6. In Fig. 3.7 we have the same circuit with the output taken from a different point, consequently an increase of the output voltage is to be expected; thus its transfer function is :

$$T(s) = \frac{Z_2 - Z_1}{(1+\eta)(Z_2 + Z_1)} \quad (3.24)$$

If Z_s and Z_L are chosen in accordance with (3.20) we get the network in Fig. 3.8 . For $\eta = 0$ this circuit and the one given in Fig. 3.6 lead to the simple and attractive L-section circuit shown in Fig. 3.9 which has the transfer function $T(s)$ in (3.23). It is mainly this circuit that shall be considered as a basic design for active RC realisations of quasi Bode-type VEs.

3.4 Active realisations.

Two examples of active realisations will be given. The first one is the design of a fan equaliser (i.e. the shaping element $X(w)$ in (3.11) is a capacitor C_o); and the second one is the design of a bump equaliser; in this case $X(w)$ is a series combination of a capacitor and an inductor.

Let us then consider the L-section circuit in Fig. 3.9 and look at the choices we have. We can either choose $Z_1 = R_o + jX$ and $Z_2 = R_v$ or $Z_1 = R_v$ and $Z_2 = R_o + jX$; apart from a multiplying constant we get, in both cases, the transfer function in (3.12). Let us, for example, take the last choice (i.e. $Z_1 = R_v$ and $Z_2 = R_o + jX$); the resulting VE will require two matched equal variable resistors (because $Z_1 = R_v$ will appear in both branches of the L-section circuit). At first sight it might have no practical interest, however in the next chapter it is shown that it can lead to the design of an interesting VE.

The circuit corresponding to the first choice (i.e., $Z_1 = R_o + jX$ and $Z_2 = R_v$) is shown in Fig. 3.10; the series combination of $-\frac{1}{2}(R_o - R_v)$ and $-\frac{1}{2}jX$ could be obtained by a NIC (Fig. 3.11). Since

this circuit requires the impractical aspect of two identical shaping elements, its performances will not be considered further.

As a next step let us proceed to the interchange of R_o and R_v , proposed in section 3.2, which leads from equation (3.12) to equation (3.14); in this case our second choice becomes $Z_1 = R_o$ and $Z_2 = R_v + jX$ and we get the circuit in Fig. 3.12 which is far more attractive than the network in Fig. 3.10 because it requires only one reactance one-port and a single variable resistor. Our design examples will be based on this combination of Z_1 and Z_2 .

3.4.1. Example I : fan equaliser.

In order to realise a simple fan equaliser the reactive element $x(\omega)$, in the circuit in Fig. 3.12, is chosen to be a capacitor C_o ; the corresponding active network is shown in Fig. 3.13 in which the physical variable element is the resistor $R'_v = \frac{1}{2} (R_o - R_v)$. One can easily verify that when R_v varies between $-R_o$ and $+R_o$, the actual resistor R'_v varies between $+R_o$ and 0. The loss frequency response of this equaliser is symmetrical about a reference flat loss 0dB. The circuit uses only one op-amp which performs simultaneously two different tasks: the realisation of $|T(s, R_v)|$ and provision of a negative range for R_v ; whereas, for example, in the case of Brglez's circuits either two amplifiers (Fig. 2.3) or an amplifier and a switch (Fig. 2.4) are required for the same task. It might be argued in practice that also the circuit in Fig. 3.13 will require a second amplifier to provide buffering for the open circuit output. However, this can be avoided by using its resistively terminated version shown in Fig. 3.14 which is based on the network in Fig. 3.7 with $\eta=1$. In this case the reference flat loss is no longer 0dB but 6dB. Going back to the open circuit operation (Fig. 3.13), it is useful, in order to avoid

tendency to instability, to provide an output series buffer resistor R_B to ensure that the real part of the output impedance of the circuit is always positive. When the circuit is driven from a grounded voltage source, the output impedance is given by

$$Z_{out} = \frac{R_o (1 - s C_o R'_v)}{1 + s C_o (R_o - R'_v)}$$

If in a practical case R'_v varies between $R_o/4$ and $3R_o/4$, we should choose a value of R_B which is greater than $3R_o$; this is because at high frequencies $\text{Re}[Z_{out}]$ is identical with

$$Z_{out} = - \frac{R_o R'_v}{R_o - R'_v}$$

and therefore $\max |Z_{out}| = 3R_o$. Thus the problem of instability in this VE can be avoided.

The practical circuit is shown in Fig. 3.15, and the measured loss frequency characteristics with the corresponding deviations from the computed results assuming ideal op-amps, are shown in Fig. 3.16.

3.4.2. Example II: bump equaliser.

The bump equaliser to be realised is also based on the network in Fig. 3.12 in which the shaping element $X(w)$ is a series combination of a capacitor C_o and an inductor L_o (i.e. $X(w) = wL_o - 1/w C_o$). Since X is a purely reactive element, a lossy inductor would not be suitable. Furthermore our aim is to achieve a bump equaliser with a minimum number of op-amps.

The basic circuit is shown Fig. 3.17. For active RC realisation it is necessary to simulate the inductor and to provide a variable negative resistor R'_V . Figs. 3.18a and 3.18b show two inductorless circuits simulating the basic circuit in Fig. 3.17, each of them using two op-amps [18]. One amplifier is used to form a NIC of the type shown in Fig. 3.11, the other one is used to form a negative impedance inverter (NII) with characteristic impedance R' , as shown in Fig. 3.19. The difference between a NIC and a NII is that when a NIC is terminated by an impedance Z , it provides an input impedance $-Z$, while a NII with a characteristic impedance R' when terminated by the same impedance Z has an input impedance $-R'^2/Z$.

The operation of the circuits in Figs. 3.18a and 3.18b is self-explanatory; as to Fig. 3.18a, we note that if $\frac{1}{Z} = \frac{1}{R} - j\omega C_1$ (i.e. R is in parallel with a negative capacitor C_1), then $-\frac{R'^2}{Z} = -\frac{R'^2}{R} + j\omega C_1 R'^2$; if we set $R^{-1} = \frac{R'_V}{R'^2}$ we get a variable negative resistor R'_V in series with an inductor $L_0 = C_1 R'^2$.

A laboratory model of the bump equaliser circuit shown schematically in Fig. 3.18a has been built. The practical circuit is shown in Fig. 3.20; measured loss frequency curves, for various values of the variable resistor R'_V , are shown in Fig. 3.21 for a resonant frequency $f_0 = 1.0 \text{ KH}_Z$. Their deviations from the ideal computed responses are also shown in Fig. 3.21. We note that the two resistors in series R'_V and R' could be, in practice, replaced by a single variable resistor $R''_V = R'_V + R'$.

An alternative option to realise the negative resistor R'_V in series with the inductor L_0 in the basic circuit 3.17 is the circuit in Fig. 3.22 [19]; its input impedance is given by

$$Z_{in} = sC_1 R_1 R_4 + \frac{1}{R_3} (R_1 R_3 - R_2 R_4) \quad (3.25)$$

by setting $R_4 = R_3 = R$ we get

$$Z_{in} = s C_1 R_1 R + (R_1 - R_2) \quad (3.26)$$

The overall resistor $(R_1 - R_2)$ can be identified with the variable resistor R'_v and its adjustment is made by varying the physical resistor R_2 which does not appear in the expression of the simulated inductor $L_o = C_1 R_1 R$. $R'_v = (R_1 - R_2)$ could be either positive or negative and it is equal to zero when $R_2 = R_1$. Since we are interested only in the negative values of R'_v we set $R_2 > R_1$. We note that if $R_2 = 0$ we obtain the simulated lossy inductor available in reference [20].

The whole bump equaliser is shown in Fig. 3.23 and the practical circuit is shown in Fig. 3.24; it has been designed to provide an amplitude range of about + 10 dB at a resonant frequency $f_o = 2.5 \text{ kHz}$. The measured loss-frequency curves and their deviations from the computed ones, assuming ideal op-amp, are shown in Fig. 3.25.

In the following we shall show that it is possible to remove the extra output buffer amplifier and the buffer resistor associated with it. Let us then reconsider the circuit in Fig. 3.22; by substituting $Z_2(s) = R_1 + 1/s C_o$ for R_1 , the expression (3.25) of its input impedance becomes

$$Z_{in} = s C_1 R_1 R_4 + \frac{1}{sC_o} + R'_v \quad (3.27)$$

where

$$R'_v = R_1 - \frac{R_2 R_4}{R_3} + \frac{C_1}{C_o} R_4 \quad (3.28)$$

Expression (3.27) suggests the replacement of the bump equaliser in Fig. 3.23 by its equivalent shown in Fig. 3.26 which is more attractive because its output can be taken from B instead of A. By doing so, we end up with a quasi Bode bump equaliser which does not need an extra buffer amplifier at its output. The required negative range of R'_v can easily be provided by varying the physical resistor R_2 . Since $-R_o \leq R'_v \leq 0$ we have

$$\frac{R_3}{R_4} [R_1 + \frac{C_1}{C_o} R_4] \leq R_2 \leq \frac{R_3}{R_4} [R_o + R_1 + \frac{C_1}{C_o} R_4] \quad (3.29)$$

By computational analysis we found that this circuit is slightly more sensitive to the finite gain bandwidth product f_T of the amplifier than the circuit in Fig. 3.23; this leads us to consider modifying the circuit. This modification consists of inserting a redundant resistor R_o between A and B and using transformation B [21] which shall be discussed in section 5.3.2. The transformation itself consists of connecting the ground terminal D to the output terminal of the op-amp and connecting C to the ground after disconnecting it from the output of the op-amp. The next step is to interchange the branches AE and AB but because they are identical, this interchange has no effect on the structure. The transfer function $T'(s)$ of the obtained circuit shown in Fig. 3.27 is related to the transfer function $T(s)$ of the original circuit (Fig. 3.26) by

$$T'(s) = -T(s) \quad (3.30)$$

A laboratory model of the transformed circuit has been built to provide a variable amplitude range of ± 10 dB at a resonant frequency of 2.5 kHz . The measured loss-frequency responses and their deviations from the computed ones, assuming ideal op-amps, are shown in Fig. 3.28.

3.5. Phase considerations and effects of the amplifier finite gain bandwidth product.

3.5.1. Phase considerations.

In this section we investigate the effect produced on the phase by a quasi Bode-type VE, i.e. the interchange of R_o and R_v as stipulated in section 3.2. We shall represent a Bode equaliser transfer function by T_B and a quasi Bode equaliser transfer function by T_{QB} .

Let us rewrite the transfer function (3.12) which represents a Bode equaliser transfer function and where M is chosen to be equal to 1.

$$T_B = \frac{R_o + jX(\omega) - R_v}{R_o + jX(\omega) + R_v} \quad (3.31)$$

Its squared modulus is

$$|T_B|^2 = \frac{(R_o - R_v)^2 + X^2(\omega)}{(R_o + R_v)^2 + X^2(\omega)} \quad (3.32)$$

Its phase Q_B , using the definition

$$T = |T| \exp(-j\phi)$$

is

$$\phi_B = \tan^{-1} \left(\frac{X(w)}{R_o + R_v} \right) - \tan^{-1} \left(\frac{X(w)}{R_o - R_v} \right) \quad (3.33)$$

For the corresponding quasi Bode equaliser (interchange of R_o and R_v), the transfer function is

$$T_{QB} = \frac{R_v + jX(w) - R_o}{R_v + jX(w) + R_o} \quad (3.34)$$

Its squared modulus function is identical with that given in (3.32) and its phase function is

$$\phi_{QB} = \tan^{-1} \left(\frac{X(w)}{R_o + R_v} \right) - \tan^{-1} \left(\frac{X(w)}{R_v - R_o} \right) \quad (3.35)$$

We are interested in $\Delta\phi = \phi_{QB} - \phi_B$. From (3.33) and (3.35) we get

$$\Delta\phi = - \tan^{-1} \left(\frac{X(w)}{R_v - R_o} \right) + \tan^{-1} \left(\frac{X(w)}{R_o - R_v} \right)$$

$$\Delta\phi = 2 \tan^{-1} \left(\frac{X(w)}{R_o - R_v} \right)$$

Thus

$$\tan \left(\frac{1}{2} \Delta\phi \right) = \frac{X(w)}{R_o - R_v} \quad (3.36)$$

Since R_v varies from $-R_o$ to $+R_o$, $(R_o - R_v)$ varies from $+2R_o$ to zero. This shows that the additional phase shift produced by using a quasi

Bode equaliser instead of a Bode equaliser is always positive, i.e. a quasi Bode equaliser is a non-minimum phase network. It should be pointed out that both ϕ_B and ϕ_{QB} are functions of the variable resistance R_v . In table 3.1 some numerical values of ϕ_B and ϕ_{QB} (in degrees) are given for four settings of R_v ; they correspond to those of a fan equaliser where $X(\omega)$ is a capacitor $C_o = 20\text{nF}$ and $R_o = 10 \text{ k}\Omega$.

$f(\text{kHz})$	$\bar{+} R_v$	$\pm \phi_B^o$	ϕ_{QB}^o
0.20	$R_o/4$	6.76	151.88
0.40		11.48	127.20
0.80		14.47	91.49
5.00		4.72	19.23
10.00		2.41	9.70
0.20	$R_o/2$	13.49	152.18
0.40		22.90	128.87
0.80		29.76	96.86
5.00		11.60	23.71
10.00		6.00	12.08

TABLE 3.1

3.5.2. Effects of the amplifier finite gain bandwidth product.

The effect of the amplifier finite gain bandwidth product on the loss-frequency responses is now investigated. We restrict ourselves to the example of a fan equaliser presented in section 3.4.1. Let us start by deriving the input impedance Z_{NI} of the NIC in Fig. 3.29; we

have

$$Z_{NI} = \frac{V_1}{i_o} \quad (3.37a)$$

$$i_o = \frac{V_1 - V_2}{R_1} \quad (3.37b)$$

$$\frac{V_2 - V_3}{R_2} = \frac{V_3}{R'_v} \quad (3.37c)$$

and

$$V_1 - V_3 = -V_2/G \quad (3.37d)$$

where

$$\frac{1}{G} = \alpha + \frac{s}{w_T} \quad (s = jw) \quad (3.38)$$

$1/\alpha$ is the d.c. gain of the amplifier and $w_T = 2\pi f_T$ where f_T is the gain bandwidth product.

Combining equations (3.37) we get

$$Z_{NI} = -R_1 \frac{R'_v - \frac{1}{G} (R_2 + R'_v)}{R_2 + \frac{1}{G} (R_2 + R'_v)} \quad (3.39)$$

which can be written under the following form

$$Z_{NI} = Z_I \frac{1 - \frac{1}{G} (1 + R_2/R'_v)}{1 + \frac{1}{G} (1 + R'_v/R_2)} \quad (3.40)$$

where

$$Z_I = - \frac{R_1 R'_v}{R_2} \quad (3.41)$$

Equation (3.41) represents the expression of the desired ideal impedance which, as can be seen, is not affected by the interchange of R_1 and R'_V [22]. By doing so and assuming $\alpha \ll 1$, equation (3.40) becomes

$$Z_{NI} = Z_I \frac{1 - \frac{s}{\omega T} (1 + R_2/R_1)}{1 + \frac{s}{\omega T} (1 + R_1/R_2)} \quad (3.42)$$

which represents the non-ideal input impedance of the circuit shown in Fig. 3.30.

Let us now set $R_1 = R_2$, to obtain

$$Z_{NI} = -R'_V \frac{1 - 2 \frac{s}{\omega T}}{1 + 2 \frac{s}{\omega T}} \quad (3.43)$$

which is in the form

$$Z_{NI} = -R'_V \exp(-j\phi) \quad (3.44)$$

This shows that the non-ideal impedance Z_{NI} is independent of R_1 and R_2 ; whereas (3.40) shows that the distortions are dependent on R'_V and R_2 . Therefore, if the NIC in Fig. 3.30 is used we should expect the deviations, from the ideal characteristics, of a quasi Bode fan equaliser to be independent of R_2 and R_1 . To illustrate this fact, let us compare the loss frequency responses of the circuits in Figs. 3.31a and 3.32a. In both cases R'_V is chosen to be equal to $R_0/5$ which produces a loss of about + 11.5 dB at an upper frequency $f = 10 \text{ kHz}$. The corresponding deviations of the computed non-ideal responses from the ideal ones are shown in Fig. 3.31b and 3.32b respectively.

It would be interesting to search for a hypothetical network (NIC) which produces no phase shift, i.e. ϕ in (3.44) is equal to zero. This has been done by adopting a strategy which consists of interchanging the inverting and non-inverting input terminals of the op-amp in Fig. 3.30 and by inserting a small capacitor C' in parallel with R'_V . But, in practice, it was found that the compensated fan equaliser was not stable.

3.6 Conclusion.

VE circuits with identical loss-frequency characteristics to those of a Bode equaliser, but of phase-frequency characteristics different from the corresponding Bode-type equaliser have been presented, and we referred to them as quasi Bode-type VEs. We have shown that they always produce an additional positive phase shift which may be unattractive in some applications. However in applications involving only speech signals, for example, loss frequency characteristics are far more important than the phase ones. In that case, in spite of the fact that the shaping impedance is restricted to a purely reactive one, it is always possible to design a VE with well defined loss-frequency characteristics. If it turns out that the phase is important or if the condition $Z_o(s) = jX(\omega)$ is not satisfied, then a quasi Bode equaliser is not suitable. In the following chapter (which is closely related to the present one), an attempt is made to overcome some of these restrictions. It is worth pointing out that the unsuitable equaliser circuit given in Fig. 1.2 becomes suitable in the context of active RC quasi Bode-type VEs; i.e. if the range of the variable resistor R_V of this circuit is chosen to be $[-R_o, 0]$ instead of $[0, \infty]$ we obtain the VE in Fig. 3.14 which satisfies the squared modulus of Bode's transfer function (1.7).

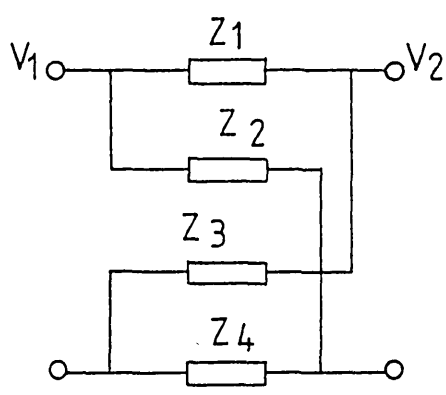


Fig. 3.1 unsymmetrical lattice circuit.

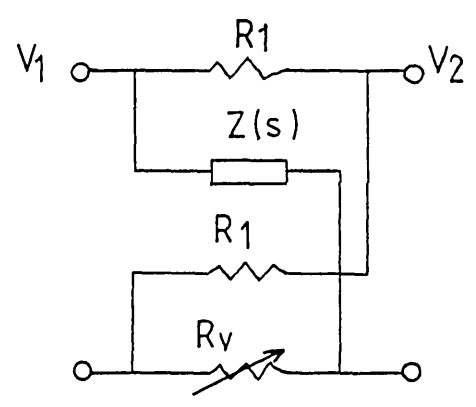


Fig. 3.2

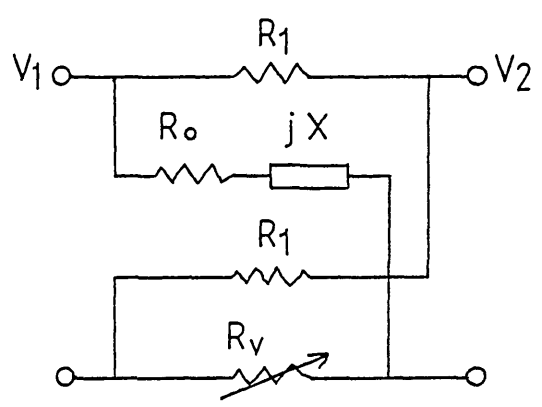


Fig. 3.3

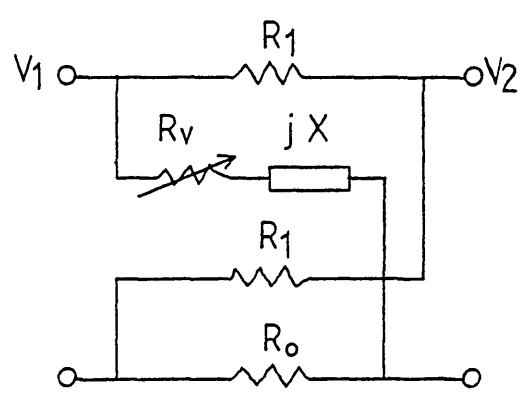


Fig. 3.4

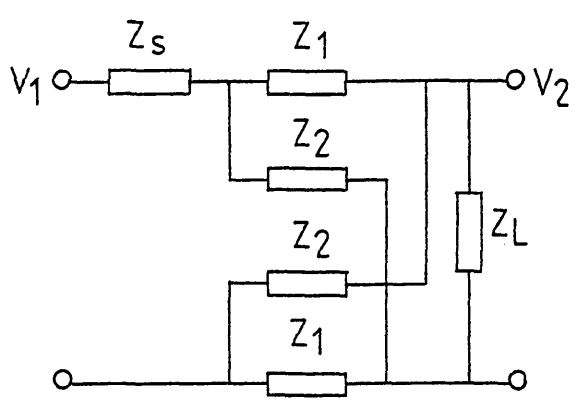
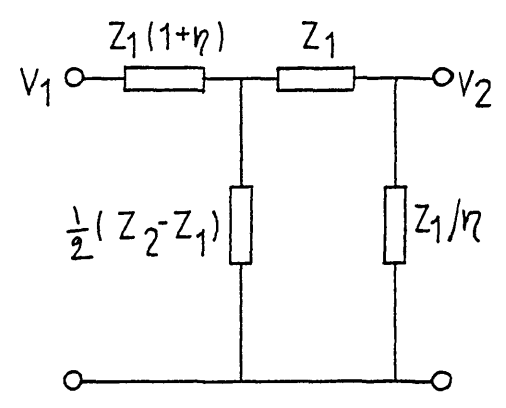


Fig. 3.5 symmetrical lattice circuit with terminating impedances.



$$T = \frac{Z_2 - Z_1}{(1 + \eta)^2 (Z_2 + Z_1)}$$

Fig. 3.6

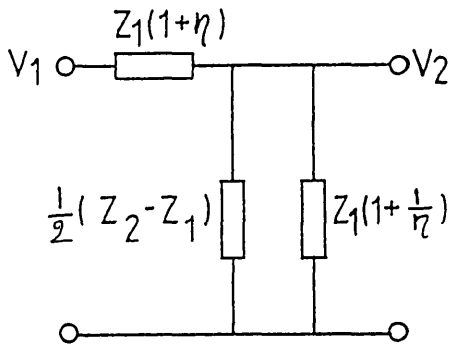


Fig. 3.7

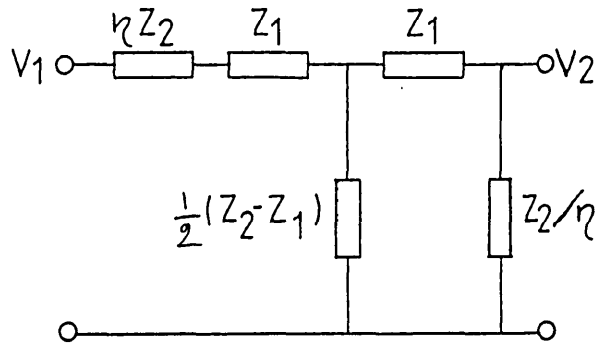
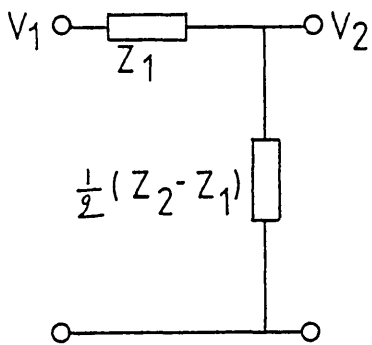
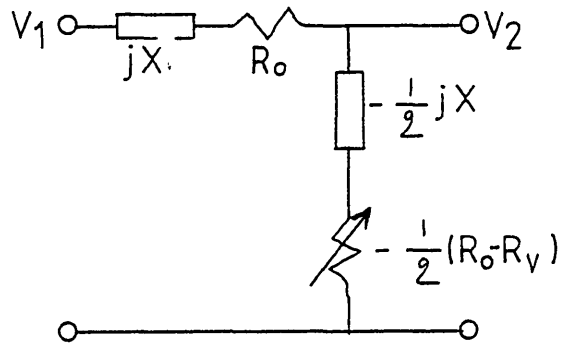


Fig. 3.8



$$T = \frac{Z_2 - Z_1}{Z_2 + Z_1}$$

Fig. 3.9



$$-R_o < R_v < R_o$$

Fig. 3.10

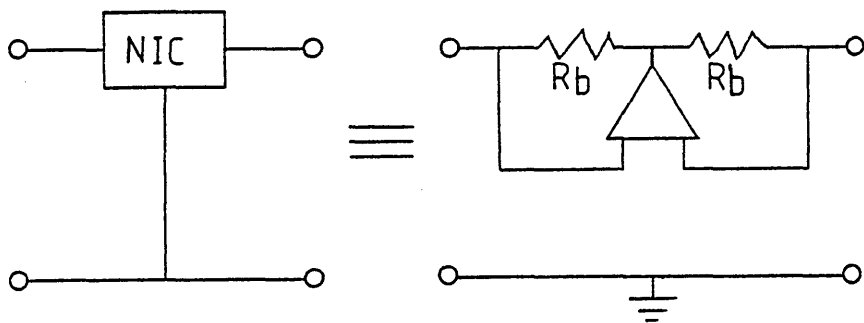


Fig. 3.11 negative impedance converter.

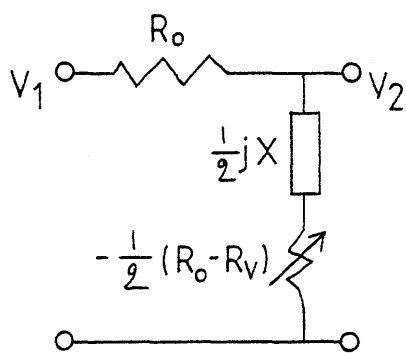


Fig. 3.12 quasi Bode-type VE.

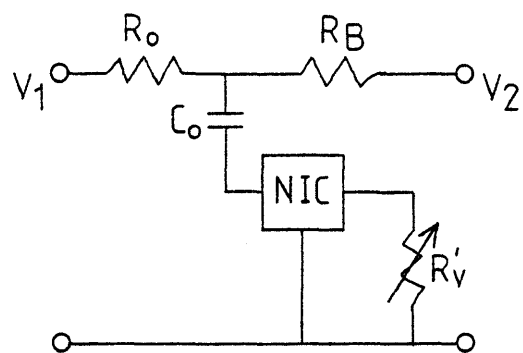


Fig. 3.13

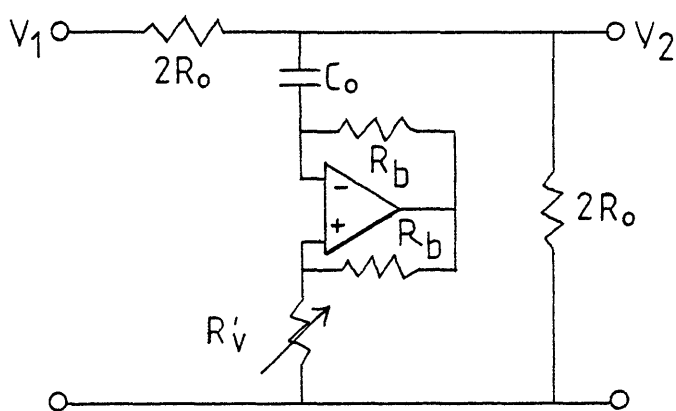


Fig. 3.14 $0 < R'_v < R_o$

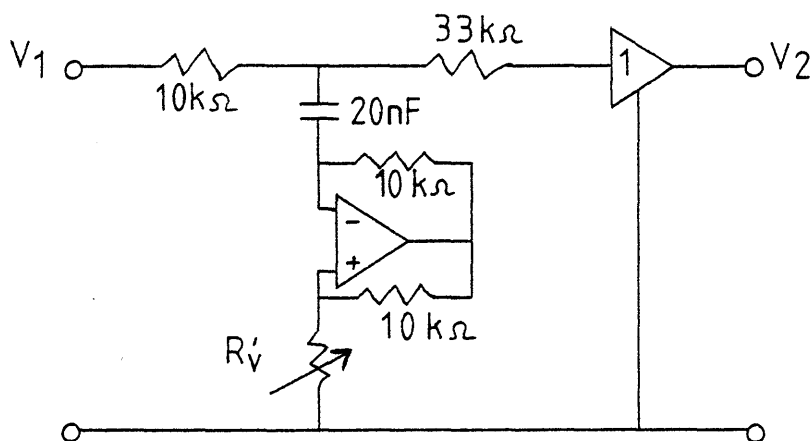


Fig. 3.15 experimental quasi Bode-type VE
op-amp TL 082 CL ($f_T = 3.0$ MHz)

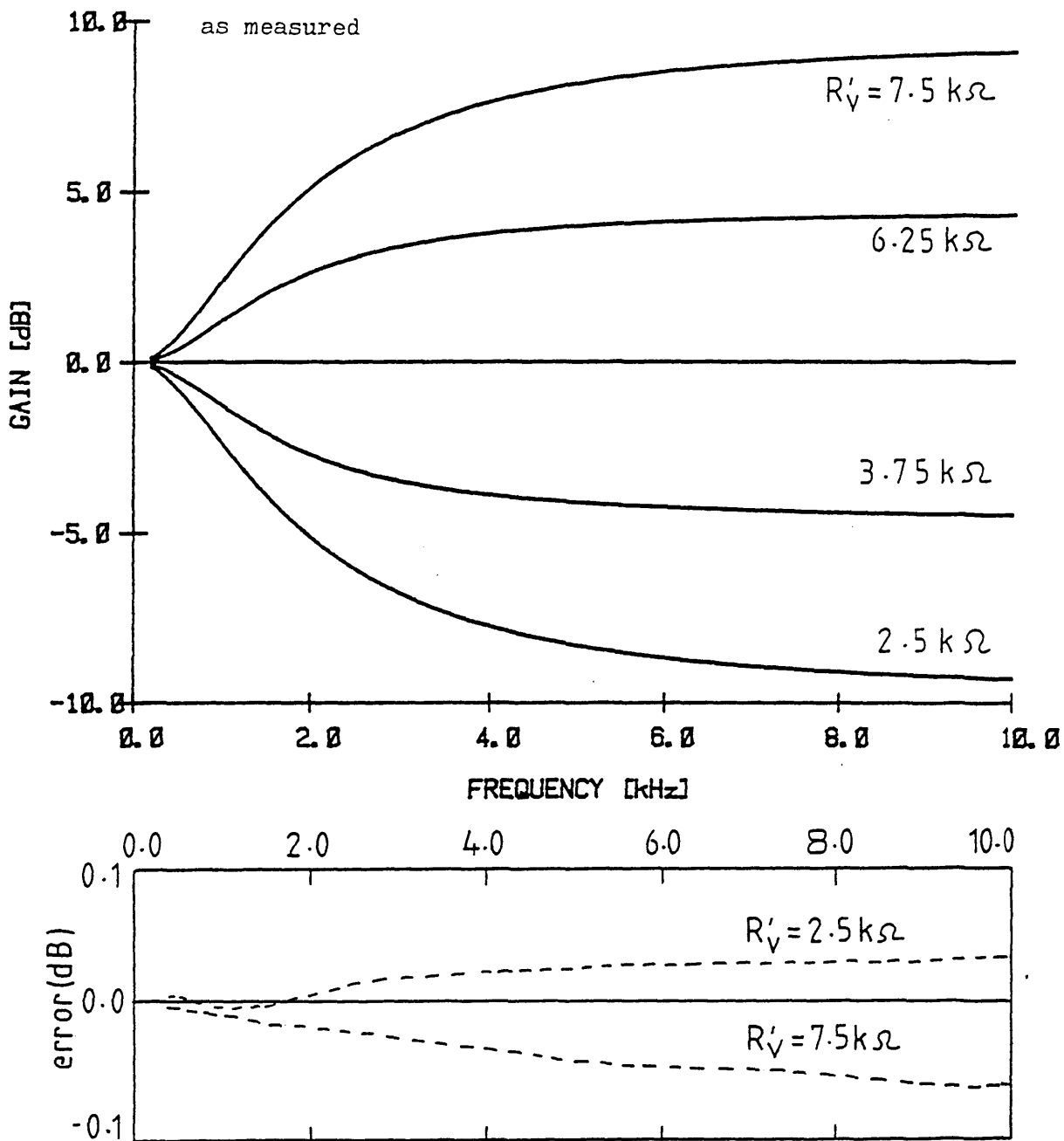


Fig. 3.16 performance evaluation responses of the quasi Bode equaliser in Fig. 3.15.

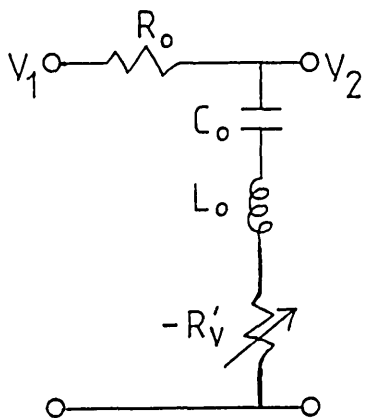


Fig. 3.17 basic quasi bump equaliser.

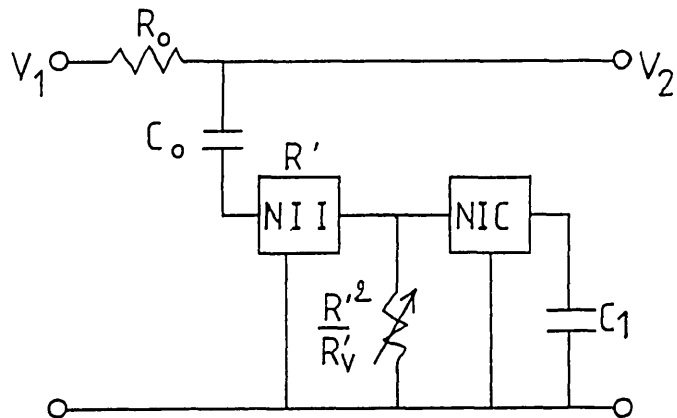


Fig. 3.18a

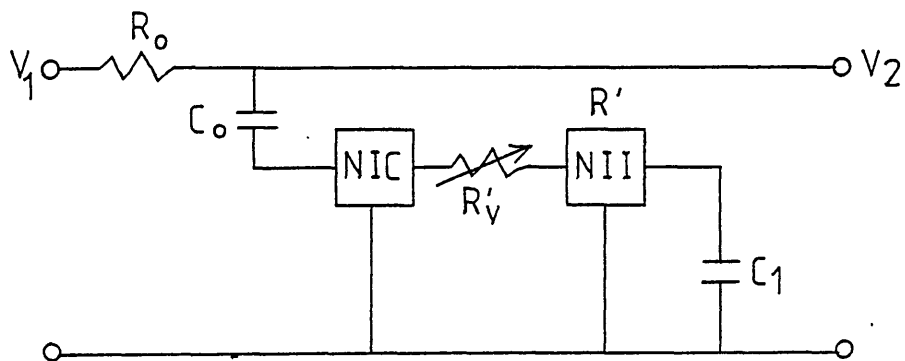


Fig. 3.18b

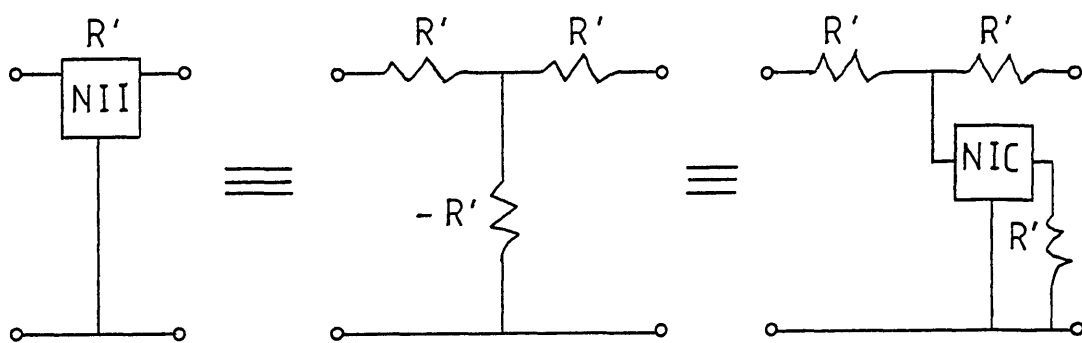


Fig. 3.19 negative impedance inverter.

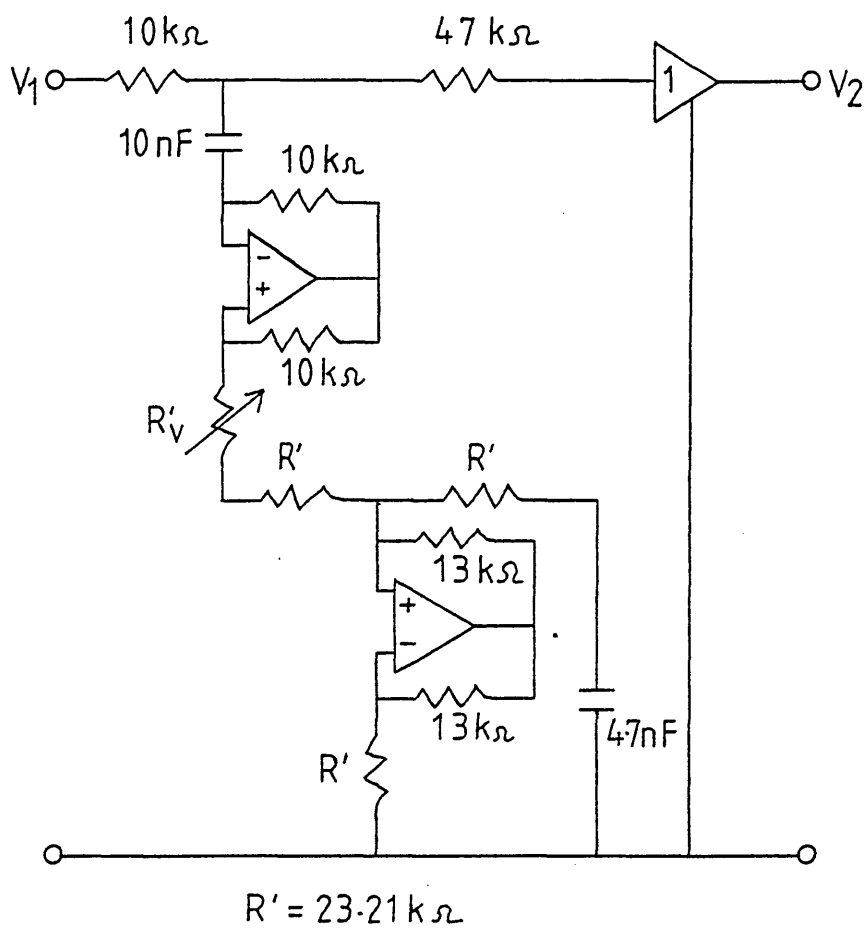


Fig. 3.20 experimental quasi bump equaliser based on the circuit in Fig. 3.18b, op-amps HA-2605-5 ($f_T = 12 \text{ MHz}$)

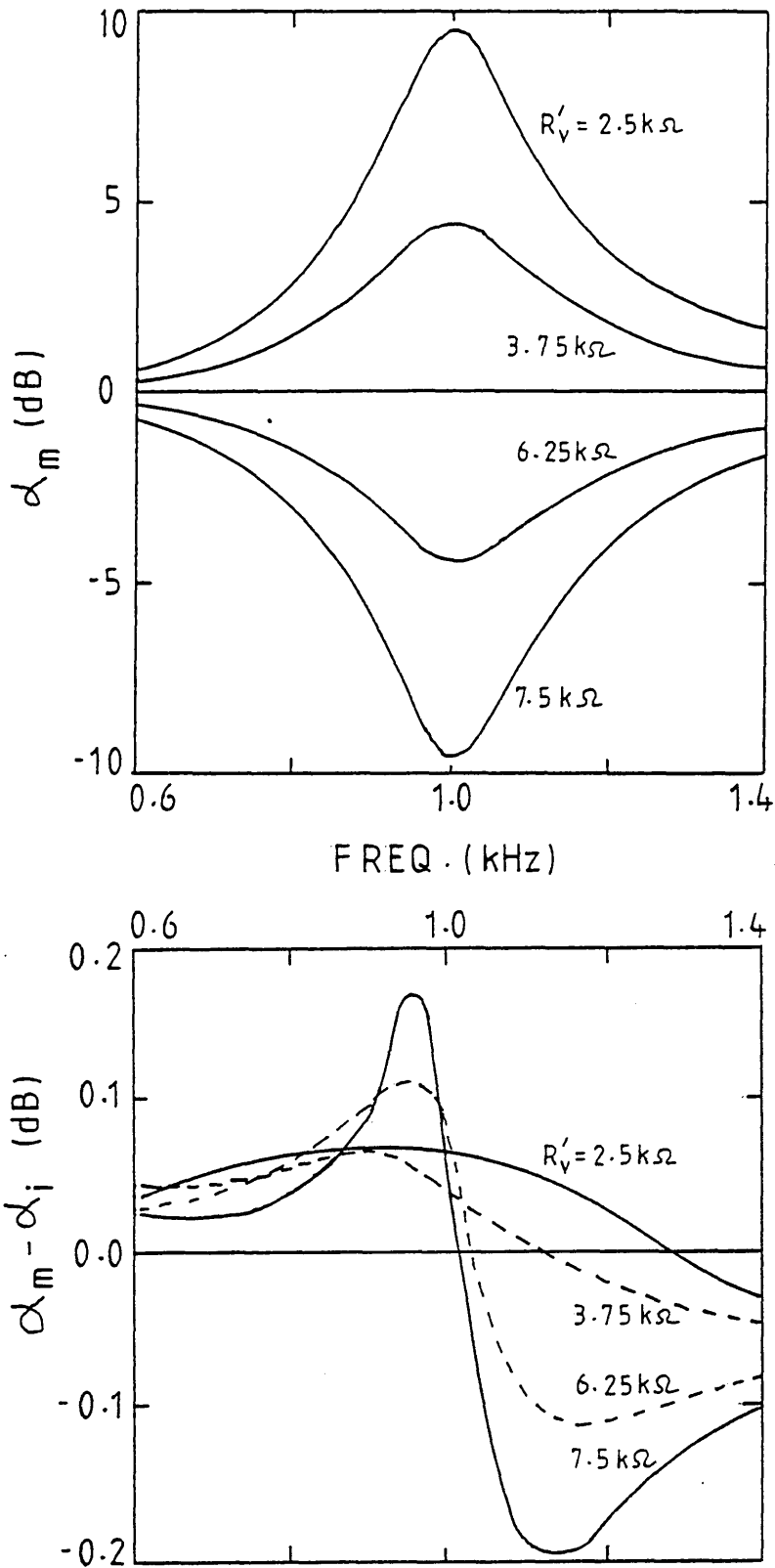


Fig. 3.21 performance evaluation responses of the quasi bump equaliser in Fig. 3.20.

α_m : measured loss

α_n : computed loss assuming ideal op-amps.

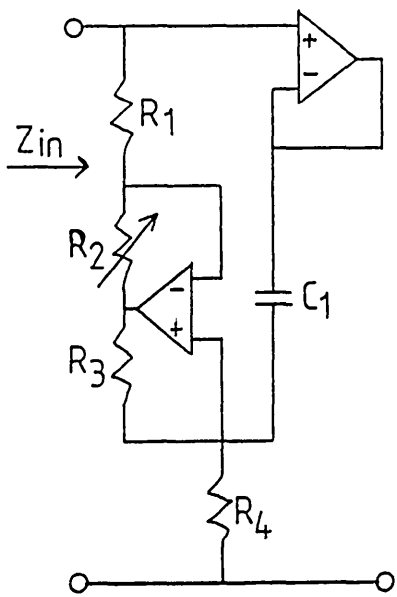


Fig. 3.22

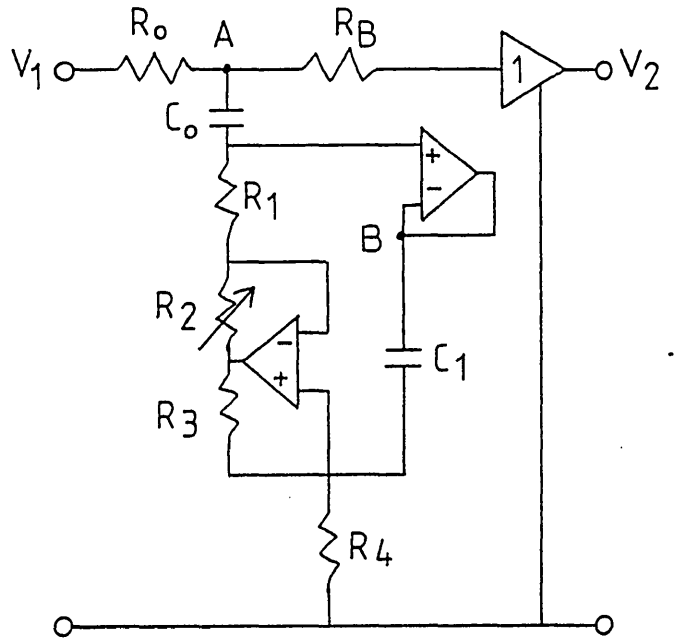


Fig. 3.23

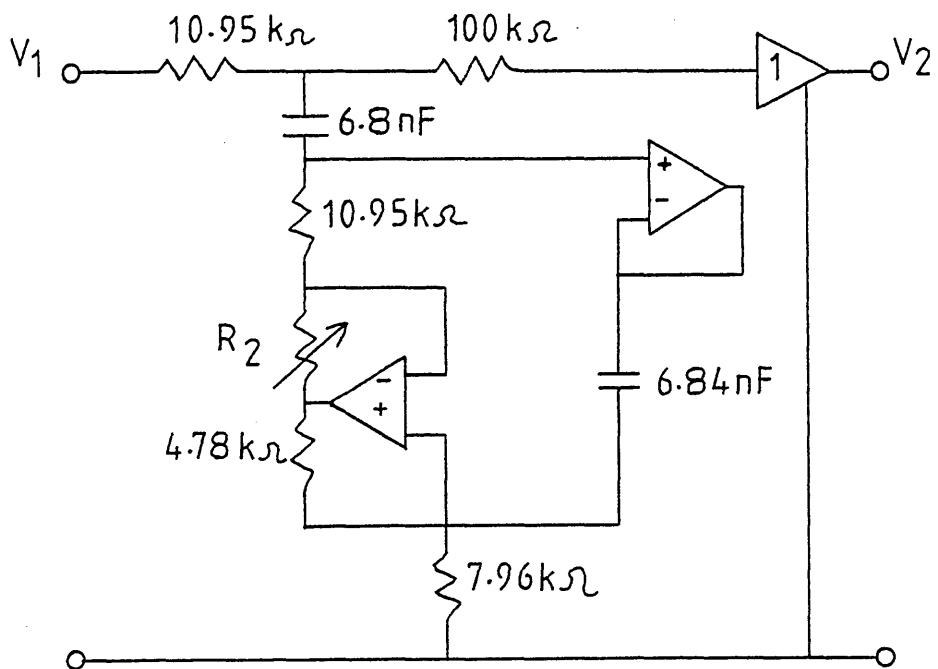


Fig. 3.24 practical quasi Bode-type bump equaliser based on the circuit in Fig. 3.23, op-amps TL 082 CL ($f_T = 3\text{ MHz}$)

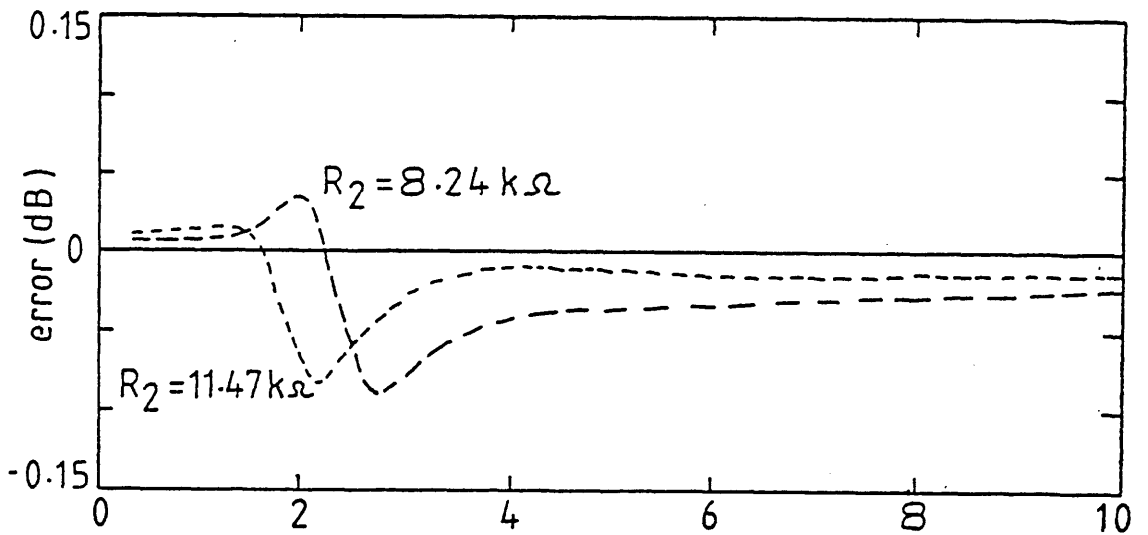
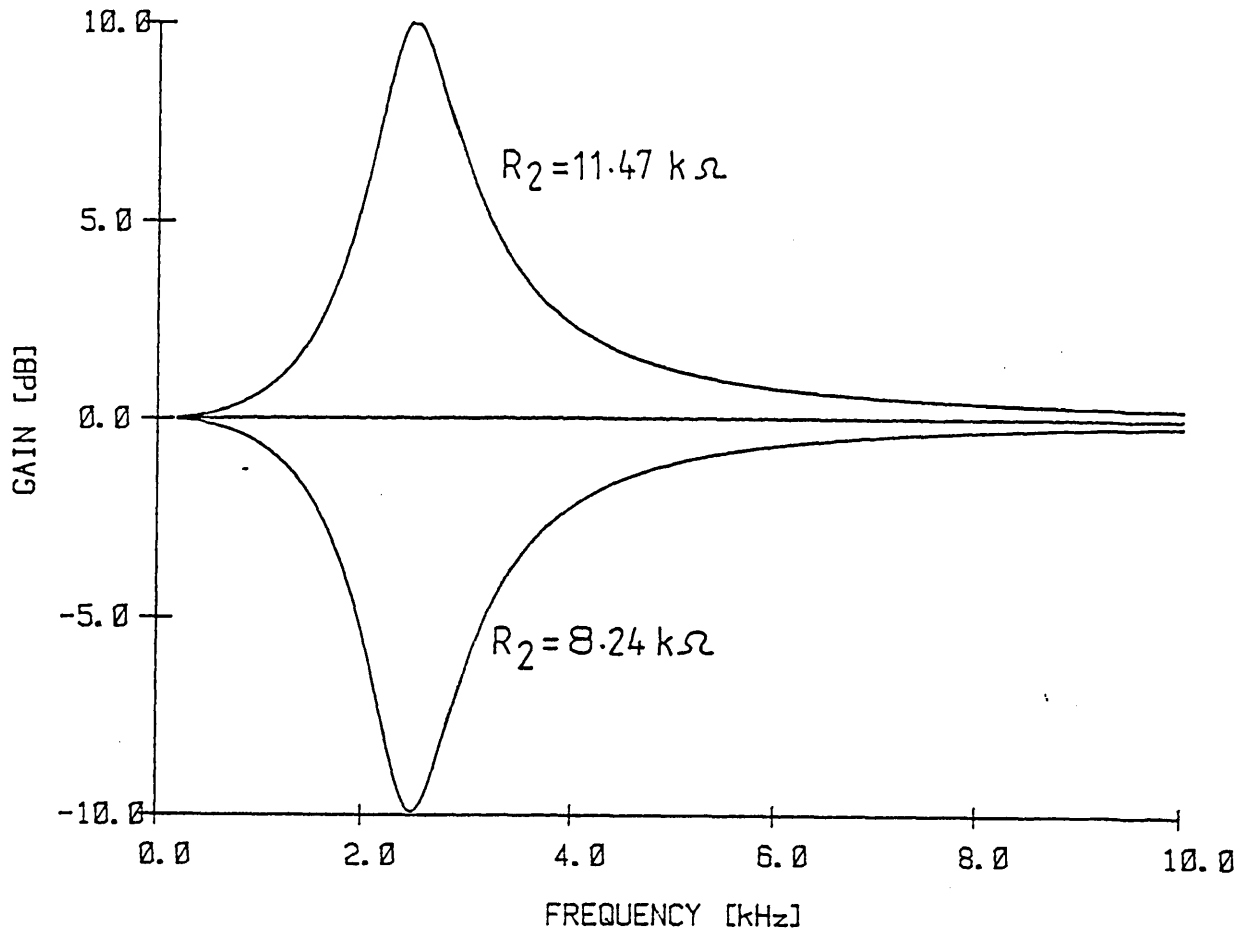


Fig. 3.25 measured frequency response of the circuit in Fig. 3.24 and deviations from the ideal case.

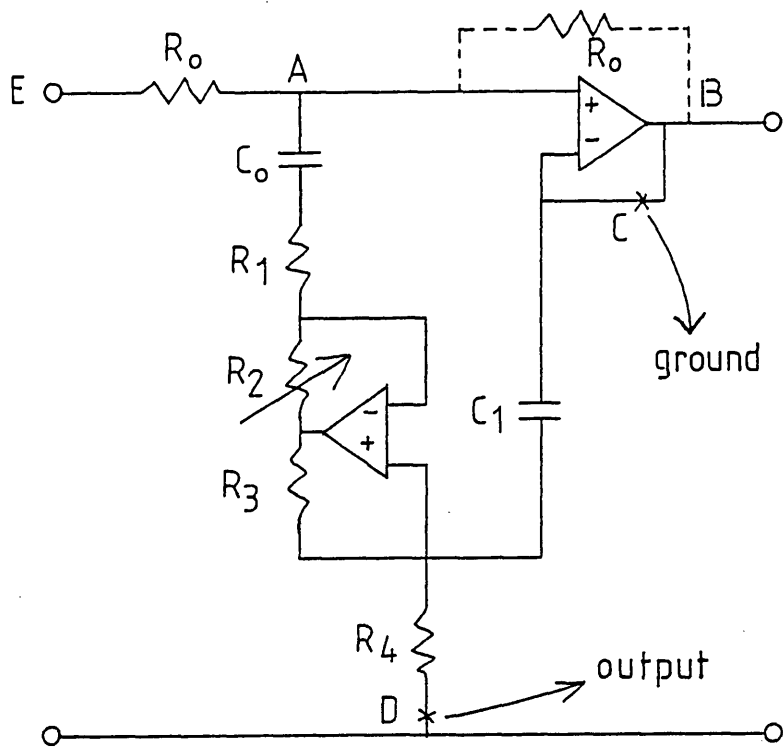


Fig. 3.26

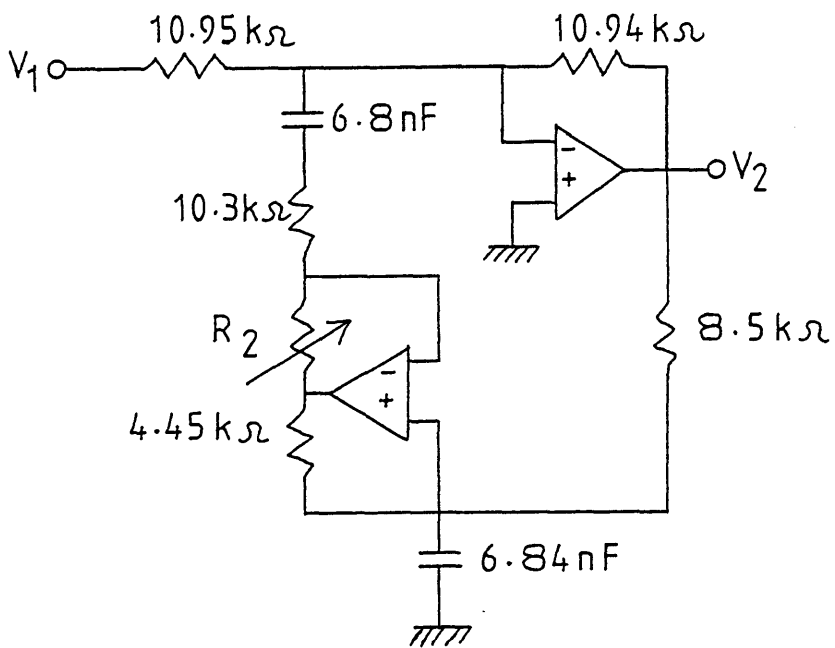


Fig. 3.27 op-amps TL 082 CL ($f_T=3\text{MHz}$)

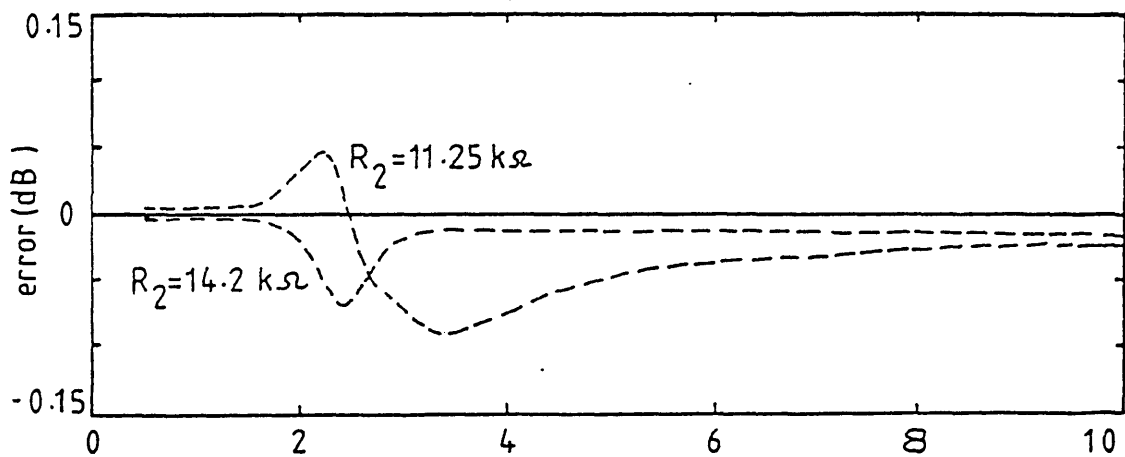
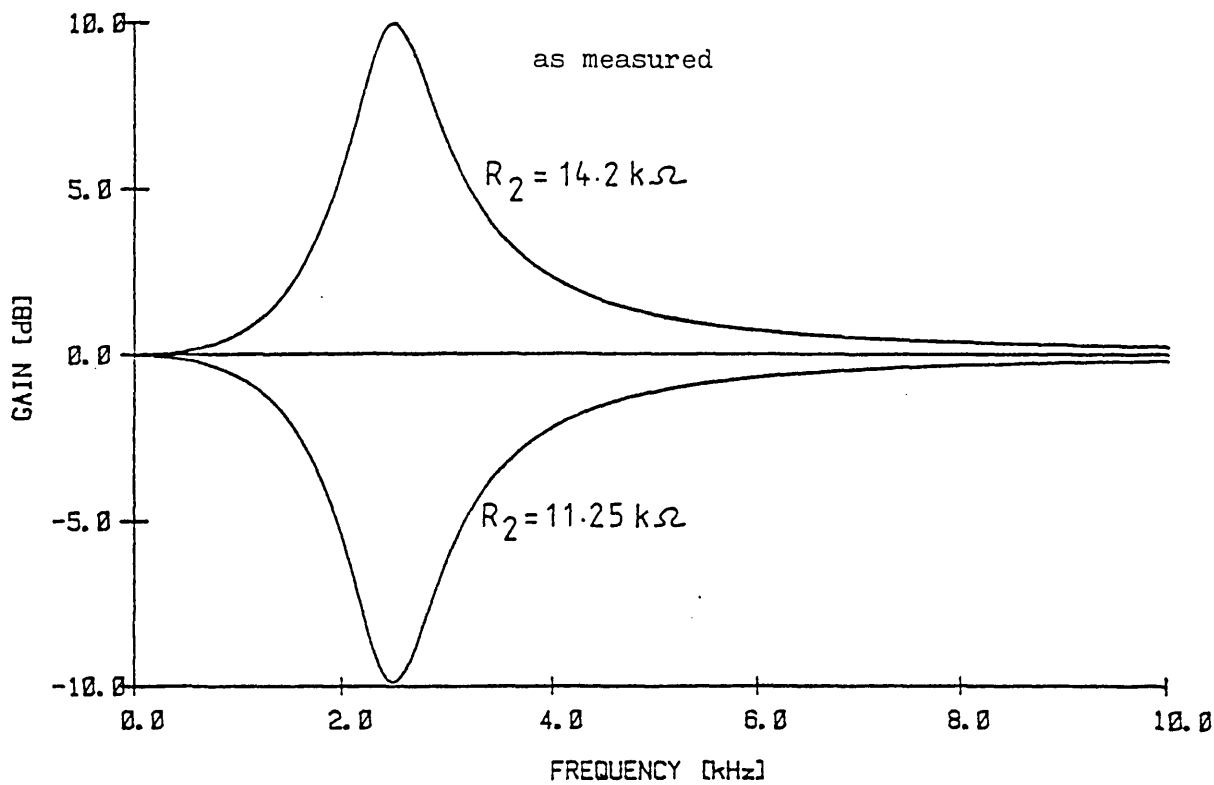


Fig. 3.28 measured frequency response of the quasi bump equaliser in Fig. 3.27 and deviations from the ideal case.

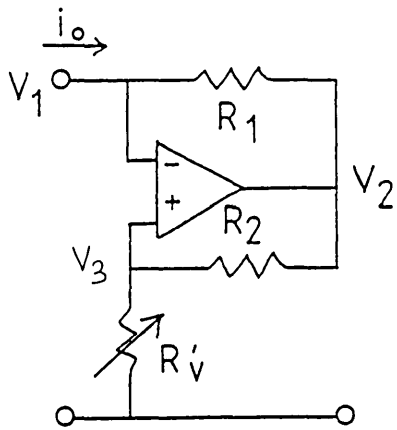


Fig. 3.29

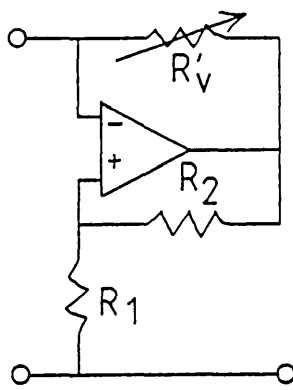


Fig. 3.30

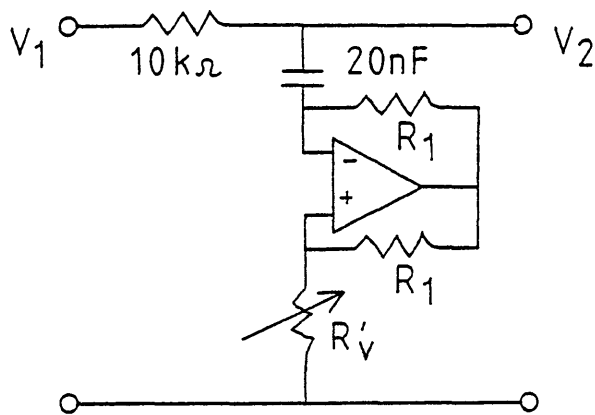


Fig. 3.31a ($f_T = 1\text{ MHz}$)

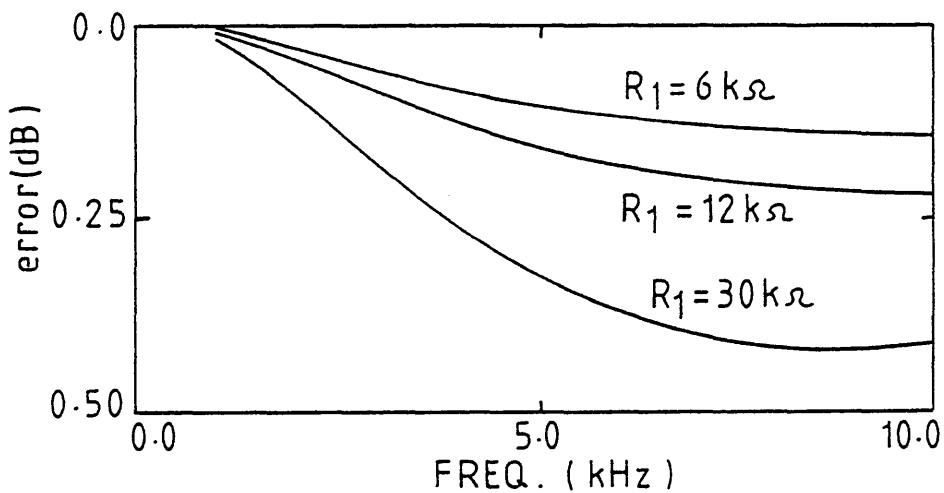


Fig. 3.31b computed deviations for various values of R_1

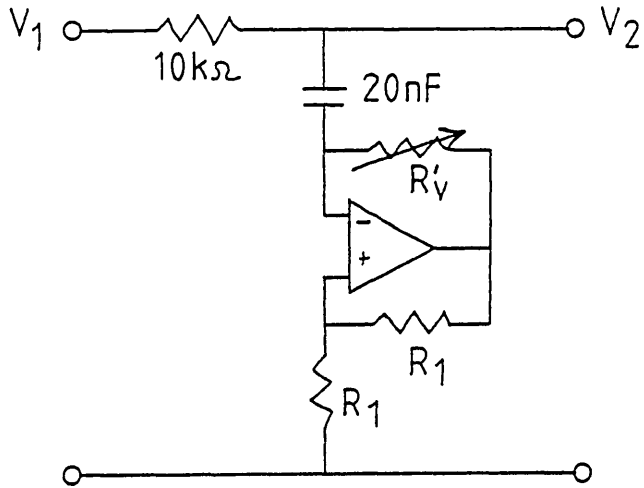


Fig. 3.32a ($f_T = 1\text{MHz}$)

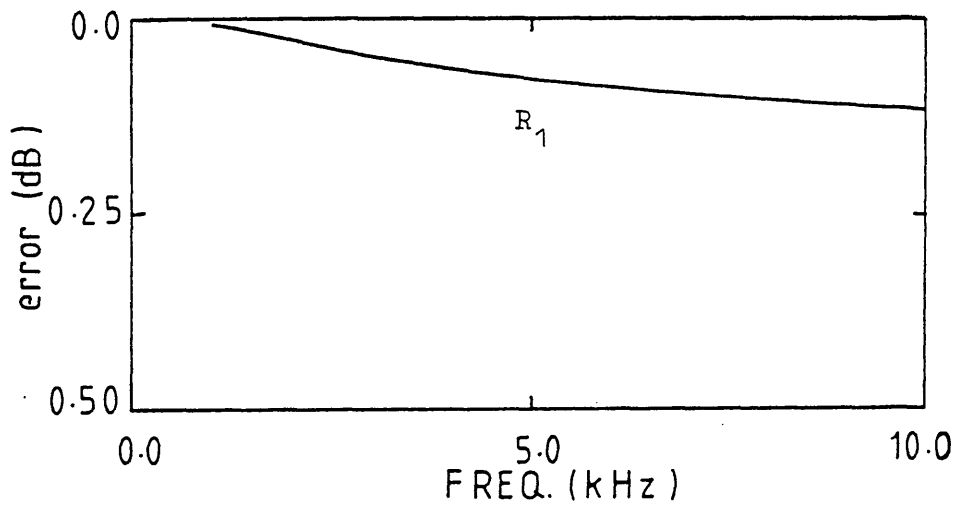


Fig. 3.32b computed deviations for $R_1 = 6, 12, 30\text{k}\Omega$

CHAPTER IV

A BODE EQUALISER USING A SINGLE OP-AMP

- 4.1 Introduction.
- 4.2 The new circuit.
- 4.3 Practical examples.
 - 4.3.1. Fan equaliser.
 - 4.3.2. Bump equaliser.
- 4.4 Discussion.

CHAPTER IV. A BODE EQUALISER USING A SINGLE OP-AMP

4.1 Introduction.

We recall from Chapter 3 that the design of a quasi Bode VE is possible only if the shaping impedance $Z_o(s)$ is purely reactive. The purpose of the present chapter is to show that it is possible to overcome this restriction by deriving a Bode VE from the passive symmetrical lattice circuit of Fig. 3.5 and which uses the same number of op-amps as its corresponding quasi Bode-type VE.

4.2 The new circuit.

Before introducing the steps to be taken in the development of the new VE, let us first give the basic transformations which lead from a T-section circuit to its equivalent Δ -configuration and vice versa

a - Transformation $T \rightarrow \Delta$

The T-section circuit in Fig. 4.1. with impedances Z_A , Z_B and Z_C has a equivalent Δ -configuration with Z'_A , Z'_B and Z'_C where

$$Z'_A = Z_A + Z_B + \frac{Z_A Z_B}{Z_C} \quad (4.1a)$$

$$Z'_B = Z_A + Z_C + \frac{Z_A Z_C}{Z_B} \quad (4.1b)$$

$$Z'_C = Z_B + Z_C + \frac{Z_B Z_C}{Z_A} \quad (4.1c)$$

if $Z_A = Z_B = Z$ we have

$$Z'_A = 2Z + \frac{Z^2}{Z_C} \quad (4.2a)$$

$$Z'_B = Z'_C = Z + 2Z_C \quad (4.2b)$$

b - Transformation $\Delta \rightarrow T$.

The Δ -configuration in Fig. 4.2 has its T equivalent with Z'_A , Z'_B and Z'_C where

$$Z'_A = \frac{Z_A Z_B}{\Sigma Z} \quad (4.3a)$$

$$Z'_B = \frac{Z_A Z_C}{\Sigma Z} \quad (4.3b)$$

$$Z'_C = \frac{Z_B Z_C}{\Sigma Z} \quad (4.3c)$$

with $\Sigma Z = Z_A + Z_B + Z_C$.

Consider now the symmetrical lattice circuit in Fig. 3.5. Its T-equivalent (for $\eta = 0$ and $Z_1 = R_v$, $Z_2 = R_o + 2Z_o$) is shown in Fig. 4.3 which, since it has an open circuit output, can be replaced by the inverted-L circuit as in Fig. 4.4. Although the circuit satisfies Bode's transfer function, it is very impracticable because it needs two variable resistors. One resistor R_v varies from $-R_o$ to $+R_o$, and the other one R'_v varies from 0 to $+R_o$, therefore the adjustment of this equaliser could be only acceptable in the case of manual control.

Let us reconsider now the circuit in Fig. 4.3. which, at first sight, seems to be very unattractive. But let us find the Δ -configuration corresponding to the T-configuration between nodes ABC. Equations (4.2a) and (4.2b) give

$$Z'_A = 2R_v + \frac{R_v^2}{\frac{1}{2}(R_o - R_v)} = \frac{(-2R_o)(2R_v)}{2R_v - 2R_o} \quad (4.4a)$$

$$Z'_B = Z'_C = R_o \quad (4.4.b)$$

Z'_A represents a resistor $2R_v$ in parallel with $-2R_o$; and we know that R_v varies between $-R_o$ and $+R_o$. This would require for the design of Z'_A at least two NICs which is not desirable. The solution lies in the fact that for the whole range of variation of R_v , the corresponding range of Z'_A is between $-R_o$ and ∞ . If we write Z'_A in the following form

$$Z'_A = -R_o + R''_v$$

we get the network in Fig. 4.5 in which the range of Z'_A remains unchanged when R''_v is positive and varies from 0 to ∞ . The problem now is to realise the floating negative resistor ($-R_o$) in series with R''_v . This can be achieved by inserting R_o between two NICs; but if the circuit is driven from a grounded voltage source only a single NIC is needed. The final VE is shown in Fig. 4.6 which has a voltage transfer function

$$T(s) = \frac{Z_o(s) (R_o + R''_v) + R_o^2}{Z_o(s) (R_o + R''_v) + R_o R''_v} \quad (4.5)$$

It is a Bode transfer function (1.7) with $M=1$,
 $\gamma = R''_v/R_o$ and $H(s) = \frac{Z_o(s)}{Z_o(s)+R_o}$

This circuit requires only one op-amp to achieve the whole operation of a Bode-type VE. It does not need a circuit modifying switch nor extra basic op-amps. However, it requires an additional buffer output amplifier. In general buffer amplifiers do not contribute to the circuit performance deterioration caused by the gain bandwidth product

f_T being finite (this is no longer valid at frequencies far above the working frequency range). Therefore we can say that a network which requires an output buffer amplifier is, in general, to be preferred to the alternative circuits requiring an op-amp as a circuit element.

In order to test the stability of the circuit let us write the expressions of its input and output impedances.

The input impedance is given by

$$Z_{in}(s) = Z_o(s) + \frac{k}{k+1} R_o \quad (4.6)$$

$$k = R''_V/R_o$$

and when the input is short circuited, the output impedance is given by.

$$Z_{out}(s) = (k-1) R_o \frac{2Z_o + R_o}{Z_o(k+1) + kR_o} \quad (4.7)$$

Equation (4.7) shows that the circuit is potentially unstable for $k < 1$ because $\text{Re}[Z_{out}(s)] < 0$. In a practical realisation we came across this problem of stability. Whenever k is less than 1 the circuit starts to oscillate. To ensure an absolute stability we add a resistor R_B of a suitable value at the output port of the circuit to make the real part of the overall output impedance positive. Thus, if Z_o is a capacitor C_o we have,

$$R_e [Z_{out}(s)] = R_o (k-1) \frac{2(k+1) + k R_o^2 C_o^2 w^2}{(k+1)^2 + (k R_o C_o w)^2} \quad (4.8)$$

and R_B should satisfy (4.9)

$$R_B > R_o (1-k) \frac{2(k+1) + k R_o^2 C_o^2 w^2}{(k+1)^2 + (k R_o C_o w)^2} \quad (4.9a)$$

at all frequencies a satisfactory R_B is given by

$$R_B > R_o \frac{1-k}{k}, \quad (k < 1) \quad (4.9b)$$

(4.9b) shows that the circuit can never be stable for $k=0$. But in practice k does not reach zero; for example to get a gain of about 20 dB at high frequencies, k should be about 0.1. In this case $R_B = 10 R_o$ is satisfactory.

4.3 Practical examples.

The circuit in Fig. 4.6 has been used for designing and testing both a fan and a bump equaliser [23].

4.3.1. Fan equaliser.

In this example Z_o is a capacitor C_o with a measured value 20.08 nF and $R_o = 10.66 \text{ k}\Omega$. The practical circuit is shown in Fig. 4.7; it is designed to provide ± 10 dB loss variation at an upper frequency of 10 KHz for four settings of R_v'' . The minimum value of R_v'' to get this ± 10 dB loss variation is $3.56 \text{ k}\Omega$; in order to ensure the stability of the circuit R_B should satisfy (4.9b), thus

$$R_B > 21.26 \text{ k}\Omega$$

we have chosen $24 \text{ k}\Omega$ which is satisfactory. The measured responses and their deviations from the ideal ones are shown in Fig. 4.8; where α_m is the measured loss and α_n is the computed loss assuming that the op-amp is ideal. The effect of the amplifier finite gain bandwidth product will be compared, in chapter 6, with non-ideal characteristics of the other VEs.

4.3.2. Bump equaliser.

We have seen in the previous chapters that a variable bump equaliser has a biquadratic transfer function of the form given by (2.8). The transfer function (4.5) of the network in Fig. 4.6 is of this form when

$$Z_o(s) = R_q + R' + j[\omega L_o - 1/(\omega C_o)] \quad (4.10)$$

where R_q represents a resistor by which the sharpness of the bump is adjusted and R' the equivalent resistor of a lossy inductor which can be simulated by an active RC circuit using one op-amp. Among the variety of those circuits we have to find a suitable one for our purpose. For reasons that will become obvious at the end of this section, it is preferable to use a simulated inductor in which $R' = 0$. However, the available single amplifier simulated inductor circuits which satisfy this condition are not easily adjustable. The example [24] of the circuit shown in Fig. 4.9 illustrates this fact. By straightforward analysis we find that if the following conditions are satisfied

$$R_2 = \frac{R_3 R_5 R_6}{R_4 (R_3 + R_6)} \quad (4.11a)$$

$$R_1 = R_5 R_6 / R_3 \quad (4.11b)$$

then the equivalent inductance is given by

$$L_o = C_o \frac{R_1 R_2 R_3 R_5 R_6^2}{R_2 R_4 (R_1 R_3 + R_3 R_4 + R_4 R_6 + R_6 R_3)} \quad (4.11c)$$

This shows that the adjustment of L_o can never be achieved by a single resistor without violating (4.11a) and (4.11b); this is also valid for the network in ref. [25]. Since the use of simulated lossy inductors becomes inevitable, let us then investigate some of those circuits.

The Prescott circuit [26] shown in Fig. 4.10 has the following input impedance

$$Z_{in}(s) = R_1 + R_2 + s C_1 R_1 R_2 \quad (4.12)$$

Here, the adjustment of $L_o = C_1 R_1 R_2$ can be achieved by a single resistor (R_1 or R_2). However, if this circuit is used in the design of our bump equaliser, the adjustment of the resonant frequency by R_1 or R_2 will result in a change of $R' = R_1 + R_2$ which will produce a variation in the bump height and this is not desirable.

We shall now show that the single amplifier active RC circuit [27] shown in Fig. 4.11 can be, in practice, satisfactory. Its input impedance is given by

$$Z_{in}(s) = R_2 \frac{1 + sC_1 R_1}{1 + sC_1 R_2} \quad (4.13)$$

The equivalent circuit of this input impedance is not unique, but (4.13) can be written in the following form

$$Z_{in}(s) = R_2 \frac{1 + (\omega C_1)^2 R_1 R_2}{1 + (\omega C_1 R_2)^2} + s \frac{C_1 R_2 (R_1 - R_2)}{1 + (\omega C_1 R_2)^2} \quad (4.14)$$

If $R_1 > R_2$, (4.14) can be interpreted as a positive inductance L_o in series with the associated resistance R' where

$$L_o = \frac{C_1 R_2 (R_1 - R_2)}{1 + (\omega C_1 R_2)^2} \quad (4.15a)$$

$$R' = R_2 \frac{1 + (\omega C_1)^2 R_1 R_2}{1 + (\omega C_1 R_2)^2} \quad (4.15b)$$

Both L_o and R' are frequency dependent; but if the circuit is in series with a capacitor $C_o = C_1$ and we assume that the resonant frequency is

$$\omega_o = 1 / C_o \sqrt{R_1 R_2}$$

then

$$L_o = \frac{C_1 R_1 R_2 (1 - \epsilon)}{1 + \epsilon} \quad (4.15c)$$

$$R' = \frac{2 R_2}{1 + \epsilon} \quad (4.15d)$$

where $\epsilon = R_2 / R_1$.

If $R_2 \ll R_1$ we get

$$L_o = C_1 R_1 R_2 \quad (4.15e)$$

$$R' = 2R_2 \quad (4.15f)$$

This is a desirable circuit because L_o can be adjusted by R_1 without changing R' . Expressions (4.15e) and (4.15f) are valid at the resonant frequency and for $\epsilon \ll 1$ with the assumption that the op-amp is ideal.

The circuit in Fig. 4.11 was selected to provide R' and L_o appearing in the expression (4.10) of $Z_o(s)$. It is relevant to point out that the capacitor C_1 should be close to C_o otherwise the above approximations are not valid. This circuit is used also in the next Chapter for designing bump equalisers.

The experimental bump equaliser is shown in Fig. 4.12, its voltage transfer function is given by

$$T(s) = \frac{\left(\frac{s}{w_o}\right)^2 + \left(\frac{s}{w_o}\right)\left(h/Q\right) + 1}{\left(\frac{s}{w_o}\right)^2 + \left(\frac{s}{w_o}\right)\left(1/Q\right) + 1} \quad (4.16a)$$

where $w_o = 1/C_o \sqrt{R_1 R_2}$ (4.16b)

$$h = \frac{(R_q + 2R_2)(1+k) + R_o}{(R_q + 2R_2)(1+k) + kR_o} \quad (4.16c)$$

$$Q = \frac{1+k}{C_o w_o [(R_q + 2R_2)(1+k) + kR_o]} \quad (4.16d)$$

and $k = R''/R_o$.

The Q defined in (4.16d) is different from the practical Q_p , an easily measurable term defined as (Fig. 4.13).

$$Q_p = \frac{w_o}{w_1 - w_2} \quad (4.17)$$

where w_o is the resonant frequency and $(w_1 - w_2)$ is the bandwidth between the two frequencies at which the maximum transmitted signal power is halved (i.e. the signal level is reduced by 3 dB).

In order to find the relationship between Q and Q_p let us write the equation which gives w_1 and w_2 ; from (4.16a) we get

$$\frac{h^2}{2} = \frac{\left[1 - \left(\frac{w}{w_o}\right)^2\right]^2 + \left(\frac{w}{w_o}\right)^2 (h/Q)^2}{\left[1 - \left(\frac{w}{w_o}\right)^2\right]^2 + \left(\frac{w}{w_o}\right)^2 (1/Q)^2} \quad (4.18a)$$

which can be written as

$$\left(\frac{w}{w_o}\right)^4 - \left(\frac{w}{w_o}\right)^2 \left(2 + \frac{h^2}{Q^2(h^2-2)}\right) + 1 = 0 \quad (4.18b)$$

the roots w_1 and w_2 of this equation are related by

$$S = \left(\frac{w_1}{w_o} \right)^2 + \left(\frac{w_2}{w_o} \right)^2 = 2 + \frac{h^2}{Q^2(h^2-2)} \quad (4.18c)$$

$$P = \left(\frac{w_1}{w_o} \right)^2 \cdot \left(\frac{w_2}{w_o} \right)^2 = 1 \quad (4.18d)$$

Inserting (4.18c) and (4.18d) into (4.17) yields.

$$Q_p = \frac{1}{\sqrt{S-2P}} = Q \sqrt{1 - \frac{2}{h^2}} \quad (4.19)$$

(4.19) shows that Q and Q_p are not equal; combining this expression with (4.16c) and (4.16d) we get

$$Q_p = \frac{(1+k) \sqrt{h^2-2}}{C_o w_o [(R_q + 2R_2)(1+k) + R_o]} \quad (4.20)$$

which gives the value of the practical Q_p in terms of the elements of the bump equaliser.

Returning to the expression of w_o (4.16b), we see that the resonant frequency can be adjusted by means of R_1 without affecting the height h (4.16c) or the sharpness of the bump (4.16d) and (4.20). The last two parameters are adjusted by means of k (i.e. R_v'') and R_q respectively. However, as shown by (4.16c) and (4.16d), any adjustment of the height h by k leads to a variation in Q , and the adjustment of Q by R_q affects the height h .

Let us now find the conditions to be satisfied in order to yield a bump with prescribed h and Q at a resonant frequency w_o . The combination of (4.16c) and (4.16d) gives

$$k = \frac{Q R_o C_o w_o + 1 - h}{Q R_o C_o w_o + h - 1} \quad (4.21a)$$

$$R_q = \frac{1+h}{2QC_o w_o} - \frac{R_o + 4R_2}{2} \quad (4.21b)$$

In the case where $h > 1$ which corresponds to $k < 1$, the frequency response of the VE corresponds to having a gain. To make sure that k and R_q are always positive we should have

$$Q \geq \frac{h-1}{R_o C_o w_o} \quad (4.21c)$$

and

$$Q \leq \frac{1+h}{(R_o + 4R_2) C_o w_o} \quad (4.21d)$$

which can be written

$$\frac{h-1}{R_o C_o w_o} \leq Q \leq \frac{1+h}{(R_o + 4R_2) C_o w_o} \quad (4.21e)$$

This shows that once the height h is chosen, Q is within limits; in order to increase the range of Q , it is advisable to choose $R_2 \ll R_o$ or at least to satisfy the following condition

$$R_2 < \frac{R_o}{2(h-1)} \quad (4.21f)$$

The bump equaliser in Fig. 4.12 was built to produce a maximum amplitude range of about ± 10 dB at a resonant frequency $f_o = 1 \text{ KH}_z$. R_q is chosen to be equal to zero and we have a Q (4.16d)

of about 5.22 which corresponds to a practical Q_p of 4.6. The measured loss-frequency responses and their deviations from the computed ones assuming ideal op-amps, are shown in Fig. 4.14. The stability of the circuit is ensured by the buffer output resistor $R_B = 68 \text{ k}\Omega$.

In practice, the lossy inductor used can be replaced by any simulated inductance using one or two op-amps, depending on the required value of its Q . It is important to mention that a very wide range of variation of k is not desirable. This could be the case if the equivalent resistance of the simulated lossy inductor is not small enough. This can be explained by investigation of equation (4.16c). For simplicity we set $R_q = 0$, in this case the values of k and k' corresponding to a pair of symmetrical loss-frequency characteristics are given by

$$k = \frac{R_o + 2(1-h)R_2}{hR_o + 2(h-1)R_2} \quad (4.22a)$$

$$k' = \frac{hR_o + 2(h-1)R_2}{R_o + 2(1-h)R_2} \quad (4.22b)$$

These equations are reciprocal and the change of h to $1/h$ leads from one of them to the other. If $h > 1$ then $k < 1$ and decreases when R_2 increases and it is equal to zero when $R_2 = R_o/2(h-1)$. On the other hand $k' > 1$ and increases rapidly when R_2 increases. Thus the minimum spread is obtainable for $R_2 = 0$ and it is infinity when R_2 reaches $R_o/2(h-1)$. In the case of the experimental

circuit (Fig. 4.12), the + 10 dB loss is obtained for $R_V'' = 1.2 \text{ k}\Omega$ and $55.83 \text{ k}\Omega$; if we had $R_2=0$ we would have $R_V'' = 2.73 \text{ k}\Omega$ and $24.55 \text{ k}\Omega$.

4.4 Discussion.

In this chapter a Bode-type VE structure has been presented. It is derived from a passive symmetrical lattice network and has the advantage of not introducing extra positive phase shift unlike the quasi Bode equaliser discussed in chapter 3. Both the structures introduced in the present chapter and the previous one require a buffer amplifier at the output; and in order to avoid a tendency to instability in the input of this buffer amplifier, it is advisable to ensure that the real part of the output impedance of the VE is always positive. This is easily achieved by providing a series buffer resistance R_B of suitable value between the VE output and the buffer amplifier input.

As far as the shaping impedance $Z_o(s)$ is concerned we have removed its restriction to being a purely reactive impedance and the structure in Fig. 4.6 can deal with any general shaping impedance.

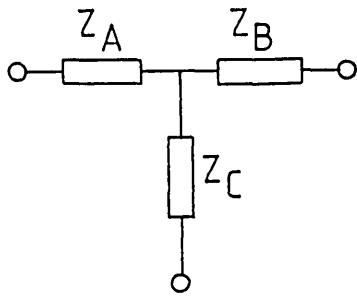


Fig. 4.1 T-configuration.

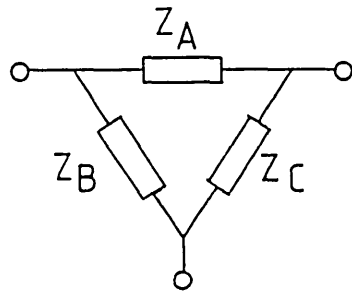


Fig. 4.2 Δ -configuration.

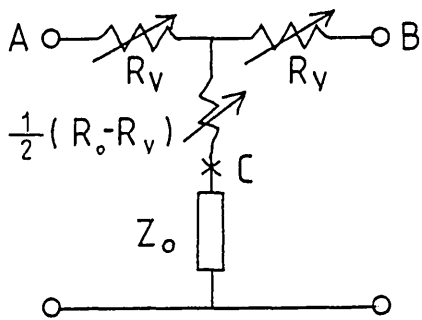


Fig. 4.3

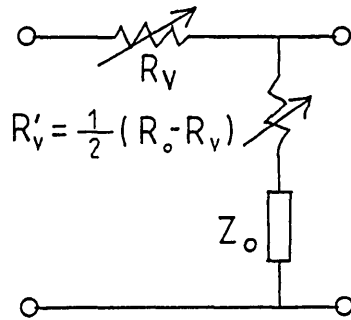


Fig. 4.4

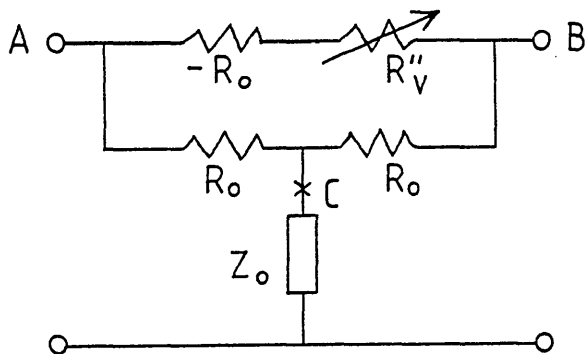


Fig. 4.5 VE equivalent to the T-section circuit given in Fig. 4.3

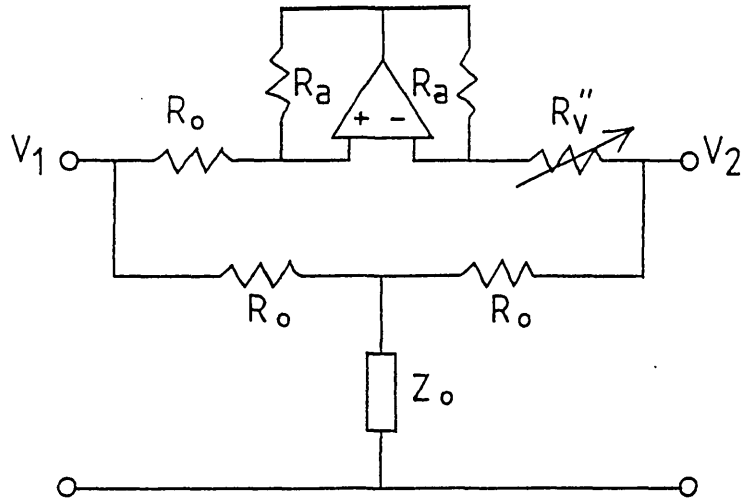


Fig. 4.6 realisation of the negative resistor of the circuit in Fig. 4.5 by a negative impedance converter.

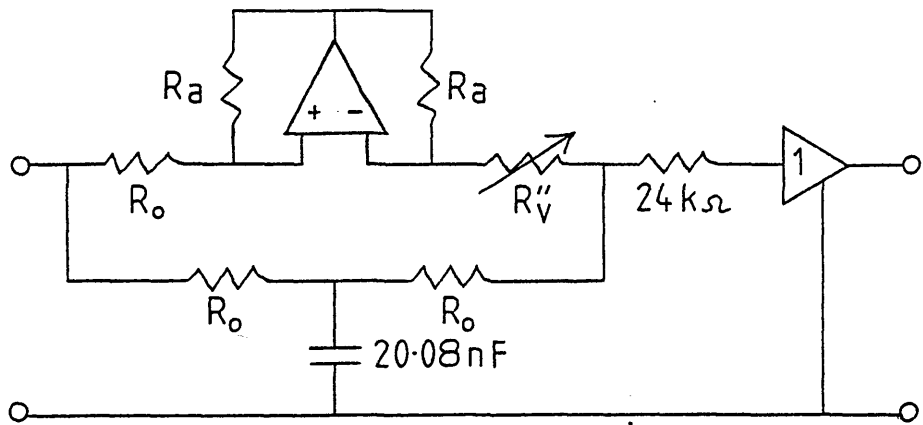


Fig. 4.7 $R_o=R_a=10.66\text{ k}\Omega$ (op-amp AD 518 JH, $f_T=12\text{ MHz}$)

Fig. 4.7 fan equaliser based on the circuit in Fig. 4.6

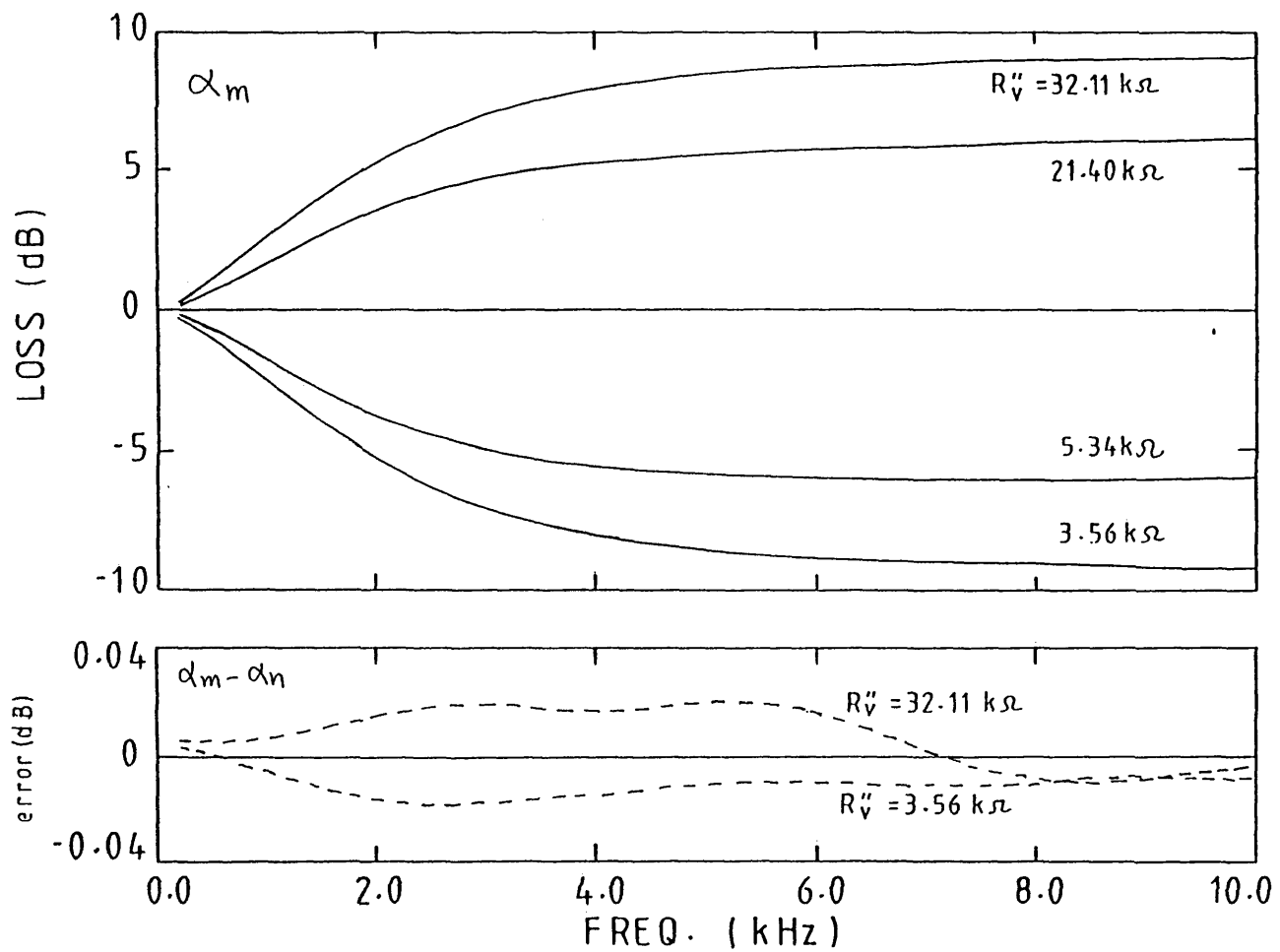


Fig. 4.8 measured frequency response of the circuit in Fig. 4.7 and deviations from the ideal case

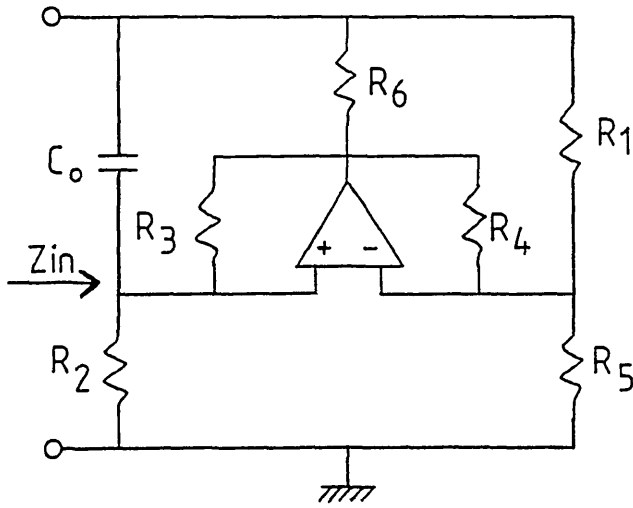


Fig. 4.9 example of simulation of an ideal inductor by a circuit using a single op-amp.

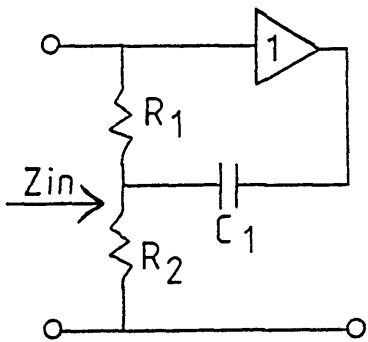


Fig. 4.10 Prescott's circuit.

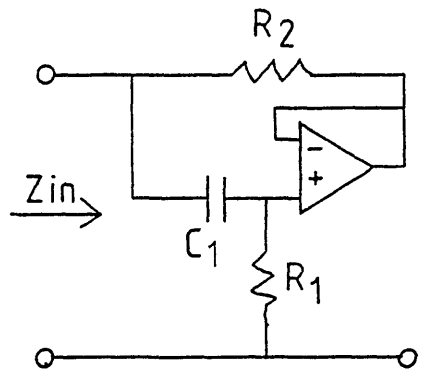


Fig. 4.11 Dutta Roy's circuit.

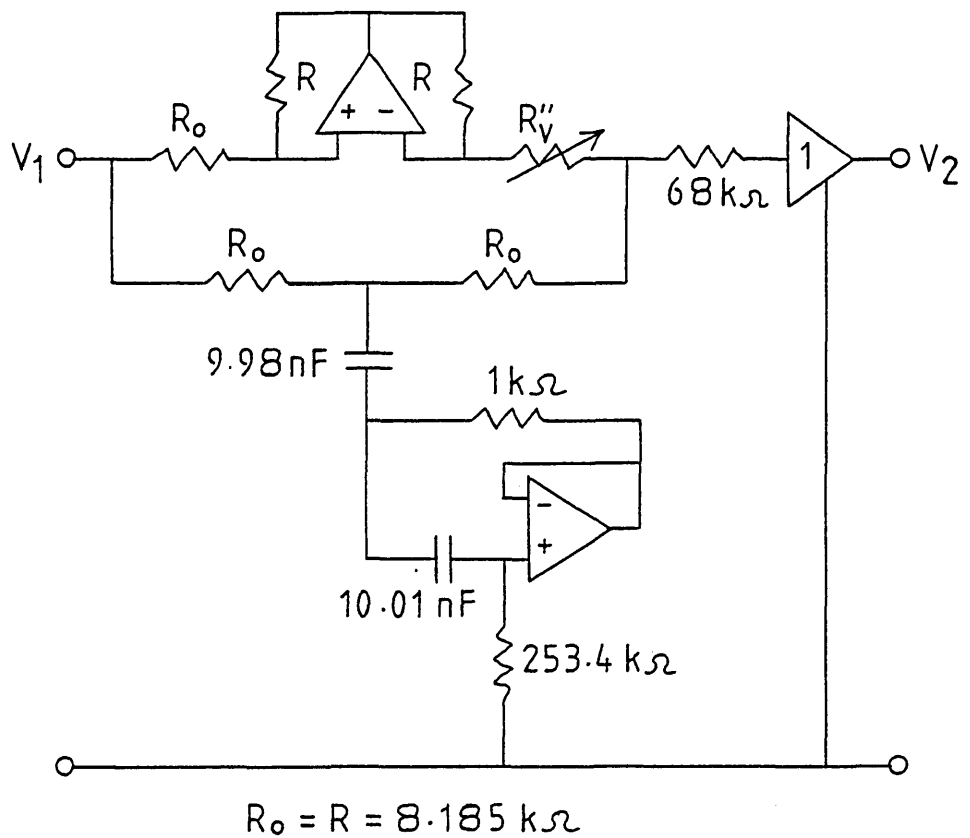


Fig. 4.12 experimental bump equaliser using the non-ideal simulated inductor in Fig. 4.11 (op-amps AD 518 JH $f_T = 12 \text{ MHz}$)

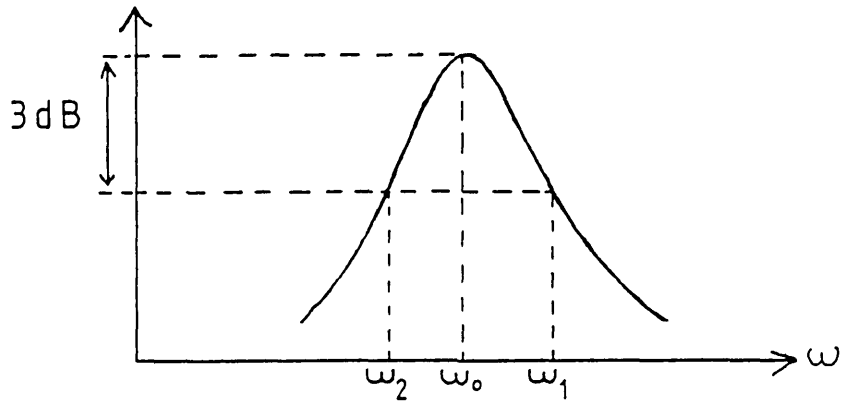


Figure 4.13

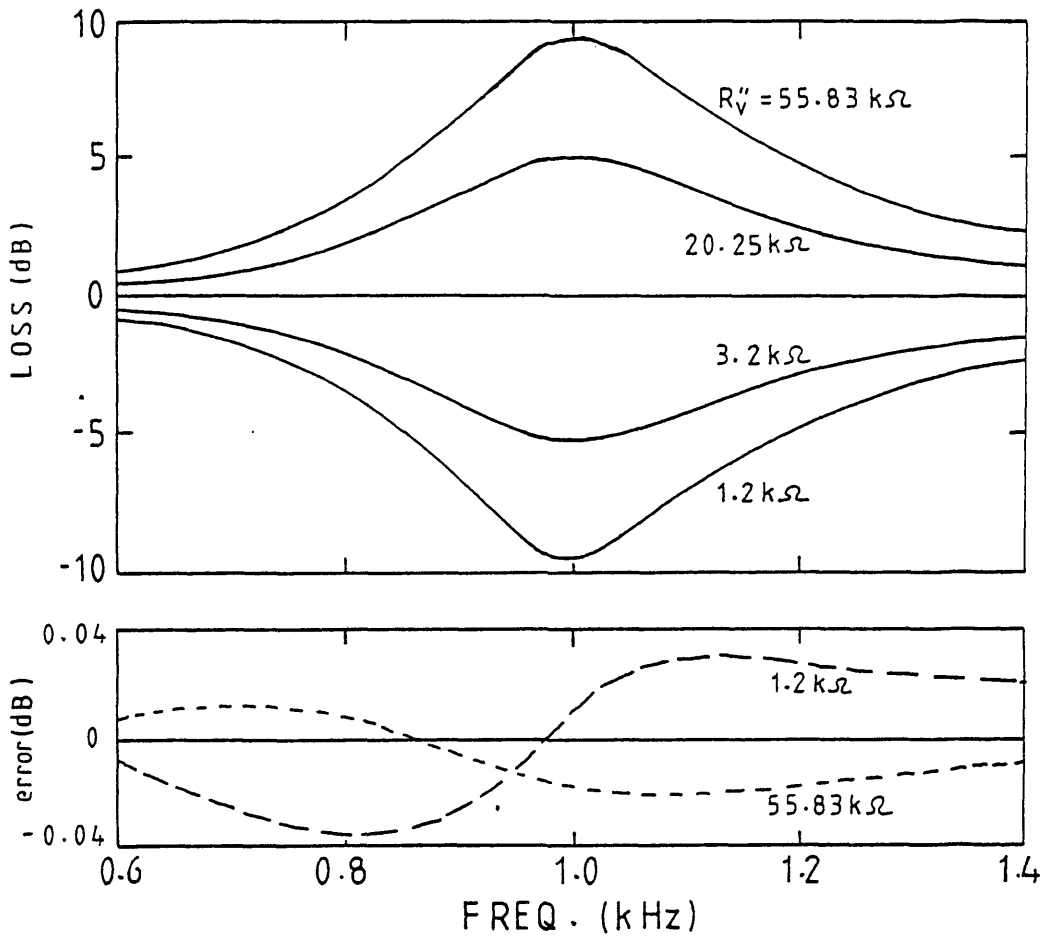


Fig. 4.14 measured frequency response of the practical bump equaliser in Fig. 4.12 and deviations from the ideal case (the error represents the difference between the measured loss and the computed loss assuming ideal op-amps).

CHAPTER V

A NEW BASIC DESIGN FOR BODE EQUALISERS

- 5.1 Introduction.
- 5.2 The basic network.
- 5.3 Some active network transformations by terminal interchange.
 - 5.3.1. Transformation A.
 - 5.3.2. Transformation B.
- 5.4 VEs derived from the basic network by terminal interchange.
- 5.5 VE with a prescribed maximum range of variation of the variable resistor.
- 5.6 A design with a grounded variable resistor.
- 5.7 Some practical results.
- 5.8 Conclusion.

CHAPTER V. A NEW BASIC DESIGN FOR BODE EQUALISERS.

5.1. Introduction.

In the previous chapters we introduced quite a number of Bode-type and quasi Bode-type VEs and we have seen that at least, in theory, they comply with Bode's transfer function for VEs or its squared modulus (in the case of quasi Bode-type VEs). However, in practice each one has its own shortcomings. First, Brglez's circuits (Fig.s. 2.3 and 2.4) need either an extra NIC or a switch modifying circuit to cover the whole range of variation. Second, quasi Bode type VEs introduce a positive phase shift; and like the network introduced in Chapter 4 (Fig. 4.6), direct cascade connection is only possible when they are provided with a buffer amplifier at the output plus the need for a buffer resistance to overcome their tendency to instability.

In this chapter a new basic design [28] for Bode VEs will be investigated and which is very useful in practice; and, as we shall see, it is a most flexible design.

5.2 The basic network [28]

Let us consider the circuit in Fig. 5.1. Its transfer function is given by :

$$T(s) = \frac{Z_A Z_F (Z_D + Z_E) + Z_A Z_B Z_E + Z_D (Z_E Z_A - Z_B Z_C)}{Z_A [Z_F (Z_D + Z_E) + Z_D (Z_E + Z_C)]} \quad (5.1)$$

let $Z_E Z_A = Z_B Z_C$ (5.2)

and $Z_B = Z_E + Z_C$ (5.3)

then we have

$$T(s) = \frac{Z_F(Z_D+Z_E) + Z_B Z_E}{Z_F(Z_D+Z_E) + Z_B Z_D} \quad (5.4)$$

We note that neither Z_F nor Z_D appear in conditions (5.2) and (5.3). Since our aim is to design a VE which does not have any constraint on its shaping impedance and on the element adjusting its loss (or gain); therefore one of the two impedances (Z_F or Z_D) can be chosen as the variable element and the other one the shaping element. However, this freedom is restricted when symmetrical loss frequency characteristics about a flat loss are desirable. Furthermore, in active RC realisation, priority is given to a grounded shaping impedance because when this shaping impedance includes a simulated inductance, the grounded one will require less op-amps than a floating one. In this case the only possibility left is to choose Z_D as the variable element and Z_F the shaping impedance.

Let us rewrite Bode's transfer function for VEs

$$T(s) = M \frac{1 + \gamma H(s)}{\gamma + H(s)} \quad (5.5)$$

Comparing (5.4) and (5.5) we get

$$M = 1$$

$$\gamma = Z_D/Z_E$$

$$\text{and } H(s) = Z_F/(Z_F+Z_B).$$

In order to cover the whole range of variation γ varies over the range $[0, \infty]$, therefore Z_D should cover the same range; the simplest way to do this is to choose Z_D as a variable resistor R_v . Z_F could be any shaping impedance $Z_0(s)$ which may consist of a number of elements. In

the practical network, shown in Fig. 5.2, we have chosen the reference resistance $R_o = Z_E = Z_C$ which makes $Z_A = Z_B = 2R_o$. The loss frequency response of this VE is symmetrical about 0dB flat loss (obtained for $R_v = R_o$), and the full range of variation is covered by varying R_v from 0 to ∞ . At the outer limits of this range, the corresponding transfer function is given by :

$$T(s) = \left[\frac{Z_o(s) + 2R_o}{Z_o(s)} \right]^{+1}$$

The advantages of the new circuit are that it uses only a single variable resistor to produce the required range of variation, it contains only a single op-amp and since the output terminal of the circuit coincides with the output terminal of the amplifier, the circuit is suitable for direct cascade connection without buffer amplifiers. This makes it more attractive than the previous designs. It might be argued that the use of a floating variable resistance to cover the range $[0, \infty]$ may not be preferable, But in practical realisations, this range is not fully covered, and in most cases it is reduced to acceptable limits. In Table 5.1 some examples of range of variation of R_v are given. $Z_o(s)$ is assumed to be a pure reactance and the maximum loss is calculated for $Z_o(s) = 0$. For example if $Z_o(s)$ is a capacitor, high frequencies are considered; and when $Z_o(s)$ is an inductor, low frequencies are considered. In the case of a series combination of a capacitor and an inductor $Z_o(s) = j[\omega L - 1/(\omega C)]$ only the resonant frequency ($f_o = 1/2\sqrt{LC}$) is considered.

R_v/R_o	Loss (dB)	range of R_v
0.562 1.778	+5 -5	1.216 R_o
0.316 3.162	+10 -10	2.846 R_o
0.178 5.623	+15 -15	5.445 R_o

TABLE 5.1

The table shows that in order to get a ± 15 dB loss R_v varies between $0.178 R_o$ and $5.623 R_o$ which is less than $6 R_o$. Therefore a floating variable resistor should not be a problem. Furthermore, as we shall see in section 5.5, it is always possible to cover the whole range of variation by varying R_v over a range $[0, mR_o]$, where m is arbitrary real and positive. It shall also be shown in Section 5.6 that the structure in Fig. 5.1 could lead to a VE with both a grounded shaping impedance and a grounded variable resistor.

5.3 Some active network transformations by terminal interchange.

In this section two network transformations by terminal interchange shall be presented and shall be used in the following sections for the development of further equalisers. These transformations are applicable to networks containing a grounded output op-amp whose

output terminal is connected to the output terminal of the network.

5.3.1. Transformation A [29,30,31]

This is the well known transformation by which a network N_1 with a voltage transfer function $T_1(s)$ leads to a network N_2 with a voltage transfer function $T_2(s)$, where

$$T_2(s) = 1/T_1(s)$$

Let us investigate this transformation and consider the network N_1 in Fig. 5.3 in which the output terminal of the assumed ideal op-amp A_1 coincides with the output terminal of the network N_1 ; and where N_0 is the network remaining after the op-amp A_1 is removed.

The potential of the two inputs of A_1 are equal

$$V_4(s) = V_5(s) \tag{5.6}$$

and can be expressed in the general form :

$$\begin{bmatrix} V_4(s) \\ V_5(s) \end{bmatrix} = \begin{bmatrix} a_{11} & a_{12} \\ a_{21} & a_{22} \end{bmatrix} \begin{bmatrix} V_i(s) \\ V_o(s) \end{bmatrix} \tag{5.7}$$

where a_{ij} depend on the structure and connections of the network N_0 .

From (5.6) and (5.7) we derive $T_1(s)$ of N_1

$$T_1(s) = \frac{V_o(s)}{V_i(s)} = \frac{a_{11} - a_{21}}{a_{22} - a_{12}} \quad (5.8)$$

The interchange of the input and output terminals of N_1 leads to the network N_2 shown in Fig. 5.4. If (5.7) represents the relation for N_1 , the corresponding relation for N_2 would be :

$$\begin{bmatrix} V_4(s) \\ V_5(s) \end{bmatrix} = \begin{bmatrix} a_{11} & a_{12} \\ a_{21} & a_{22} \end{bmatrix} \begin{bmatrix} V_o(s) \\ V_i(s) \end{bmatrix} \quad (5.9)$$

and the voltage transfer function $T_2(s)$ of N_2 is

$$T_2(s) = \frac{a_{22} - a_{12}}{a_{11} - a_{21}} \quad (5.10)$$

Comparing (5.8) and (5.10) we get

$$T_2(s) = 1/T_1(s) \quad (5.11)$$

we can therefore say if the conditions set above, are satisfied, the interchange of the input and output terminals of a network N_1 with a voltage transfer function $T_1(s)$ gives a network N_2 with a voltage transfer function $T_2(s) = 1/T_1(s)$.

5.3.2. Transformation B [21].

This second transformation and its result shall be presented followed by an attempt to outline its proof.

Let us consider the network N_1 (Fig. 5.5) whose output is connected to the output terminal of the op-amp A2 (A2 is assumed to be ideal) and which has a voltage transfer function $T_1(s)$.

The transformation consists of interchanging Z_1 and Z_2 , and connecting terminal 2 to the ground and terminal 6 to the output terminal of A₂; the obtained circuit with a voltage transfer function $T_2(s)$ is shown in Fig. 5.6.

$T_2(s)$ and $T_1(s)$ are related by :

$$T_2(s) = - \frac{Z_1}{Z_2} T_1(s) \quad (5.12)$$

The network in Fig. 5.5 can be represented by Fig. 5.7 in which the output voltage is represented by a voltage source eT_1 . The interchange described above leads to the networks in Fig. 5.8. The network in Fig. 5.8b is identical with the network in Fig. 5.6; where $V_i = e$ and $V_o = -e \frac{Z_1}{Z_2} T_1$

$$\text{therefore } T_2 = \frac{V_o}{V_i} = - \frac{Z_1}{Z_2} T_1$$

obviously, if $Z_1 = Z_2$ then $T_2 = - T_1$.

5.4 VEs derived from the basic network by terminal interchange.

The two transformations described above are used here for the development of further Bode-type VEs.

The interchange of the input and output terminals of the circuit in Fig. 5.2 (i.e. transformation A) leads to the circuit shown in Fig. 5.9; its transfer function is

$$T(s) = \frac{Z_o (R_v + R_o) + 2R_v R_o}{Z_o (R_v + R_o) + 2R_o^2} \quad (5.13)$$

We note that the loss-frequency characteristics obtained from the circuit in Fig. 5.2 by varying R_v over the range $[0, \infty]$ are obtained from the circuit in Fig. 5.9 by varying R_v over the range $[\infty, 0]$; and, of course, the flat loss 0dB is obtained from both circuits by setting $R_v = R_o$. The two circuits are 'inverse' one of the other and the choice in dealing with one or the other depends on the user. However, the circuit in Fig. 5.9 is more sensitive to the amplifier finite gain bandwidth product f_T than the basic circuit. This shall be shown in chapter 6.

Let us now apply transformation B to the circuit in Fig. 5.9; the resulting circuit with a voltage transfer function

$$T(s) = - \frac{Z_o (R_v + R_o) + 2R_v R_o}{Z_o (R_v + R_o) + 2R_o^2} \quad (5.14)$$

is shown in Fig. 5.10. If transformation A is applied to this last circuit we get the VE shown in Fig. 5.11 whose transfer function is

$$T(s) = - \frac{Z_o (R_v + R_o) + 2R_o^2}{Z_o (R_v + R_o) + 2R_v R_o} \quad (5.15)$$

It shall be shown, in chapter 6, that this VE and the one in Fig. 5.2 have identical reaction to the effect of amplifier imperfections. The distortions due to this effect are also identical for the circuits in Figs. 5.9 and 5.10.

The shaping impedance Z_o of the VEs in Figs. 5.10 and 5.11 should be treated as grounded because in the first case it is connected to the output terminal of the op-amp, and the second case it is connected to the input terminal of the VE which is driven from a grounded voltage source. All the four circuits are stable; to prove this, let us examine the expressions of their respective input impedances shown in Table 5.2.

Fig. number	Zin(s)
5.2	$\frac{2}{3} \cdot \frac{2R_o R_v + Z_o (R_o + R_v)}{R_v}$
5.11	$2R_o \cdot \frac{2R_o R_v + Z_o (R_o + R_v)}{R_o (2R_o + 3R_v) + Z_o (R_o + R_v)}$
5.9	$\frac{2}{2R_o - R_v} \left[2R_o^2 + Z_o (R_o + R_v) \right]$
5.10	$2R_o \cdot \frac{2R_o^2 + Z_o (R_o + R_v)}{R_o (2R_o + R_v) + Z_o (R_o + R_v)}$

TABLE 5.2

The circuits in Figs. 5.2, 5.11 and 5.10 are short-circuit stable and the real part of their respective input impedances are always positive. The circuit in Fig. 5.9 is also short-circuit stable and the fact that $\text{Re} [Zin (s)]$ becomes negative for $R_v > 2R_o$ does not imply that the circuit is not stable; it only means activity. Passivity, which is one of the requirements of stability, could be

violated without disturbing stability [32] . One of the practical means of testing stability is the evaluation of the amount of positive feedback (which is less than the negative one in the case of the circuit in Fig. 5.9).

5.5 VE with a prescribed maximum range of variation of the variable resistor.

It has been mentioned in section 5.2 that it is always possible to reduce the range of variation of the floating variable resistor R_v of the basic circuit in Fig. 5.2 from $[0, \infty]$ to $[0, mR_o]$, where m is arbitrary real and positive. To do this let us reconsider the network in Fig. 5.1 and let

$$\begin{aligned} Z_A &= aR_o \\ Z_B &= bR_o \\ Z_C &= cR_o \\ Z_D &= kR_o \\ Z_E &= eR_o \quad \text{and} \quad Z_F = Z_o(s) \end{aligned}$$

where a, b, c, k, e are positive and real.

The corresponding transfer function can be written in the following form

$$T(s) = \frac{Z_o(s) + \frac{[k(ae-bc) + abe] R_o}{a(k+e)}}{Z_o(s) + \frac{k(c+e)}{k+e} R_o} \quad (5.17)$$

In this equation $Z_o(s)$ is the shaping impedance and k corresponds to the variable element. (5.17) is a Bode's VE transfer function if the

two following conditions are satisfied

$$m = \frac{abe}{bc - ae} \tag{5.18}$$

$$b = \frac{a(c+2e)}{a+c} \tag{5.19}$$

Condition (5.18) gives the maximum range of variation of the variable element (in this case k in (5.17) is equal to m); condition 5.19 allows the loss-frequency characteristics of (5.17) to be symmetrical around a flat loss 0dB. It can easily be verified that when $a=b=2$ and $e=c=1$ we get the circuit in Fig. 5.2 where the range of variation of the variable element is $[0, \infty]$. If we assume that the needed range of variation should be $[0,1]$, in this case $m=1$ and condition (5.18) becomes

$$bc - ae = abe \tag{5.20}$$

with the additional constraint

$$bc > ae \tag{5.21}$$

Combining (5.19) and (5.20) we get

$$c^2 + ce(1-a) - ae(1+2e) = 0 \tag{5.22}$$

(5.22) has infinite (a,c,e) solutions. For the sake of simplicity let $a=1$, then we get

$$c = \sqrt{e(1+2e)} \tag{5.23}$$

(5.23) gives infinite couple (c,e) ; but if we choose $e=\frac{1}{2}$, then $c=1$ and $b=1$.

And if we make another choice for example $e=4$ we get $c=6$ and $b=2$.

The first choice gives the circuit shown in Fig. 5.12 with the transfer function

$$T(s) = \frac{Z_o (R_o + 2R_v) + R_o (R_o - R_v)}{Z_o (R_o + 2R_v) + 3R_o R_v} \quad (5.24)$$

and the 0dB flat loss is obtained for $R_v = R_o/4$.

The second choice leads the VE shown in Fig. 5.13 with the transfer function

$$T(s) = \frac{Z_o (4R_o + R_v) + 8R_o (R_o - R_v)}{Z_o (4R_o + R_v) + 10 R_o R_v} \quad (5.25)$$

and the 0dB flat loss is obtained for $R_v = \frac{4}{9} R_o$.

The last two circuits (in Figs. 5.12 and 5.13) are not the only Bode-type VEs which have the range of variation of the variable element $[0, 1]$ ($0 \leq R_v \leq R_o$), but there is an infinite number of circuits depending on the solutions of equation (5.22). This range $[0, 1]$ could be reduced or extended depending on the value of m in condition (5.18). Transformations A and B (section 5.3) can be applied to all those circuits. However, one should be careful when applying transformation B because the flat loss of the obtained circuits might not be any longer 0dB. This fact is illustrated by the VE in Fig. 5.13: when transformation A is applied to this circuit we get the inverse of the transfer function in (5.25) and the flat loss is 0dB. Transforming, the obtained circuit, by B gives the following transfer function

$$T(s) = -2 \frac{Z_o (4R_o + R_v) + 10 R_o R_v}{Z_o (4R_o + R_v) + 8R_o (R_o - R_v)} \quad (5.26)$$

which indicates that the flat loss is at 6dB and not 0dB. On the other hand if we apply the successive transformations to the VE in Fig.5.12, the flat loss 0dB remains unchanged. In general the obtained flat loss, after transformation B, is given by $20 \log b/a$.

In order to illustrate the capabilities of the basic structure in Fig. 5.1, the following section will show another attractive feature of this structure which is the development of a VE with both a grounded shaping impedance and a grounded variable resistor.

5.6 A design with a grounded variable resistor.

In this section we shall show that the basic network in Fig. 5.1 could lead to the design of a Bode-type VE where the variable resistor and the shaping impedance are both grounded. By "grounded" we mean that the relevant element is directly connected to the ground terminal or it is either connected to a grounded output terminal of an op-amp or the input terminal of a network driven from a grounded voltage source. In the basic network the impedances Z_A , Z_B , Z_C and Z_F are regarded as grounded. The only combination of these four impedances that produces a Bode-type VE is when Z_C is the variable resistor and Z_F the shaping impedance $Z_o(s)$.

If R_o is a reference resistor and we set

$$\begin{aligned}
 Z_A &= a R_o \\
 Z_B &= b R_o \\
 Z_D &= d R_o \\
 Z_E &= e R_o \\
 Z_C &= R_v = kR_o
 \end{aligned}
 \tag{5.27}$$

where a, b, d, e and k are positive and real; the transfer function (5.1) becomes

$$T(s) = \frac{Z_o(s) + R_o A(k)}{Z_o(s) + R_o B(k)}
 \tag{5.28}$$

where

$$\begin{aligned}
 A(k) &= \frac{abe + d(ae - bk)}{a(d+e)} \\
 B(k) &= \frac{d(e+k)}{d+e}
 \end{aligned}
 \tag{5.29}$$

Since k is positive, $B(k)$ is always positive but $A(k)$ becomes negative when

$$k > \frac{ae(b+d)}{bd}$$

It is therefore essential to find the upper limit of the range $[0, k_m]$ within which k should vary in order to produce symmetrical loss-frequency characteristics.

The lower limit which is zero gives

$$\begin{aligned}
 A(o) &= \frac{e(b+d)}{d+e} \\
 B(o) &= \frac{de}{d+e}
 \end{aligned}
 \tag{5.30}$$

the upper limit km should satisfy

$$\begin{aligned}
 A(km) &= B(o) \\
 A(o) &= B(km)
 \end{aligned}
 \tag{5.31}$$

then the unique value of km is

$$km = \frac{ae}{d}$$

we can therefore say that the basic network (Fig. 5.1) is a Bode-type VE with both a grounded variable resistor and a grounded shaping impedance only if

$$\begin{aligned}
 Z_A &= Z_B = aR_o \\
 Z_C &= R_v = kR_o \\
 Z_F &= Z_o(s)
 \end{aligned}$$

the corresponding network is shown in Fig. 5.14; its transfer function is

$$T(s) = \frac{(d+e)Z_o(s) + [e(a+d) - dk] R_o}{(d+e) Z_o(s) + d(e+k) R_o}
 \tag{5.32}$$

$$0 \leq k \leq \frac{ae}{d}$$

Comparing (5.32) and (5.5) we get

$$M = 1$$

$$\gamma = \frac{d(e+k)}{e(a+d) - dk}$$

$$H(s) = \frac{(d+e) Z_o(s)}{(d+e)Z_o(s) + e(a+2d) R_o}$$

It can easily be verified that when k varies from 0 to $\frac{ae}{d}$, γ varies from $\frac{d}{a+d}$ to $\frac{a+d}{d}$. This means that the whole range of variation $[0, \infty]$ of γ can never be fully covered by this new VE. Consequently the maximum symmetrical variable amplitude is within limits which have to be specified.

We know that for any k ($0 \leq k \leq \frac{ae}{d}$), the maximum amplitude is obtained for $Z_o(s) = 0$; in this case (5.32) becomes

$$T(k) = \frac{e(a+d) - dk}{d(e+k)} \tag{5.33}$$

at the outer limits of k , the maximum loss (or gain) in dB is given by

$$\alpha \text{ (dB)} = \pm 20 \log \frac{a+d}{d} \tag{5.34}$$

This shows that the maximum amplitude that can be obtained by the VE in Fig. 5.14 depends on the ratio $(a+d)/d$. It is up to the designer to choose this ratio and also the other parameters depending on the requirements to be met by the equaliser.

Let us give an example : the aim is to design a VE (based on the network in Figs. 5.14) which gives a maximum loss of about ± 6 dB when k varies between 0 and 1 (i.e. $0 \ll R_v \ll R_o$). Equation (5.34) gives

$$\pm 6 = \pm 20 \log 2 = \pm 20 \log \frac{a+d}{d}$$

which gives $a=d$; and since the maximum value of k is $1 = \frac{ae}{d}$, we get $e=1$; we can always choose $a=d=1$ which leads to the circuit shown in Fig. 5.15 with a transfer function

$$T(s) = \frac{2Z_o(s) + (2-k)R_o}{2Z_o(s) + (1+k)R_o} \quad (5.35)$$

Depending on the special application, $Z_o(s)$ and R_o have been left to be chosen accordingly. Whatever $Z_o(s)$ and R_o are, the loss-frequency characteristics of the VE are symmetrical about 0dB flat loss (obtained for $k = \frac{1}{2}$) and the maximum loss (or gain) that can be reached is 6dB.

Laboratory models of the VE in Fig. 5.14 have been built; they can provide a maximum loss of about ± 14 dB. The practical results shall be presented in section 5.7.

Like all the circuits presented in this chapter, transformations A and B (Section 5.3) can be applied also to the circuit in Fig. 5.14; and because $Z_A = Z_B$, the 0dB flat loss remains unchanged after the B transformation.

5.7 Some practical results.

Some of the VEs we have presented in this chapter have been built and tested. The circuit in Fig. 5.2 was built for designing both a fan and a bump VE. Its corresponding practical fan equaliser is shown in Fig. 5.16. The measured responses and their deviations from the computed ideal ones are shown in Fig. 5.17. The practical bump equaliser is shown in Fig. 5.18. It was built to provide a range of the variable loss of about ± 10 dB at a centre frequency $f_0 = 1.5 \text{ kHz}$. The lossy inductor used here is the same one as that in Fig. 4.11 and the comments given in sub-section 3.3.2 regarding the adjustment of the height and the sharpness of the bump are relevant in the context of the circuit in Fig. 5.18; these adjustments should be achieved in the same way. The measured loss-frequency characteristics and the error characteristics of the VE are shown in Fig. 19.

A fan equaliser, based on the network in Fig. 5.9, was built to provide ± 10 dB variable loss at an upper frequency 10 kHz . The experimental circuit and the measured results are shown in Figs. 5.20 and 5.21 respectively. It can be seen that the responses obtained by this circuit when R_v varies from $2.0 \text{ k}\Omega$ to $28.13 \text{ k}\Omega$ are identical to those obtained by the circuit in Fig. 5.16 when R_v varies from $28.13 \text{ k}\Omega$ to $2.0 \text{ k}\Omega$.

The last practical example is based on the circuit in Fig. 5.14. It was designed to produce a maximum variable loss of ± 14 dB when R_v varies between 0 and $14.2 \text{ k}\Omega$. The experimental fan and bump equalisers are given in Figs. 5.22a and 5.23a, and the respective measured responses and their deviations from the computed ones (assuming ideal op-amps) are shown in Figs. 5.22b and 5.23b .

5.8 Conclusion.

A new basic structure for Bode-type VEs has been presented. It is a very simple and flexible structure; it requires only a single op-amp to provide the basic operation of a VE. Moreover, the output terminal of this op-amp is directly connected to the output terminal of the VE which makes the structure suitable for direct cascade connection without extra buffer amplifiers. Potentially, the network in Fig. 5.1 is capable of producing an unlimited number of Bode equalisers. We have produced some of them via transformations by terminal interchange and others by changing the position of the variable element, i.e. the VE in Fig. 5.14 for which, at the expense of a constraint on the symmetrical variable loss, it was possible to have both the shaping impedance and the variable resistor grounded. It is worth pointing out that, for the network in Fig. 5.14, the variations of R_v are no longer of the form $1/R_v$ ($0 \leq R_v \leq \infty$) but they become linear.

The effects of the amplifier gain bandwidth product on the VEs discussed in this chapter and the previous ones shall be investigated in the following chapter.

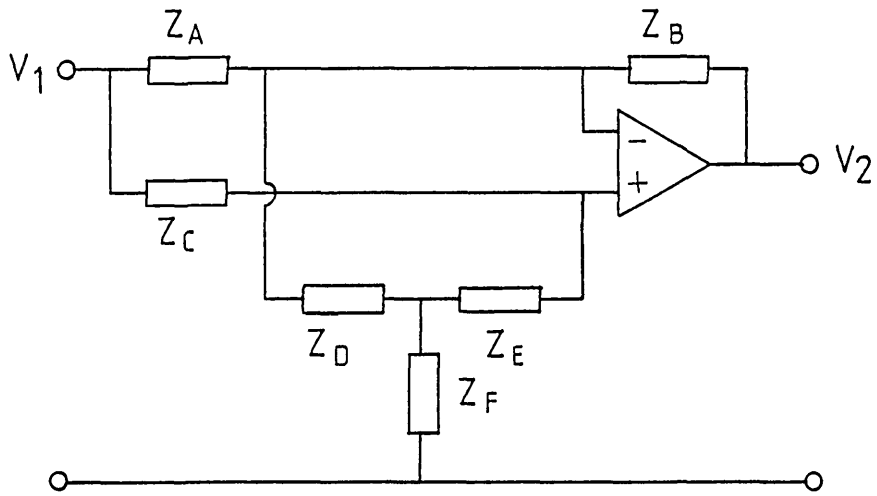


Fig. 5.1 new basic structure for Bode-type VE.

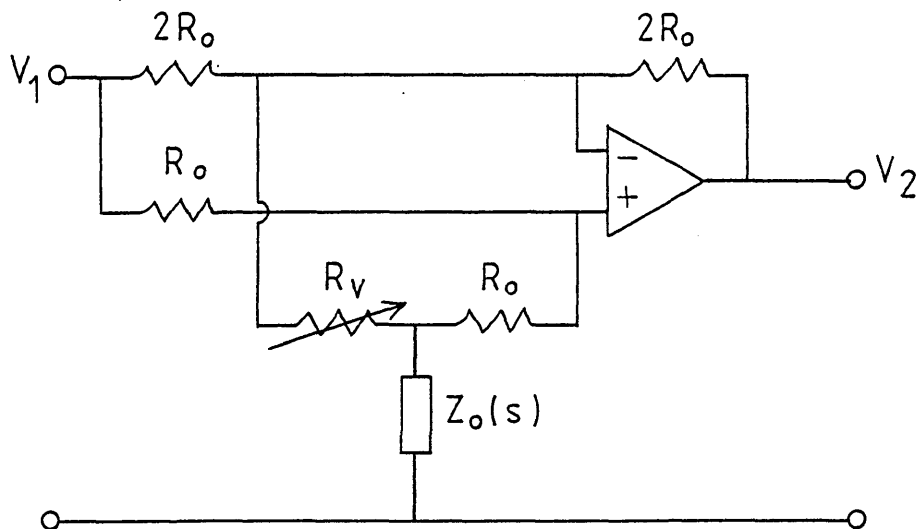


Fig. 5.2 VE obtained from the above structure by making $Z_A = Z_B = 2R_o$, $Z_C = Z_E = R_o$ and $Z_D = R_v$.

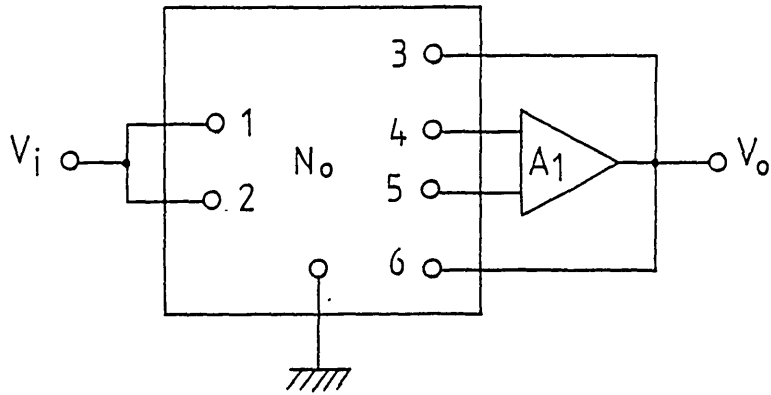


Fig. 5.3 network N_1 with transfer function T_1 .

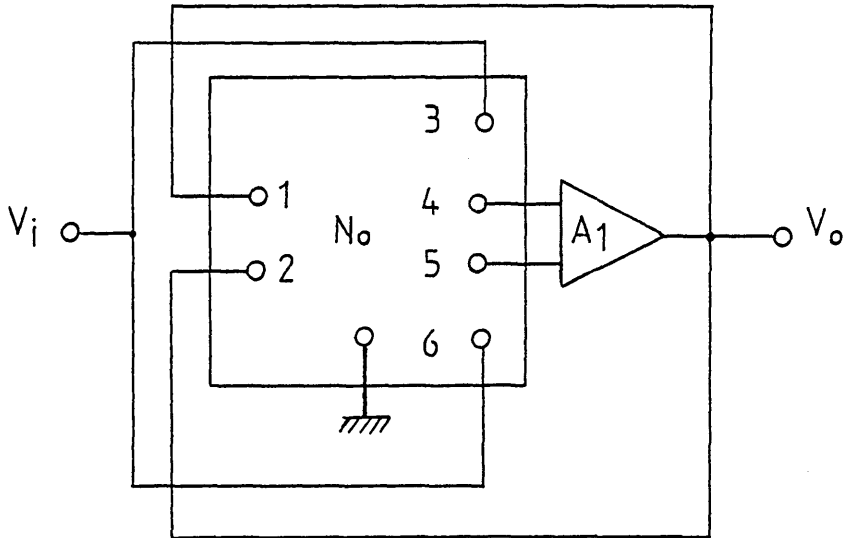


Fig. 5.4 network N_2 with transfer function $1/T_1$.

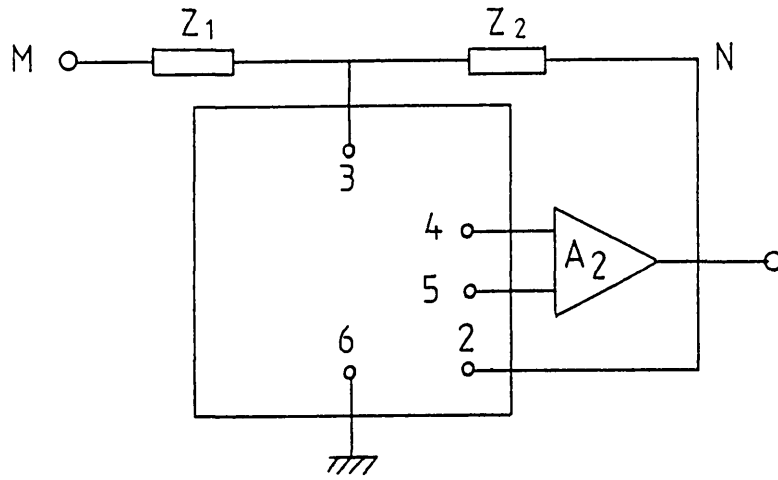


Fig. 5.5 network N_1 to be transformed by transformation B.

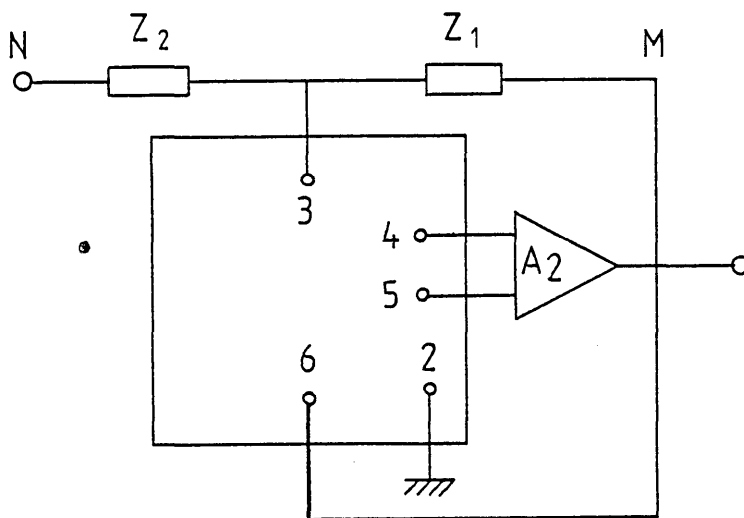
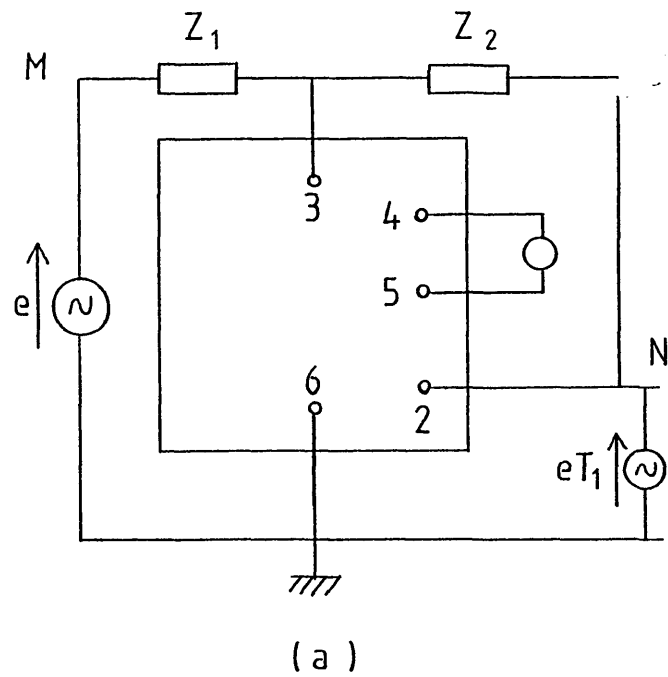


Fig. 5.6 network N_2 obtained from network N_1 by transformation B.



≡

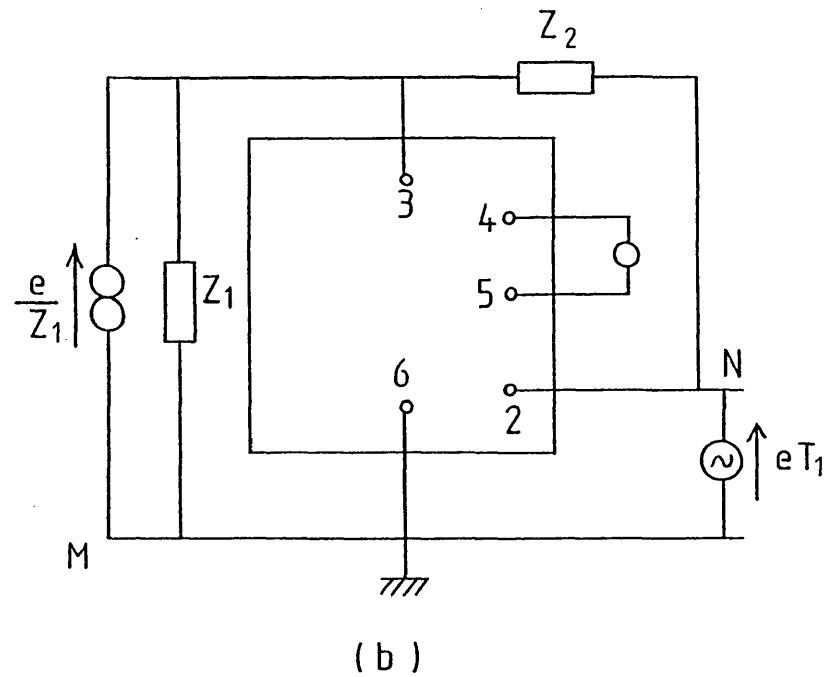
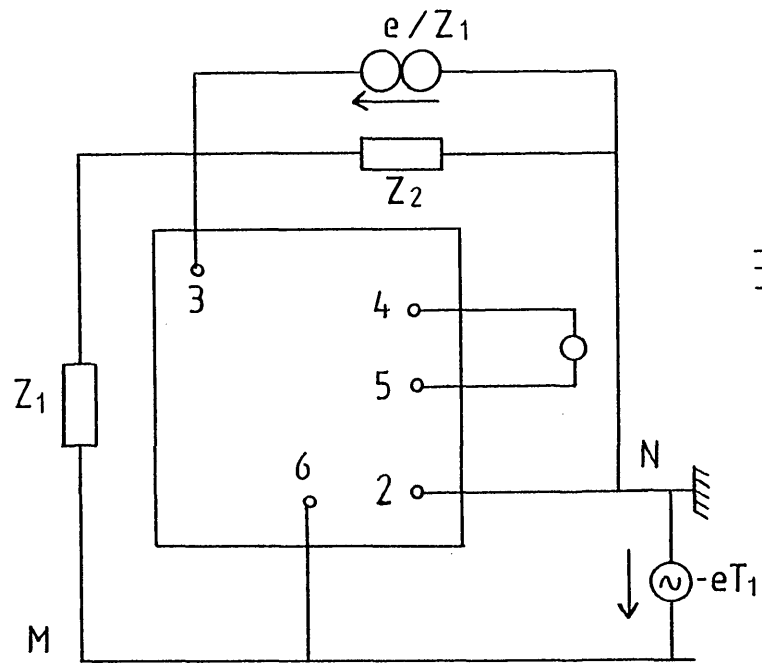
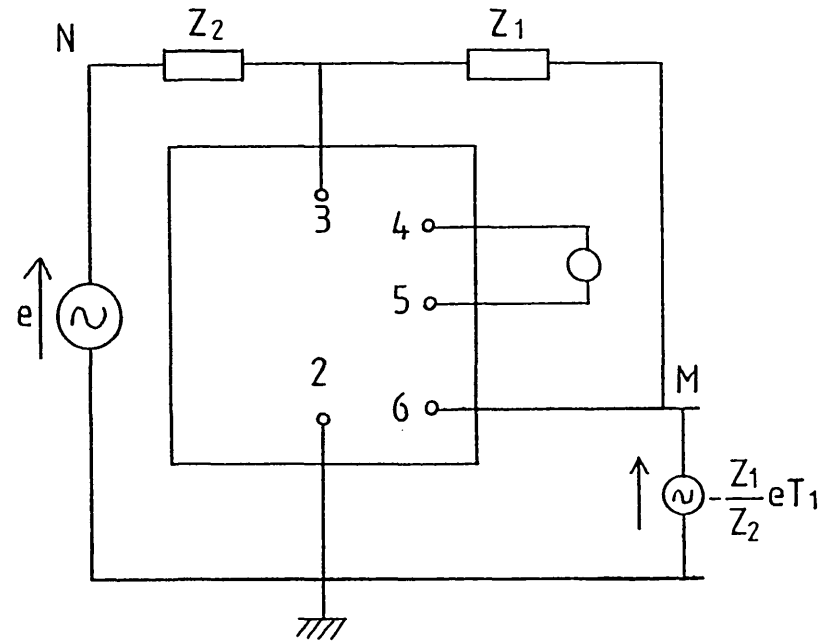


Figure 5.7 networks equivalent to the one shown in Fig. 5.5 where a nullator is inserted between nodes 4 and 5 (it replaces the input terminals of the op-amp). In (b) the current source e/Z_1 replaces the voltage source e in (a).



(a)

≡



(b)

Figure 5.8 networks identical with the one shown in Fig. 5.6

(a) is obtained from 5.7b by transformation B

(b) is identical with (a) where the input current source e/Z_1 is replaced by a voltage source e .

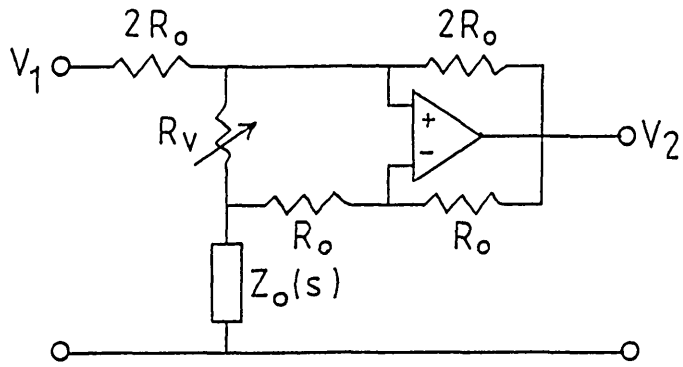


Fig. 5.9 VE obtained from the circuit in Fig.5.2 by transformation A.

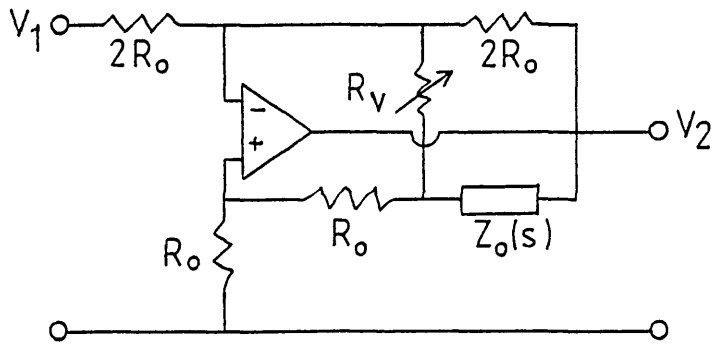


Fig. 5.10 VE obtained from the above circuit by transformation B.

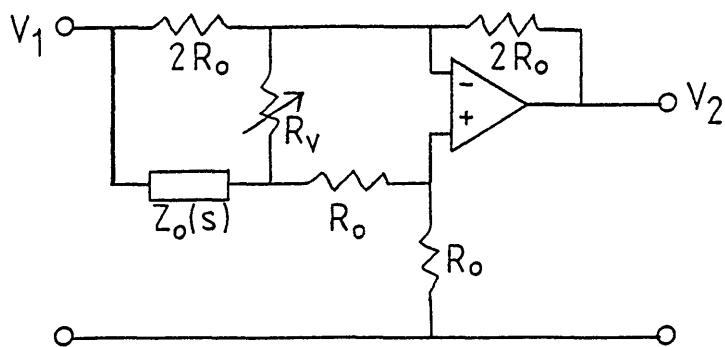


Fig. 5.11 VE derived from the circuit of Fig. 5.10 by transformation A.

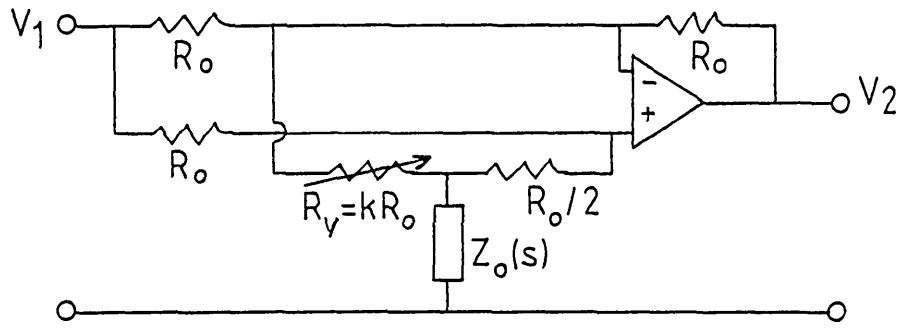


Fig. 5.12 VE with prescribed range of variation of R_v .
($0 \leq k \leq 1$)

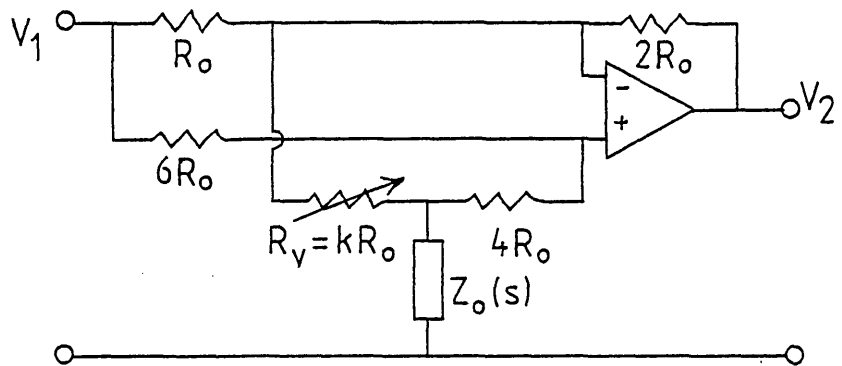


Fig. 5.13 $0 \leq k \leq 1$

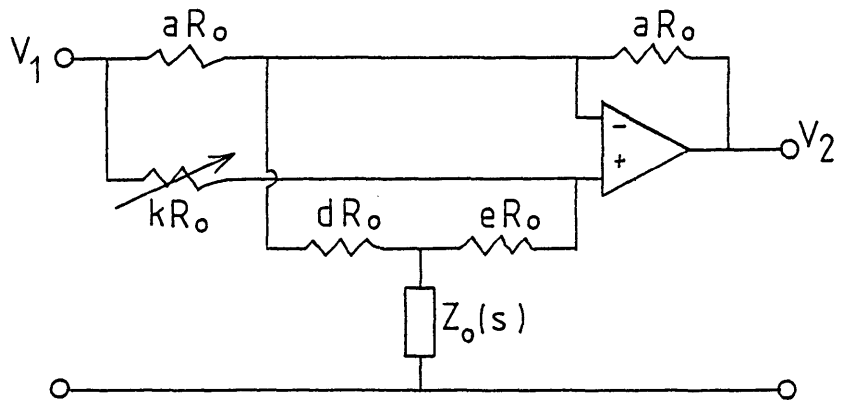


Fig. 5.14 VE with R_v and $Z_0(s)$ grounded ($0 \leq k \leq ae/d$).

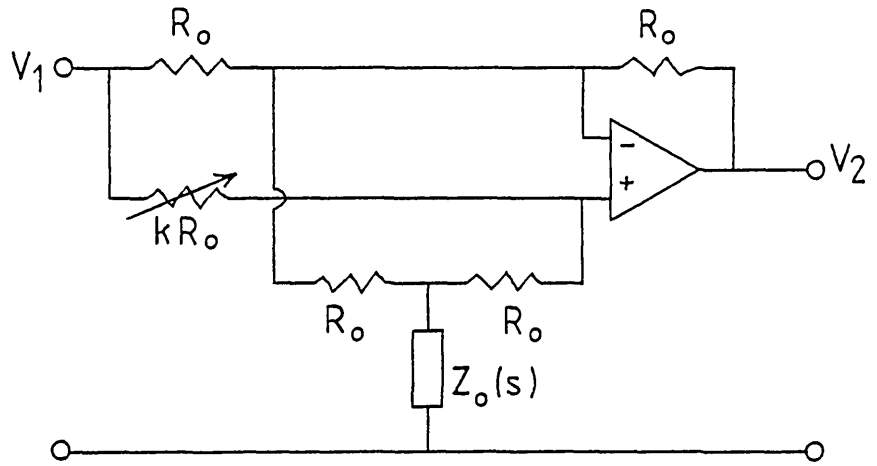


Fig. 5.15 $0 \leq k \leq 1$

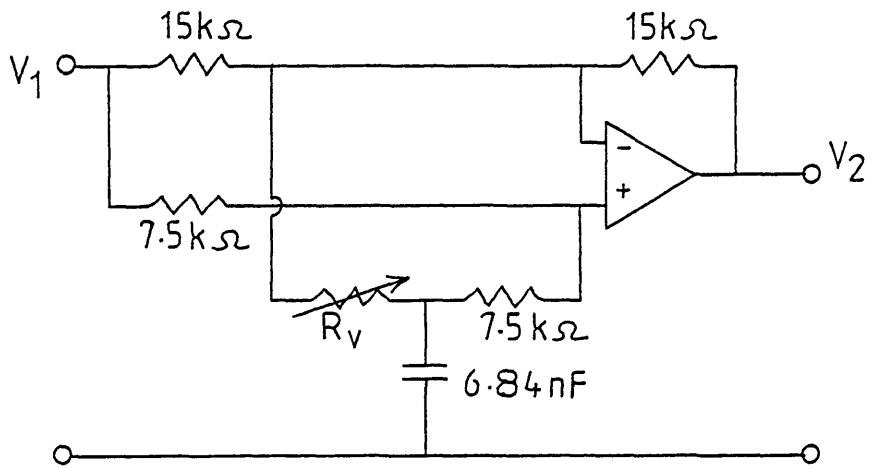


Fig. 5.16 experimental fan equaliser based on the circuit in Fig. 5.2 (op-amp TL 082 CL, $f_T=3\text{MHz}$).

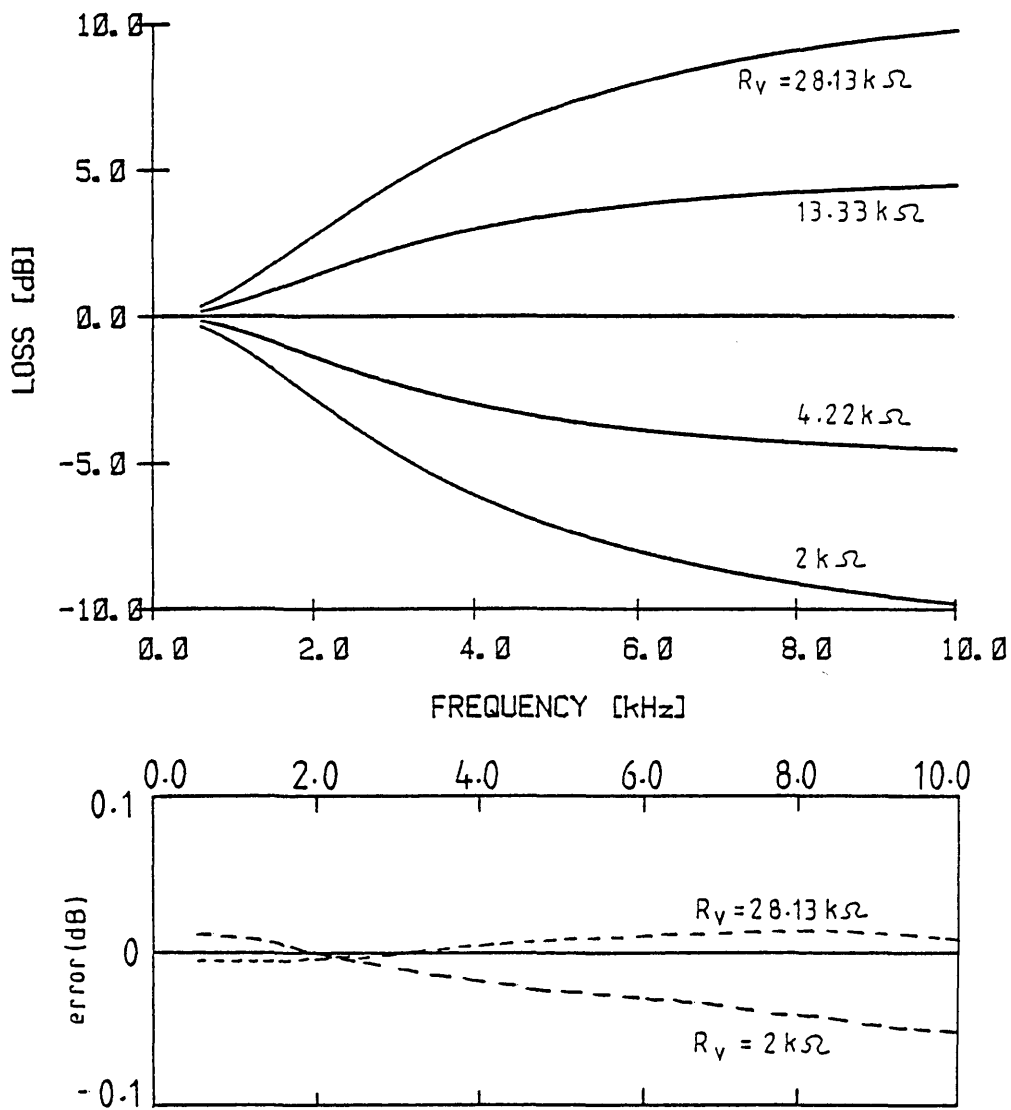


Fig. 5.17 measured frequency response of circuit in Fig. 5.16 and deviations from the ideal case.

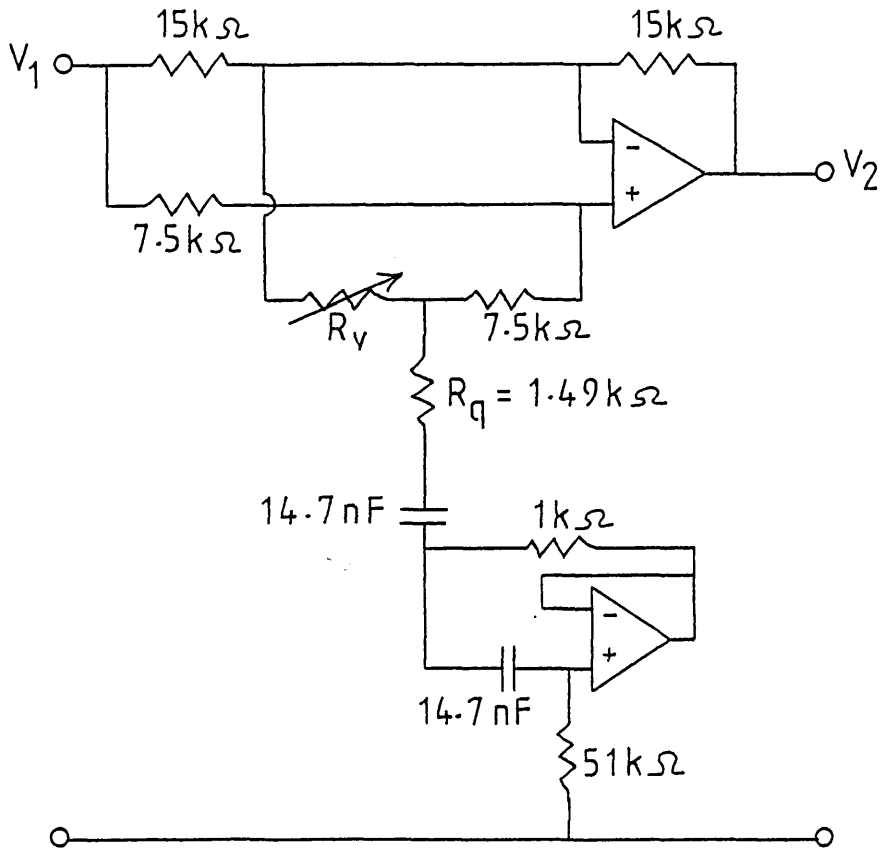


Fig. 5.18 experimental bump equaliser based on the circuit in Fig. 5.2 (op-amps TL 082 CL, $f_T=3$ MHz).

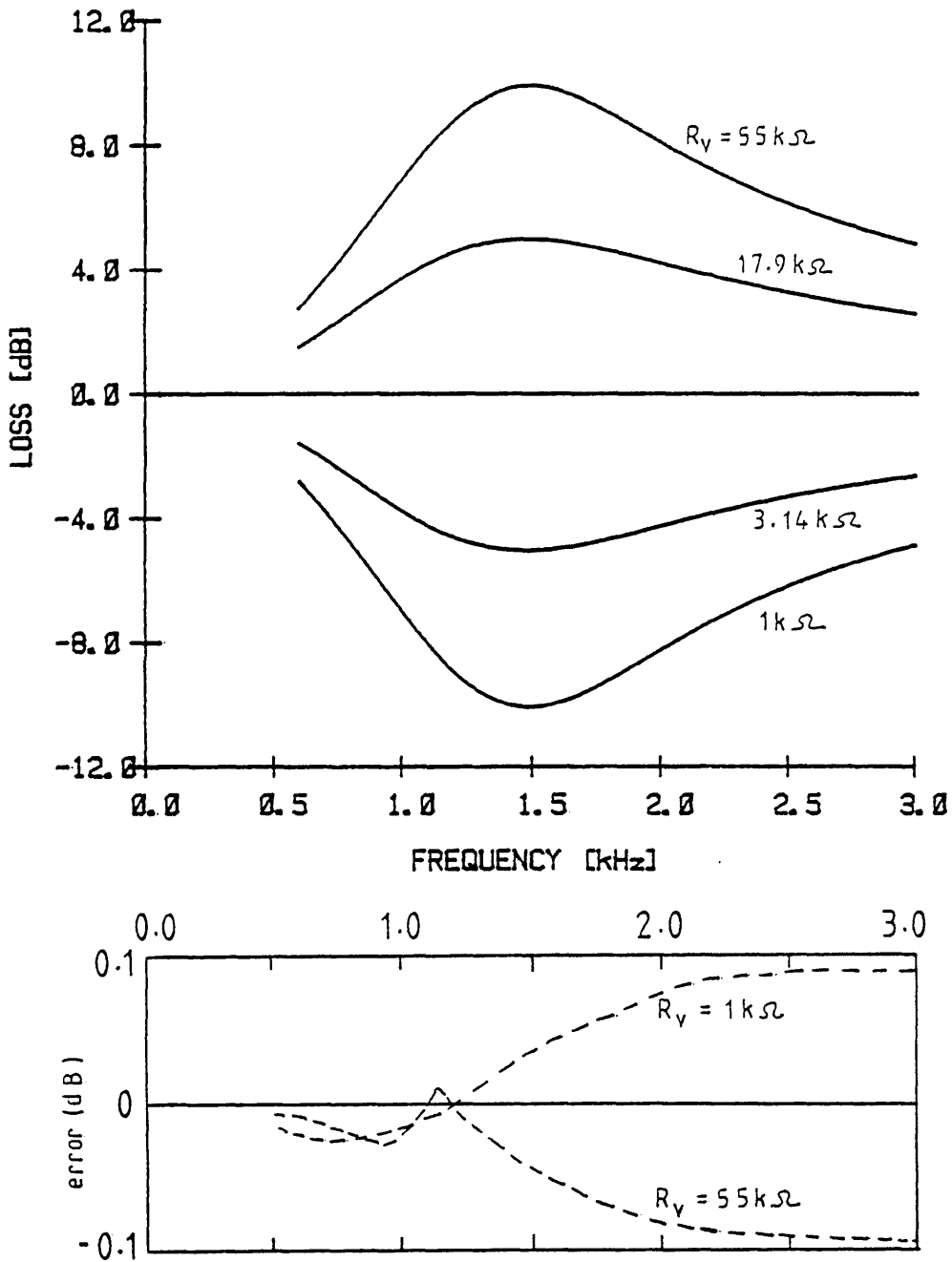


Fig. 5.19 measured frequency response of bump equaliser in Fig. 5.18 and deviation from the ideal case.

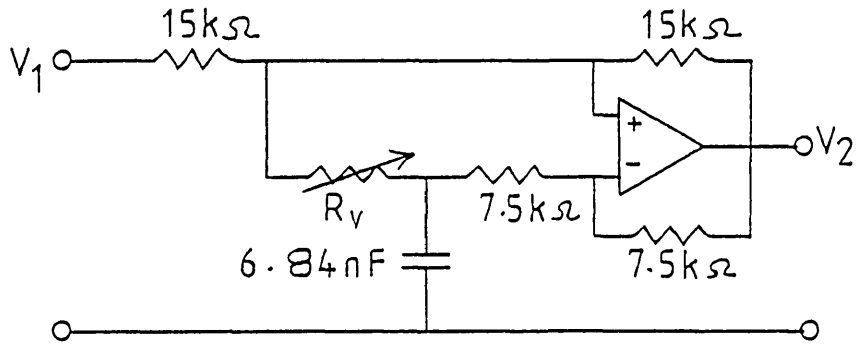


Fig. 5.20 practical fan equaliser based on the circuit in Fig. 5.9, op-amp TL 082 CL ($f_T = 3\text{MHz}$).

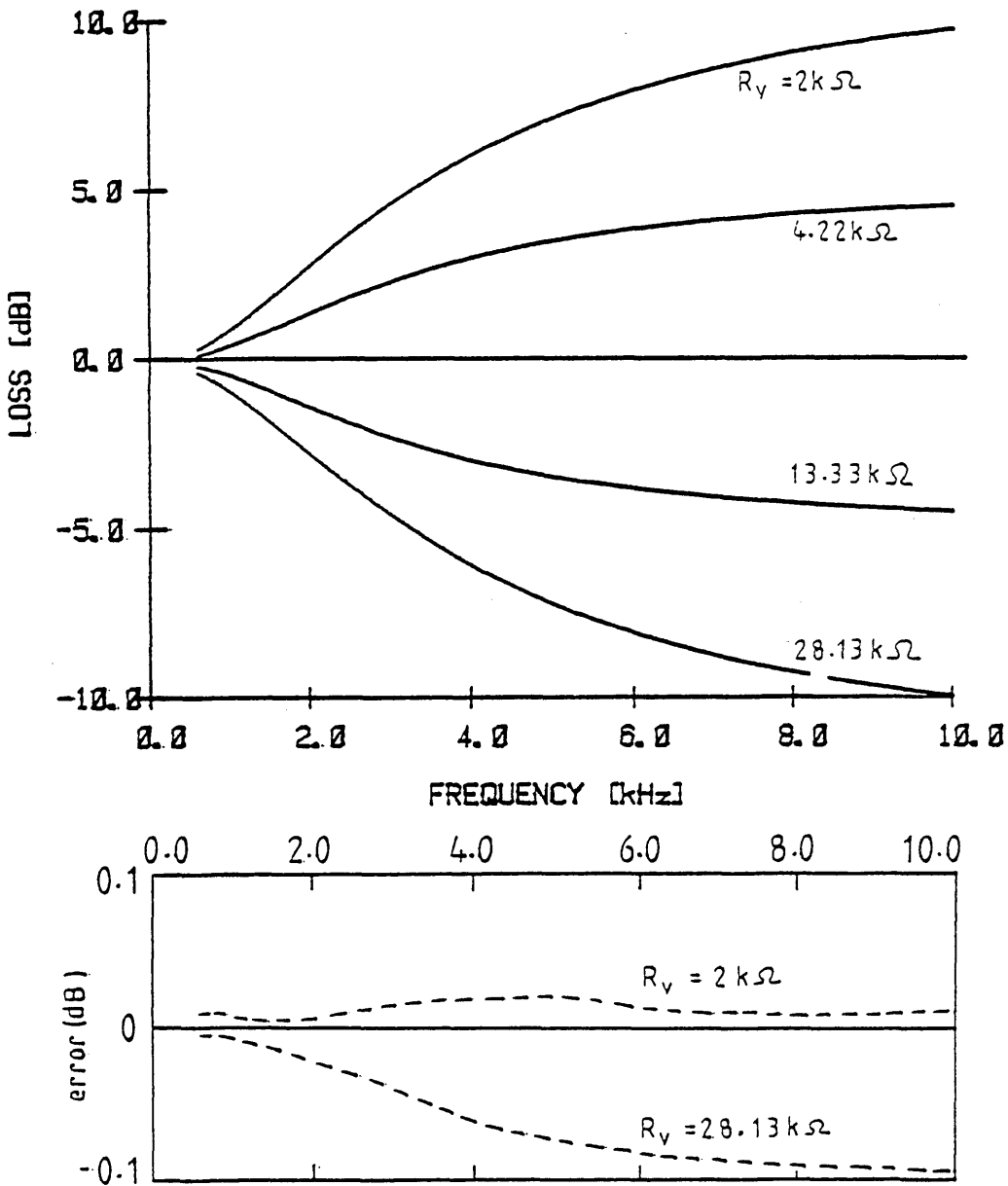


Fig. 5.21 measured frequency response of the above circuit and deviations from the ideal case

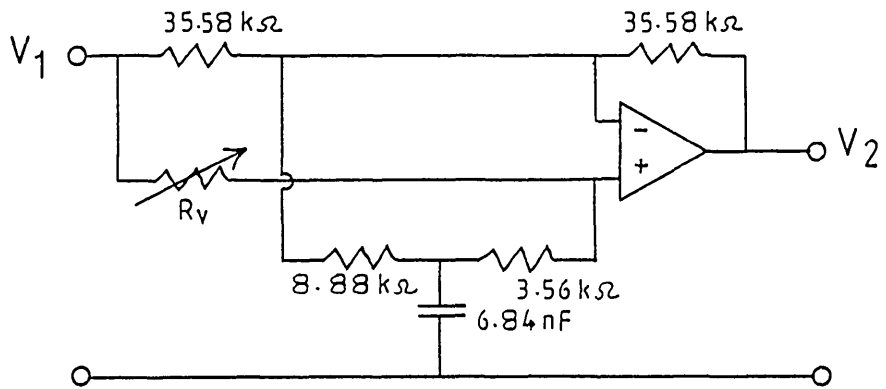


Fig. 5.22a practical fan equaliser corresponding to the circuit in Fig. 5.14 ($f_T = 3 \text{ MHz}$)

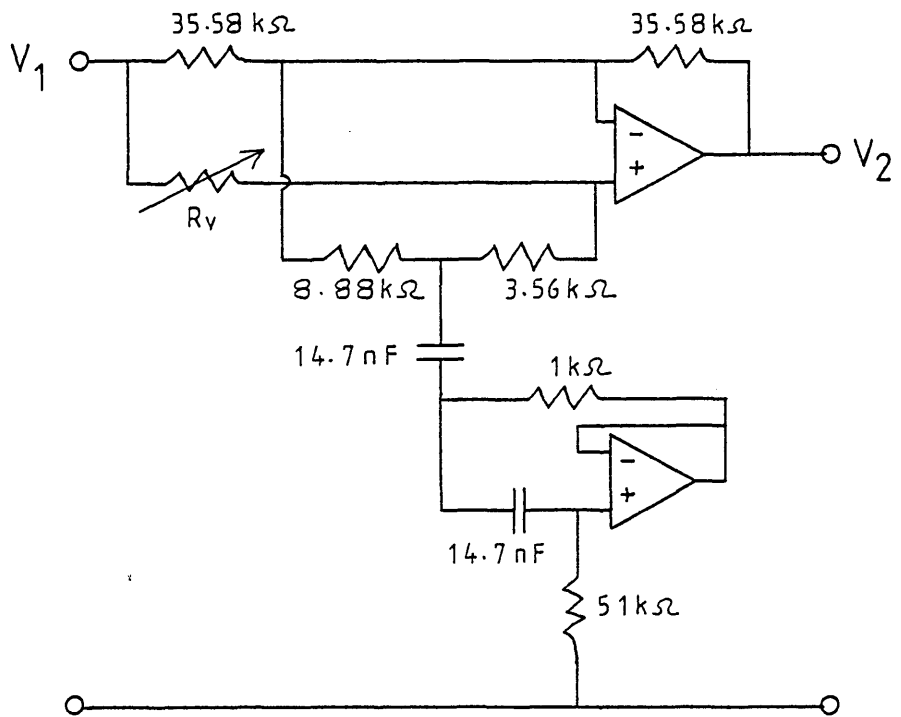


Fig. 23a practical bump equaliser corresponding to the circuit in Fig. 5.14 ($f_T = 3 \text{ MHz}$)

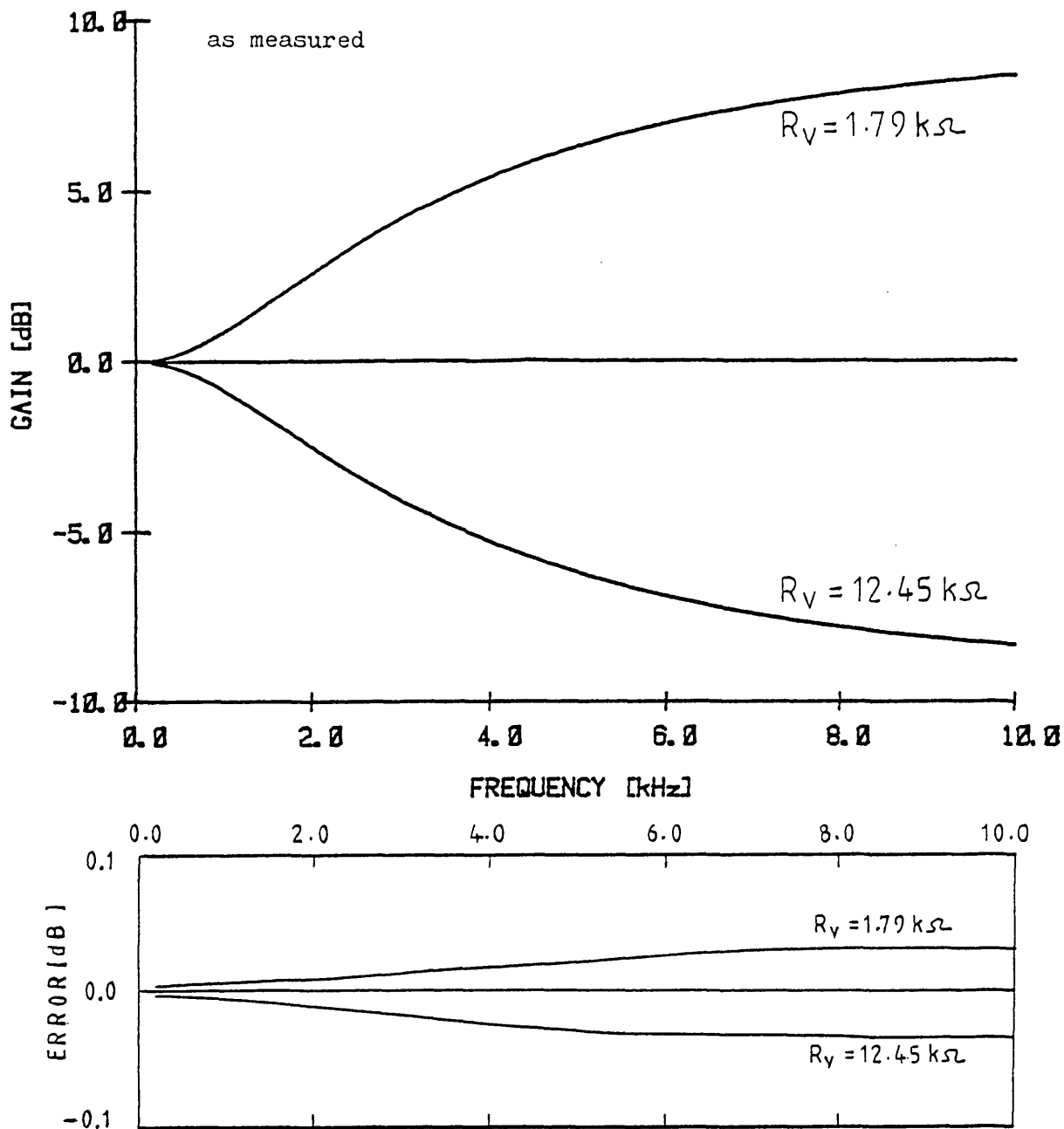


Fig. 5.22b frequency response of the practical fan equaliser in Fig. 5.22a and deviation from the ideal case.

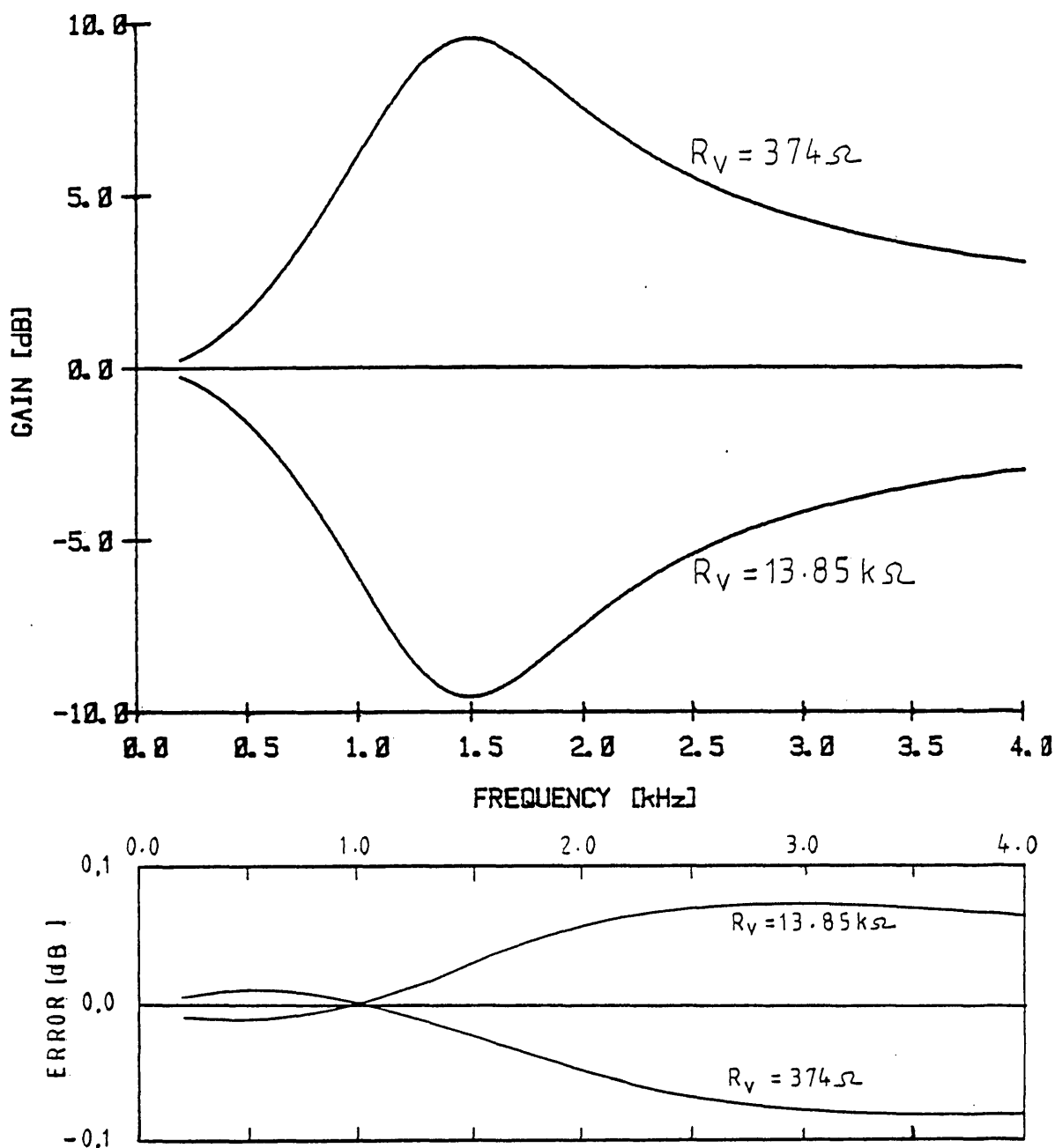


Fig. 5.23b measured frequency response of the bump equaliser in Fig. 5.23a and deviations from the ideal case.

CHAPTER VI

EFFECTS OF THE AMPLIFIER FINITE GAIN BANDWIDTH PRODUCT

- 6.1 Introduction.
- 6.2 The comparison method.
 - 6.2.1. Fan equalisers.
 - 6.2.2. Bump equalisers.
- 6.3 The optimisation method.
- 6.4 Some computed results.

CHAPTER VI EFFECTS OF THE AMPLIFIER FINITE GAIN
BANDWIDTH PRODUCT.

6.1 Introduction

In practice the distortions due to the amplifier imperfections are characterised by the finite gain bandwidth product f_T of the amplifier. It will be assumed that all op-amps in the VEs under consideration here are identical and have the same f_T . The investigation will not include the distortions caused by the variations of f_T due to environmental factors such as temperature. A comparison method between the various VEs shall be presented followed by an attempt to minimise the effects of f_T . Finally some computed results shall be given.

6.2 The comparison method.

The purpose of this section is to show that some conditions should be met before proceeding at any comparison of the performances of the VEs we have presented in the previous chapters. Thus, two fan equalisers, for example, with different structures are not comparable unless they produce identical loss-frequency characteristics which means that the modulus of their respective voltage transfer function should be equal. In the following the circuit in Fig. 4.6 will be used as reference for comparison.

6.2.1. Fan equalisers.

The transfer function of the reference VE in Fig. 4.6 is given by

$$T(s) = \frac{Z_o(s) (1+k_o) + R_o}{Z_o(s) (1+k_o) + k_o R_o} \quad (6.1)$$

where $k_o = R_v/R_o$ varies from 0 to ∞ and $Z_o(s)$ is a capacitor C_o which is assumed to be the same for all the VEs to be considered.

Let us find under which conditions the circuit in Fig. 5.1 produces identical loss-frequency characteristics with those of the reference VE. First let

$$\begin{aligned} Z_A &= aR \\ Z_B &= bR \\ Z_C &= cR \\ Z_D &= R_v = kR \\ Z_E &= eR \\ Z_F &= Z_o(s) = 1/C_o s. \end{aligned}$$

where R is positive and arbitrary and the parameters a, b, c, k and e to be defined are positive and real. Then we have

$$\frac{(1+k_o)^2 + (R_o C_o \omega)^2}{(1+k_o)^2 + (k_o R_o C_o \omega)^2} = \frac{a^2(k+e)^2 + [k(ae-bc) + abe]^2 (RC_o \omega)^2}{a^2[(k+e)^2 + k^2(c+e)^2 (RC_o \omega)^2]} \quad (6.2)$$

which gives

$$k = \frac{abe k_o}{a(c+e) - k_o (ae-bc)} \quad (6.3)$$

and

$$a^2(k+e)^2 (k_o^2 - 1) R_o^2 + \{ [k(ae-bc) + abe]^2 - a^2 k^2 (c+e)^2 \} (1+k_o)^2 R^2 = 0 \quad (6.4)$$

Combining these two equations with conditions (5.18) and (5.19) and assuming that the parameter 'a' is arbitrary we get

$$b = R_o / R \quad (6.5a)$$

$$e = \frac{mb^2}{(a-b)(b+m) + 2bm} \quad (6.5b)$$

$$c = \frac{ab(b+m)}{(a-b)(b+m)+2bm} \quad (6.5c)$$

$$k = \frac{mbe k_o}{bek_o + m(c+e)}$$

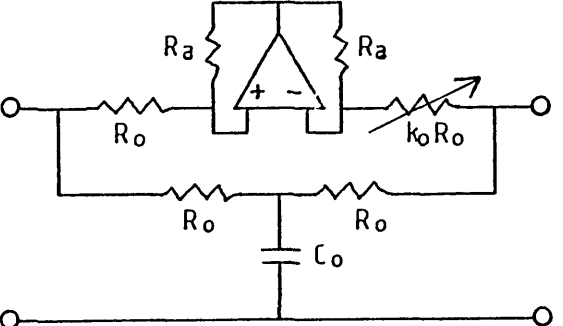
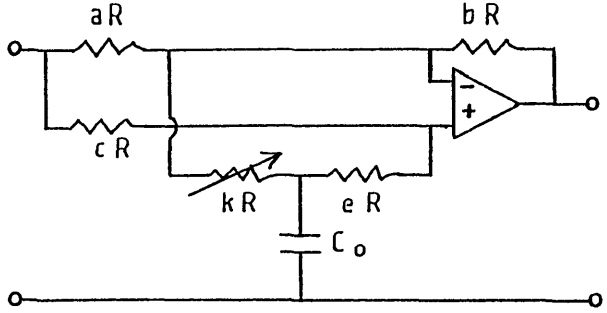
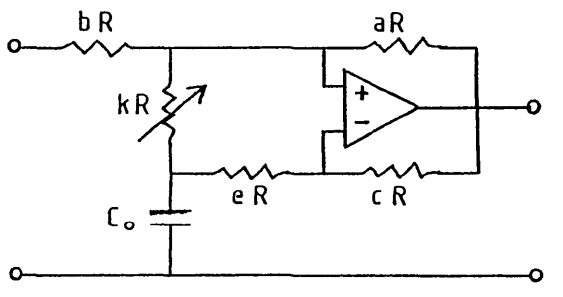
k varies within the range [0, m] where m is positive and real and could be infinity. Equations (6.5) give the design parameters of the network in Fig. 5.1 which has the same loss-frequency characteristics as the reference fan equaliser.

A set of VEs with identical loss-frequency characteristics is shown in Table 6.1 in which k represents the variable element of the VE to be compared with the reference VE; and m is the upper limit of the range k. In the case of the circuit No:4 (table 6.1), h_o represents a maximum amplitude.

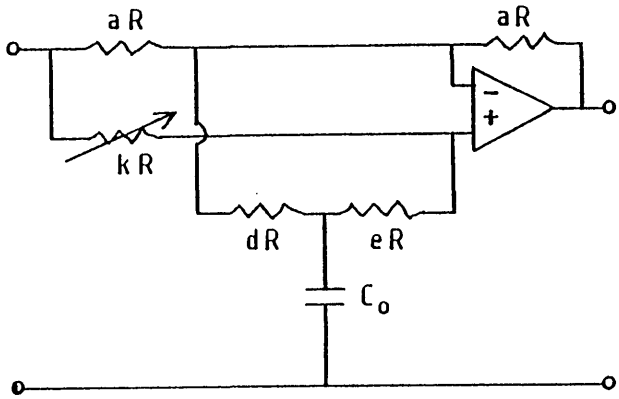
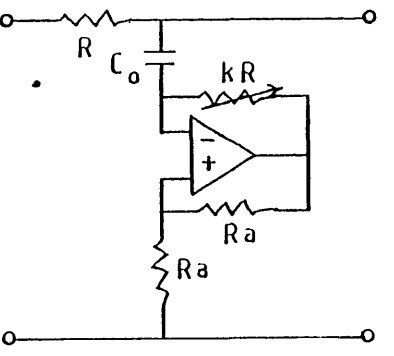
6.2.2. Bump equalisers.

For simplicity, the bump equalisers to be compared contain a purely reactive shaping impedance which is realised by means of an active RC simulated inductor in series (or in parallel) with a capacitor C_o . Table 6.2 gives some bump equalisers with identical loss-frequency characteristics where the circuit No:1 is the reference VE; w_o represents the centre frequency of the bump. The design parameters are found by following the procedure used for fan equalisers. However,

TABLE 6.1

VE	DESIGN PARAMETERS	TRANSFER FUNCTION
 <p>Reference VE - No:1</p>	$0 \leq k_0 \leq \infty$	$T_1(s) = \frac{1+k_0 + s C_0 R_0}{1+k_0 + s k_0 C_0 R_0}$
 <p>No:2</p>	$b = R_0/R$ $e = \frac{mb^2}{(a-b)(b+m)+2mb}$ $c = \frac{ab(b+m)}{(a-b)(b+m)+2mb}$	$T_2(s) = \frac{a(k+e)+sC_0R[k(ae-bc)+abe]}{a[(k+e)+sC_0Rk(c+e)]}$
 <p>No:3</p>	$k = \frac{mb e k_0}{e b k_0 + m(c+e)}$ $0 \leq k \leq m$	$T_3(s) = 1/T_2(s)$

Continued:- (Table 6.1)

VE	DESIGN PARAMETERS	TRANSFER FUNCTION
 <p style="text-align: center;">No:4</p>	$e = \frac{m}{h_o - 1}$ $a = \frac{m R_o}{e(h_o + 1)R - R_o}$ $d = \frac{a}{h_o - 1}$ $k = \frac{e(k_o h_o - 1)}{k_o + 1}$ $0 \leq k \leq m$	$T_4(s) = \frac{(d+e) + sC_o R [e(a+d) - kd]}{(d+e) + s C_o R d(e+k)}$
 <p style="text-align: center;">No:5</p>	$R = R_o$ $k = \frac{1}{k_o + 1}$ $0 \leq k \leq 1$	$T_5(s) = \frac{1 - skC_o R}{1 + s(1-k) C_o R}$

Continued..

Continued:-

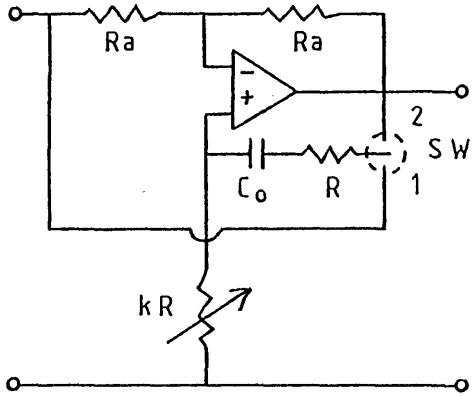
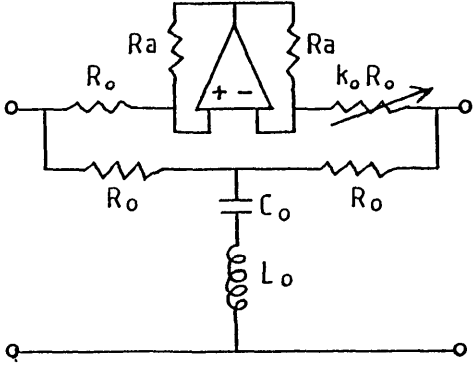
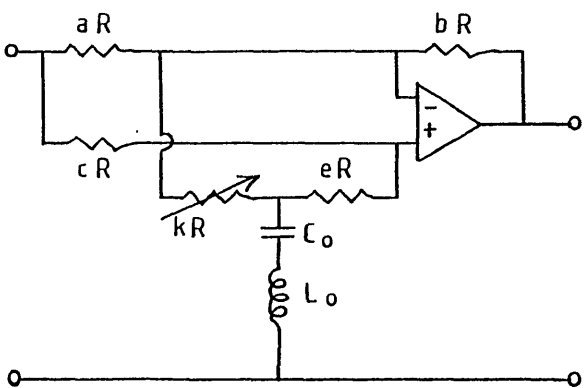
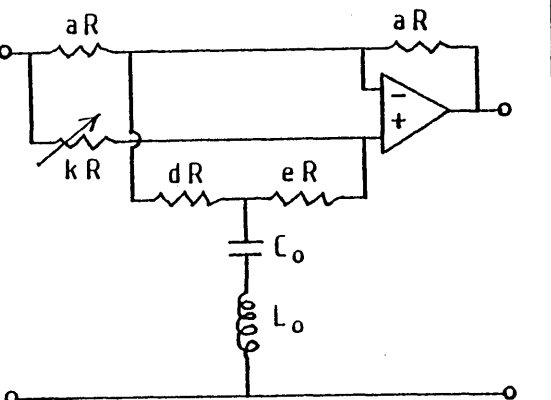
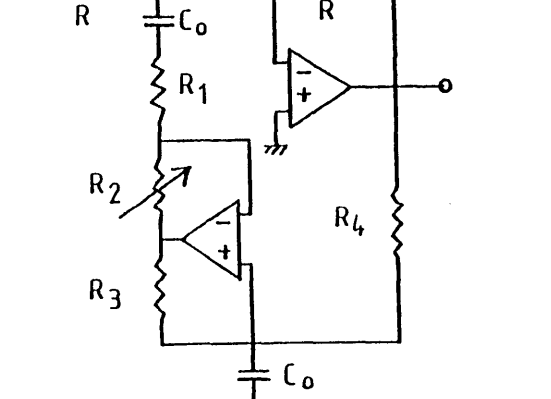
VE	DESIGN PARAMETERS	TRANSFER FUNCTION
 <p>No: 6</p>	$R = R_o / 2$ $k = \frac{k_o - 1}{k_o + 1} ; \text{ for } k_o \geq 1$ $k = \frac{1 - k_o}{1 + k_o} ; \text{ for } 0 \leq k_o \leq 1$ $0 \leq k \leq 1$	<p>SW 1 $T_6(s) = - \frac{1 + s C_o R (1 - k)}{1 + s C_o R (1 + k)}$</p> <p>SW 2 $T'_6(s) = 1/T_6(s)$</p>

TABLE 6.1

TABLE 6.2

CIRCUIT NUMBER	DESIGN PARAMETERS	TRANSFER FUNCTION
 <p>reference VE <u>1</u></p>	$0 \leq k_o \leq \infty$	$T_{21}(s) = \frac{\left[1 - \left(\frac{\omega}{\omega_o}\right)^2\right] (1 + k_o) + s C_o R_o}{\left[1 - \left(\frac{\omega}{\omega_o}\right)^2\right] (1 + k_o) + s C_o k_o R_o}$
 <p>No: 2</p>	$b = R_o / R$ $e = \frac{mb^2}{(b+m)(a-b) + 2mb}$ $c = \frac{ab(b+m)}{(b+m)(a-b) + 2mb}$ $k = \frac{mebk_o}{ebk_o + m(c+e)}, 0 \leq k \leq m$	$T_{22}(s) = \frac{a \left[1 - \left(\frac{\omega}{\omega_o}\right)^2\right] (k+e) + \left[k(ae-bc) + abe\right] RC_o s}{a \left[\left(1 - \left(\frac{\omega}{\omega_o}\right)^2\right) (k+e) + k(c+e) RC_o s \right]}$

Continued:- (Table 6.2)

CIRCUIT NUMBER	DESIGN PARAMETER	TRANSFER FUNCTION
 <p style="text-align: center;">No: 4</p>	$e = \frac{m}{h_o - 1}$ $a = \frac{mR_o}{e(h_o + 1)R - R_o}$ $d = \frac{a}{h_o - 1}$ $k = \frac{e(k h_o - 1)}{k_o + 1}$ <p style="text-align: right;">$0 \leq k \leq m$</p>	$T_{24}(s) = \frac{\left[1 - \left(\frac{w}{w_o}\right)^2\right] (d+e) + sC_o R \left[e(a+d) - kd\right]}{\left[1 - \left(\frac{w}{w_o}\right)^2\right] (d+e) + s C_o R d(e+k)}$
 <p style="text-align: center;">No: 5</p>	$R = R_o R_3$ $R_2 = \frac{R_3}{R_4} \left(R_1 + R_4 + \frac{R}{1+k_o}\right)$ $\frac{R_3}{R_4} (R_1 + R_4) \leq R_2 \leq \frac{R_3}{R_4} (R_1 + R_4 + R)$	$T_{25}(s) = \frac{\left[1 - \left(\frac{w}{w_o}\right)^2\right] + sC_o \left[R_1 + R_4 - \frac{R_2 R_4}{R_3}\right]}{\left[1 - \left(\frac{w}{w_o}\right)^2\right] + sC_o \left[R_1 + R_4 - \frac{R_2 R_4}{R_3} + R\right]}$

Continued:-

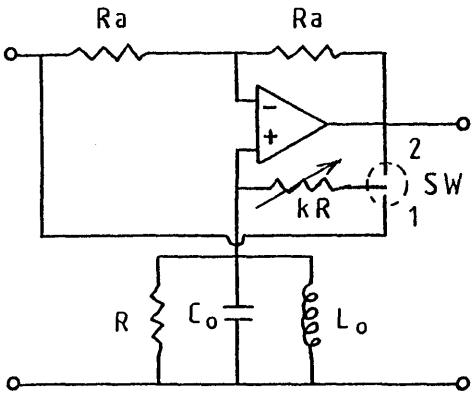
CIRCUIT NUMBER	DESIGN PARAMETERS	TRANSFER FUNCTION
 <p style="text-align: center;">No: 6</p>	<p>for $k_o < 1$</p> $R = \frac{2(1 + k_o)}{w_o^2 C_o^2 R_o (1 + k_o)}$ $k = \frac{1 - k_o}{1 + k_o}$	$T_{26}(s) = \frac{\frac{s}{w_o^2 C_o} (1+k) + kR \left[1 - \left(\frac{w}{w_o}\right)^2 \right]}{\frac{s}{w_o^2 C_o} (1+k) - kR \left[1 - \left(\frac{w}{w_o}\right)^2 \right]}$ <p style="text-align: center;">S W 2</p>

TABLE 6.2

it might be useful to treat the circuit No:4 (Tables 6.1 and 6.2) as an example.

By equating the respective squared modulus of $T_{21}(s)$ and $T_{24}(s)$ we get

$$k_o^2 [e(a+d)-kd]^2 - d^2(e+k)^2 = 0 \quad (6.6)$$

$$(d+e)^2 (k_o^2 - 1) R_o^2 + \{ [e(a+d)-kd]^2 - d^2(e+k)^2 \} (1+k_o)^2 R^2 = 0 \quad (6.7)$$

Combining these two equations yields

$$k = e \frac{(a+d) k_o - d}{d(1+k_o)} \quad (6.8)$$

$$(d+e) R_o = e(a+2d)R \quad (6.9)$$

From chapter 5 (Section 5.6) we know that the upper limit of k is given by

$$m = \frac{ae}{d} \quad (6.10)$$

and the maximum amplitude that can be obtained (in this case at the resonant frequency) is given by

$$h_o = \frac{a+d}{d} \quad (6.11)$$

(6.10) and (6.11) give the first design parameter

$$e = \frac{m}{h_o - 1} \quad (6.12a)$$

by eliminating d from (6.9) and (6.11), and using (6.12a) we get

$$a = \frac{m R_o}{e(h_o+1) R-R_o} \quad (6.12b)$$

with

$$R > \frac{R_o}{e(h_o+1)}$$

Since a and e are known we can derive d either from (6.10) or (6.11).

Finally the variable element k is easily found by dividing (6.8) by d and replacing $(a+d)/d$ by h_o , thus

$$k = e \frac{k_o h_o - 1}{k_o + 1} \quad (6.12c)$$

$$0 \leq k \leq m .$$

6.3 The optimisation method.

For most of the VEs we have discussed in the previous chapters, there is no obvious method to compensate for the distortions caused by the finite gain bandwidth product f_T of the amplifier. And even if there is any compensation method, it will complicate the structure of the VE; and because, usually, some approximations have to be made to achieve this compensation, consequently the effect of f_T is not completely removed.

In the case of the VE using transistors (Fig. 2.14), two capacitors have been used [12] to compensate for the error due to the amplifier limitation. The method we have used for the circuit in Fig. 3.31 seems more attractive because it reduces the error without incorporating extra components into the structure.

In this section a method of minimising the effects of the amplifier finite gain bandwidth product f_T shall be presented. It is mainly efficient when applied to the VEs discussed in chapter 5. This method consists of finding the values of the components of a VE for which the deviations from an ideal reference response, within a working frequency range, are minimum. This, of course, does not involve any extra devices to be added to the basic structure of the VE.

The method to be followed is exactly the same for all the circuits. By saying that, let us give an illustrative example.

We have chosen the circuit No.2 in Table 6.1 whose non-ideal transfer function is given by

$$T(s) = \frac{Z_o(s) a(k+e) + R [k(ae-bc) + abe]}{a[Z_o(s)(k+e) + k(c+e)R] + \frac{1}{G} \{R(c+e)[ab+k(a+b)] + Z_o(s)[ab+(a+b)(k+c+e)]\}}$$

(6.13)

where $Z_o(s) = 1/s C_o$ and $\frac{1}{G} = \alpha + j \frac{f}{f_T}$, where $1/\alpha$ represents the DC gain of the op-amp and f_T its finite gain bandwidth product.

An optimisation programme is set to calculate the modulus of (6.13); but first we have to find the parameters a,b,c,e and k.

If the range of k is chosen to be $[0, \infty]$ then m should be equated to infinity in the expressions of the above parameters. R_o , C_o and k_o are defined by the reference VE (circuit No:1 in Table 6.1). Because the parameter 'a' is arbitrary we can set it to any positive value; then the procedure is very simple : the programme is initiated with an arbitrary value of R which gives

$$b = R_o/R$$

since 'b' is known, we have

$$e = \frac{b^2}{a+b}$$

$$c = \frac{ab}{a+b}$$

$$k = \frac{eb k_o}{c+e}$$

All the parameters are known for the initial value of R; this enables the programme to find, within the working frequency range, the maximum error (in dB) $ER_1 = 20 \log \left| \frac{T(s)}{T_o(s)} \right|$ ($T_o(s)$ is obtained from (6.13) by setting $1/G = 0$). Then ER_1 is compared with an arbitrary reference error (ERMAX) which is high enough and cannot be obtained in practice, therefore $|ER_1| < |ERMAX|$, and ER_1 becomes the new reference error. The next step is to find the error

ER_2 for $R + \Delta R$; if $|ER_2| > |ER_1|$ another error ER_3 is calculated for $(R + \Delta R) - \Delta R/2$; if $|ER_3| < |ER_2|$ then the new reference error is ER_3 . The process of decreasing each new value of R continues till we reach $(R + \Delta R) - \frac{m\Delta R}{2}$ for which the error is ER_i ; if $|ER_i| < |ER_{i-1}|$ the process continues otherwise the error ER_{i+1} is calculated for $(R + \Delta R) - \frac{m\Delta R}{2} + \frac{\Delta R}{4}$. The programme continues increasing and decreasing each new value of R until it reaches an error ER_j for which $|ER_j - ER_{j-1}| < \epsilon$, where ϵ is a very small error (for example 10^{-6} dB). This means that no significant improvement of the distortions is to be expected in changing the new value of R by $\pm \delta R$. At this stage, the programme stops and gives the values of the parameters b, c, e, k , the error ER_j and R . Table 6.3 gives the design parameters of the circuit No:2 (Table 6.1) for different values of R . For each value, the circuit produces the same frequency response as the reference VE (circuit No:1 Table 6.1) for which $R_o = 15 \text{ k}\Omega$, $k_o = 1/3$ corresponding to a loss of -8.297 dB at an upper frequency 10 kHz .

$R(\text{k}\Omega)$	$f_T(\text{MHz})$	a	b	c	e	k	maximum error (dB)
15			1	0.5	0.5	1/6	-0.03598
13	3	1	1.1538	0.5357	0.6181	0.206	-0.03352
7.5			2	0.6666	1.3333	0.4444	-0.02642
2			7.5	0.8823	6.6176	2.2059	-0.01483

TABLE 6.3

In some cases the improvement is not very significant; moreover, the value of ER_j depends on f_T and on the arbitrary value of 'a'; it is advisable to test the programme for different values of a.

In the case of bump equalisers, apart from the quasi Bode-type ones (chapter 3), the inductor L_o is simulated by the positive impedance converter (PIC) shown in Fig. 6.1 where $R_3 = R_4$ and $R_2 = \frac{1}{C_o w_o}$ (w_o corresponds to the resonant frequency $f_o = w_o/2\pi$). This choice can be justified by investigating the non-ideal input impedance of the PIC. If we assume that the gain function G is identical for both op-amps we get

$$Z_{in}(s) = R_1 \frac{R_2 R_4 + \frac{1}{G} (1 + \frac{1}{G}) (R_3 + R_4) (R_2 + Z_o(s))}{R_3 Z_o(s) + \frac{1}{G} (1 + \frac{1}{G}) (R_3 + R_4) (R_2 + Z_o(s))} \quad (6.14)$$

where $\frac{1}{G} = \alpha + \frac{s}{w_T}$ and $Z_o(s) = 1/s C_o$; assuming that α is very small and ignoring second and higher terms proportional to $1/w_T$, we find the following expression

$$Z_{in}(s) = s C_o \frac{R_1 R_2 R_4}{R_3} \cdot \frac{1 + \frac{1}{w_T C_o R_2} \left(1 + \frac{R_3}{R_4}\right) + \frac{s}{w_T} \left(1 + \frac{R_3}{R_4}\right)}{1 - \frac{w_T^2 C_o R_2}{w_T} \left(1 + \frac{R_4}{R_3}\right) + \frac{s}{w_T} \left(1 + \frac{R_4}{R_3}\right)} \quad (6.15)$$

which can be written

$$Z_{in}(s) = sL_o [R_e(\epsilon) + j I_m(\epsilon)] \quad (6.16)$$

where

$$L_o = C_o \frac{R_1 R_2 R_4}{R_3}$$

$$Re(\epsilon) = \frac{1 - \frac{w^2}{w_T} C_o R_2 (1 + R_4/R_3) + \frac{1}{w_T C_o R_2} (1 + R_3/R_4)}{1 - 2 (1 + R_4/R_3) R_2 C_o \frac{w^2}{w_T}}$$

$$I_m(\epsilon) = \frac{w}{w_T} \frac{R_3/R_4 - R_4/R_3}{1 - 2 \frac{w^2}{w_T} R_2 (1 + R_4/R_3)}$$

If $R_3 = R_4$ then $I_m(\epsilon) = 0$ and the Q-factor of the simulated inductor is not affected by w_T [33] ; in this case

$$Re(\epsilon) = 1 + \frac{2}{w_T} \left[\frac{1}{C_o R_2} + R_2 C_o w^2 \right]$$

This function is minimum when $R_2 = \frac{1}{C_o w}$; if w is the resonant frequency w_o and R_2 is chosen accordingly, we can say that the effect of f_T on the simulated inductor is minimum at a fixed resonant frequency [34] . The PIC optimised by this method will be used as an element of the shaping impedances of the bump VEs to be compared; but it is not guaranteed that the optimisation method, described above, of the whole equaliser will lead to the optimum circuit.

However, as it shall be shown, the computed results are very close to the ideal. As far as the comparison is concerned, it would be simpler to use ideal inductors but this would have the disadvantage of depriving the reader from appreciating the non-ideal effect of amplifiers on the loss-frequency characteristics of RC fan equalisers and RC bump equalisers.

6.4 Some computed results.

We recall that in order to be able to make any comparison between the performances of the various VEs, regardless of their structure, we should make sure first that they are designed in such a way that they produce identical frequency responses. The ideal transfer function (6.1), corresponding to the circuit No.1 (Table 6.1), is chosen as reference. In the case of fan equalisers we have : $R_o = 15 \text{ k}\Omega$ and Z_o is a capacitor $C_o = 6.8 \text{ nF}$; the variable element k_o is either equal to 3 or $1/3$. These two values of k_o bring a maximum loss of + 8.297 dB at 10 kHz . For each of the circuits given in Table 6.1, the deviations of the non-ideal responses from the ideal ones have been computed. Table 6.4 gives the design parameters of the various VEs and it is stated whether a particular circuit is optimised or not. As for the circuits 1,5 and 6, the optimisation method described in section 6.3 does not substantially improve their performances; for this reason it is not stated that they have been optimised.

A glance at the error-frequency characteristics of the circuits 2 and 4 shows that the optimisation method has been successfully applied to them. A comparison of the error-frequency characteristics (from Fig. 6.2 to Fig. 6.15) of the whole set of fan equalisers leads to the following remarks :

TABLE 6.4

Circuit number	Design parameters	optimised	f_T (MHz)	Error-frequency Characteristics.
1	$R_o = 15 \text{ k}\Omega$ $k_o = 3, 1/3$		3	Fig. 6.2
	$m \rightarrow \infty$ $R = 15 \text{ k}\Omega$ $a = b = 1$ $c = e = 0.5$ $k = 3/2, 1/6$	No	3	Fig. 6.3
	1		Fig. 6.4	
2	$m \rightarrow \infty$ $R = 2 \text{ k}\Omega$ $a = 1, b = 7.5$ $c = 0.882, e = 6.617$ $k = 19.852, 2.2$	Yes	3	Fig. 6.5
	$m \rightarrow \infty$ $R = 3 \text{ k}\Omega$ $a = 1, b = 5$ $c = 5/6, e = 25/6$ $k = 12.5, 1.388$		1	Fig. 6.6
3	$m \rightarrow \infty$ $R = 15 \text{ k}\Omega$ $a = b = 1$ $c = e = 0.5$ $k = 1/6, 3/2$	No	3	Fig. 6.7

Table 6.4. - continued.

4	$m = 4, h_o = 5$ $R = 7.5 \text{ k}\Omega$ $a=2, d=0.5, e=1$ $k=3.5, 0.5$	NO	3	Fig. 6.8
			1	Fig. 6.9
	$m=4, h_o=5$ $R= 3.5 \text{ k}\Omega$ $a=10, d=2.5, e=1$ $k = 3.5, 0.5$	YES	3	Fig. 6.10
			1	Fig. 6.11
	$m=9, h_o = 10$ $R= 10 \text{ k}\Omega$ $a= 1.421, d= 0.1579$ $e = 1$ $k = 7.25, 1.75$	NO	3	Fig. 6.12
	$m = 9, h_o = 10$ $R = 1.8 \text{ k}\Omega$ $a = 28.125$ $d = 3.125$ $e = 1$ $k = 7.25, 1.75$	YES	3	Fig. 6.13
5	$R = 15 \text{ k}\Omega$ $R_a = 10 \text{ k}\Omega$ $k = 0.25, 0.75$		3	Fig. 6.14
6	$R = 7.5 \text{ k}\Omega$ $R_a = 10 \text{ k}\Omega$ $k= 0.5$		3	Fig. 6.15

TABLE 6.4

- the VEs derived from symmetrical lattice networks (i.e. circuits 1 and 5) are affected most by the finite gain bandwidth product of the amplifier.
- the circuit 4 derived from the new basic structure is thought to be the best circuit because, when optimised, the f_T of the op-amp has only a minor effect on its frequency response.

We note that the error-frequency characteristics in Figs. 6.3 and 6.4 of the circuit 2 are identical with those of the circuit in Fig. 5.11. Apart from a multiplying constant (-1), their non ideal transfer function is the one given by (6.13) where $a=b$. This is also valid for the circuit 3 and the circuit in Fig.5.10 which have the error frequency characteristics shown in Fig. 6.7. When $a=b$ and $c=e$, their non-ideal transfer function is given by

$$T(s) = + \frac{Z_o(s)(k+c) + 2kcR}{Z_o(s)(k+c) + acR + \frac{1}{G} \{2c(a+2k)R + Z_o(s)(a+4c+2k)\}} \quad (6.17)$$

The second set of error-frequency characteristics to be compared are those of bump equalisers. Apart from the quasi Bode-type equaliser, we have used the PIC in Fig. 6.1 to simulate the inductor needed for each of the VEs in Table 6.2. The values of the elements of this PIC are : $R_1 = R_2 = R_3 = R_4 = 9.35 \text{ k}\Omega$ and $C_o = 6.8 \text{ nF}$ which gives a resonant frequency $f_o = 2.5 \text{ kHz}$. For all of the bump equalisers, the maximum loss at the centre frequency is about + 9.544 dB

corresponding to the two values 3 and $1/3$ of the variable element k_o (k_o corresponds to the adjustable resistor of the reference circuit 1 in Table 6.2). Table 6.5 shows the design parameters of bump equalisers with identical frequency responses, they correspond to the VEs given in their most general form in Table 6.2.

A comparison of the computed error-frequency characteristics (from Fig. 6.16 to Fig. 6.22) shows that the equalisers derived from symmetrical lattice networks (circuits 1 and 5 in Table 6.2) are the most affected by the finite f_T of the amplifiers. Figs. 6.18 and 6.20 show the error-frequency characteristics of the circuits 2 and 4 where the two op-amps of the PIC are assumed to be ideal; comparing these two figures with Figs. 6.17 and 6.19 we get an idea of the contribution to the distortions due to the simulated inductor being non-ideal.

The non-ideal effect of the op-amps on the frequency response of a bump equaliser is characterised by a slight change in the amplitude and by a shift in the resonant frequency, mainly due to the non-ideal simulated inductor. The obtained shapes of the error-frequency characteristics are explained by Fig. 6.23, where it can be seen that the error changes sign around the centre frequency, and its modulus is maximum at the flanks of the bump. In practice this maximum error can be reduced by a readjustment of the resonant frequency. A final point to be mentioned is that only the circuit 5 (Table 6.2) can be optimised by the method described in Section 6.3; in the other cases the improvement is of no significance.

Circuit number	Design parameters	f_T (MHz)		error-frequency characteristic
		basic op-amp	PIC	
1	$R_o = 11 \text{ k}\Omega$ $k_o = 3, 1/3$	3	3	Fig. 6.16
2	$m \rightarrow \infty$ $R = 11 \text{ k}\Omega$ $a = b = 1$ $c = e = 0.5$ $k = 3/2, 1/6$	3	3	Fig. 6.17
		3	ideal	Fig. 6.18
4	$m = 4, h_o = 5$ $R = 3.5 \text{ k}\Omega$ $a = 4.4$ $d = 1.1$ $e = 1$ $k = 3.5, 0.5$	3	3	Fig. 6.19
		3	ideal	Fig. 6.20
5	$R = 11 \text{ k}\Omega$ $R_1 = 10.31 \text{ k}\Omega, R_3 = 4.445 \text{ k}\Omega$ $R_4 = 8.5 \text{ k}\Omega$ $R_2 = 11.3, 14.18 \text{ k}\Omega$	3		Fig. 6.21
6	$R_a = 20 \text{ k}\Omega$ $R = 31.87 \text{ k}\Omega$ $k = 0.5$	3	3	Fig. 6.22

TABLE 6.5

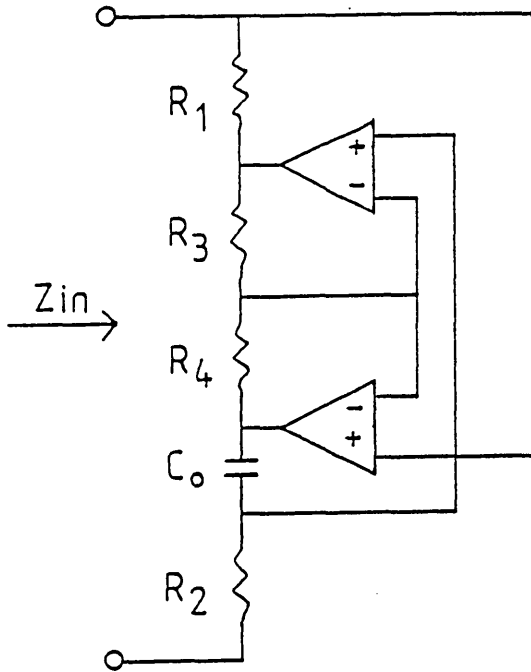


Figure 6.1 PIC simulating the inductance L_o

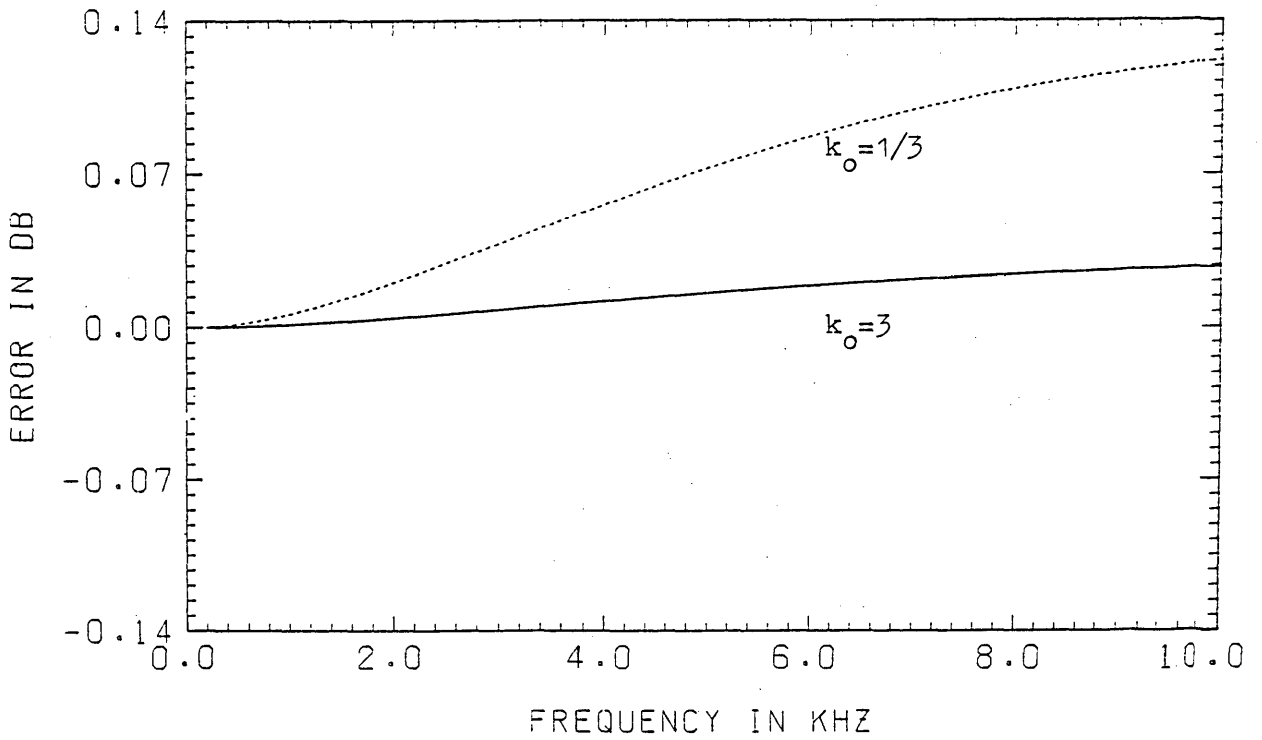


Figure 6.2

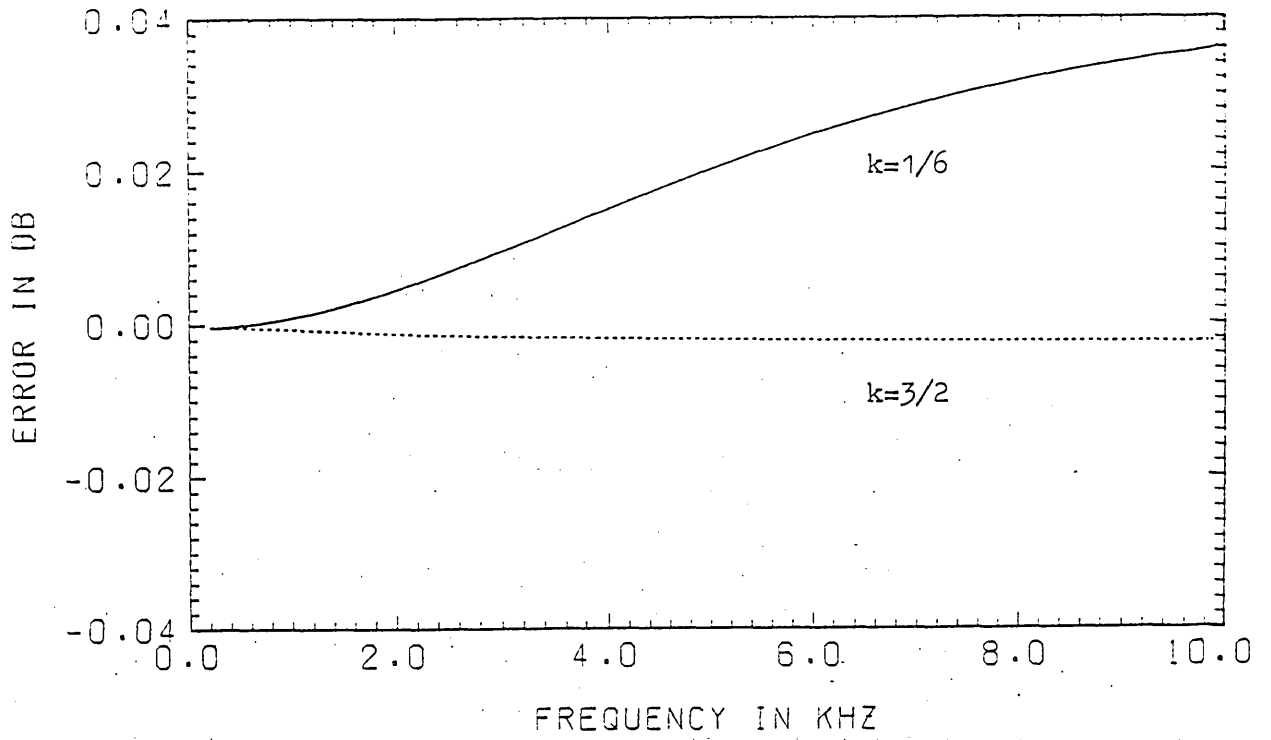


Figure 6.3

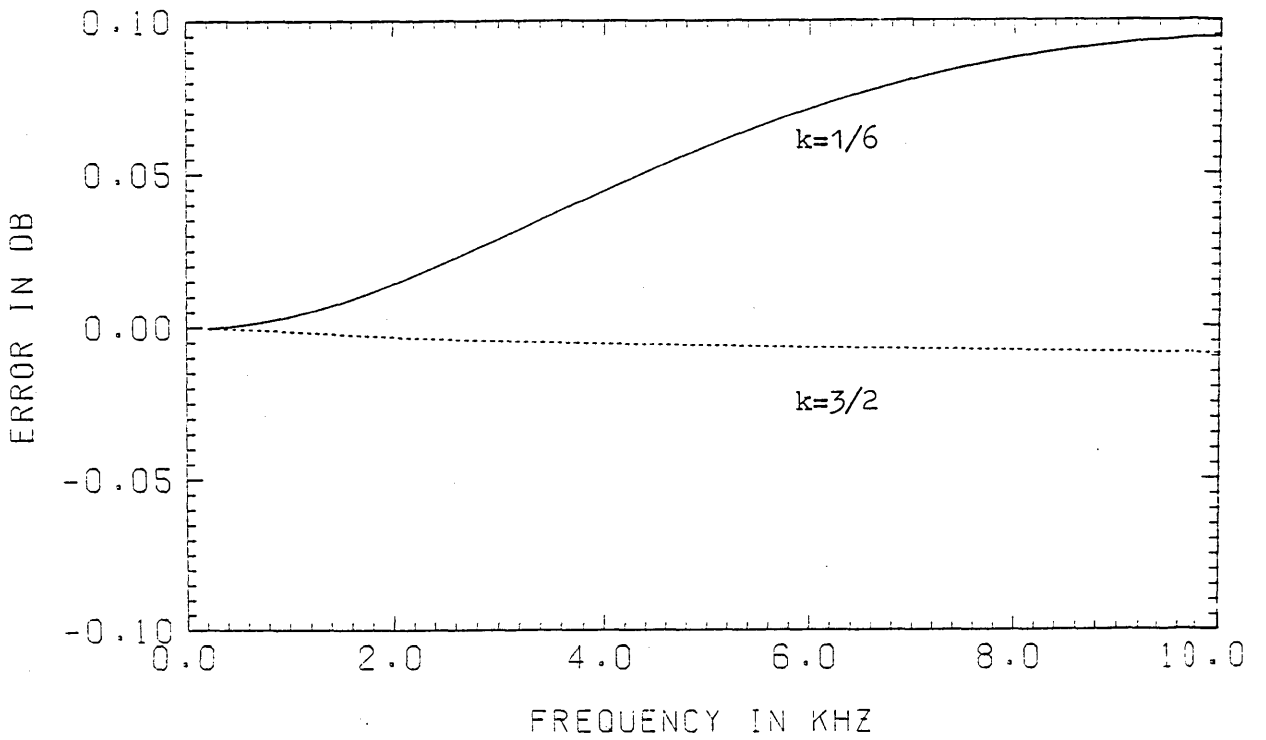


Figure 6.4

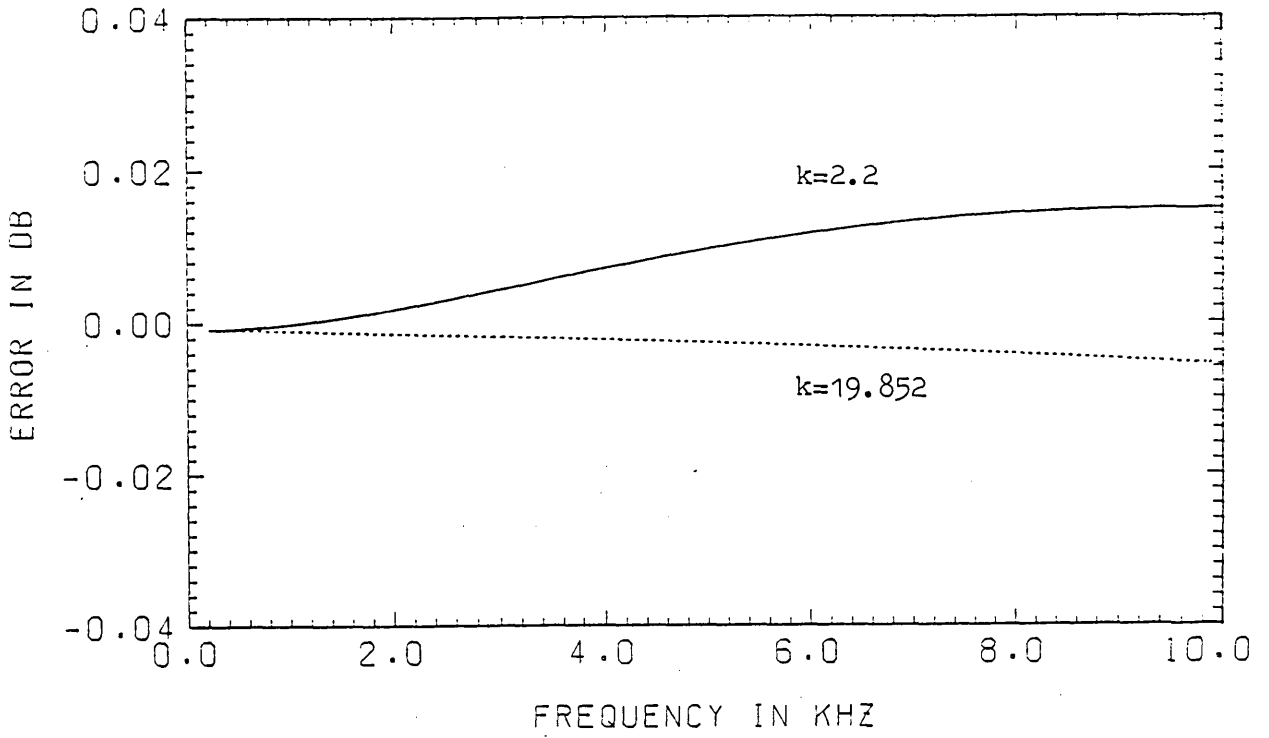


Figure 6.5

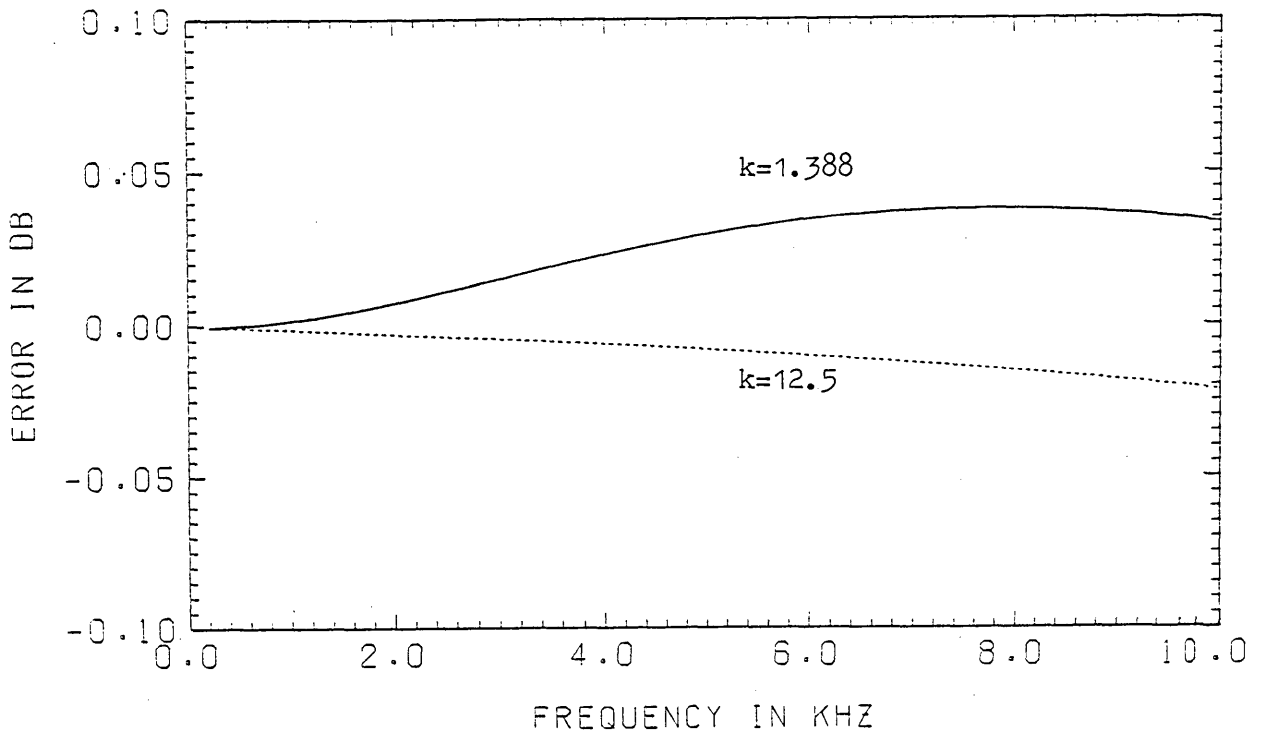


Figure 6.6

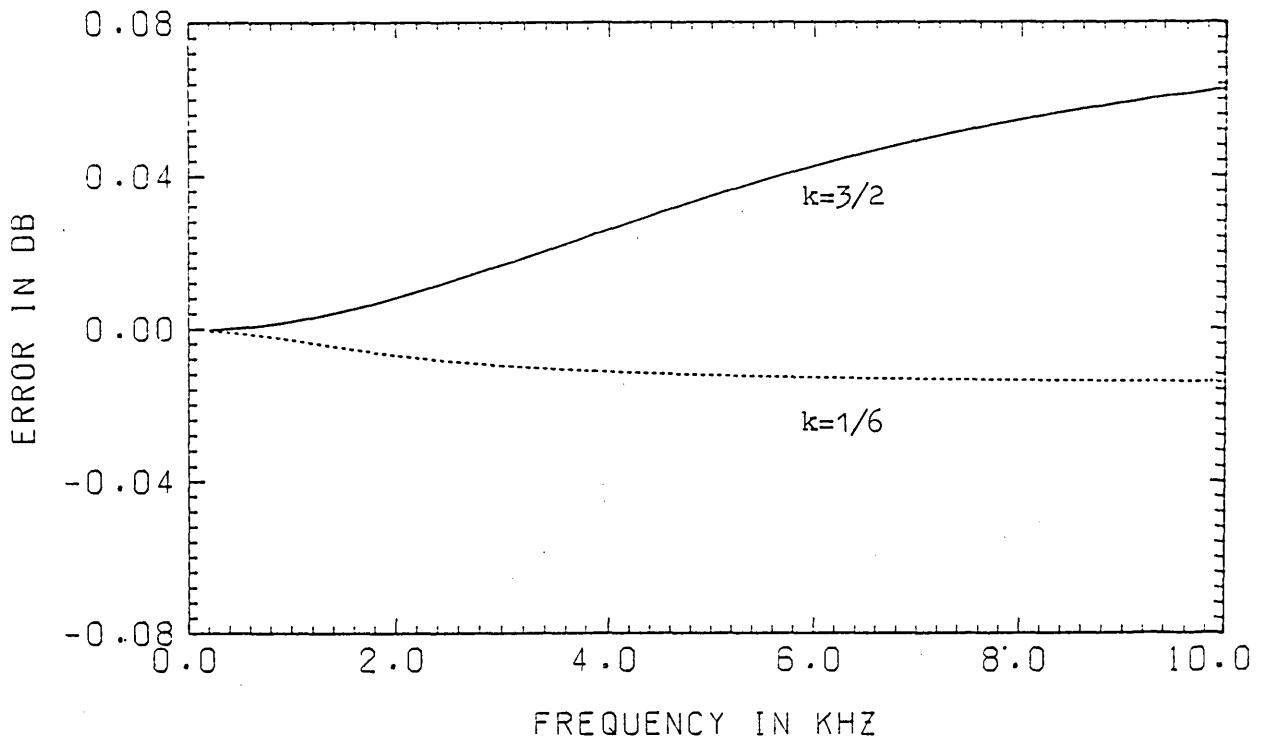


Figure 6.7

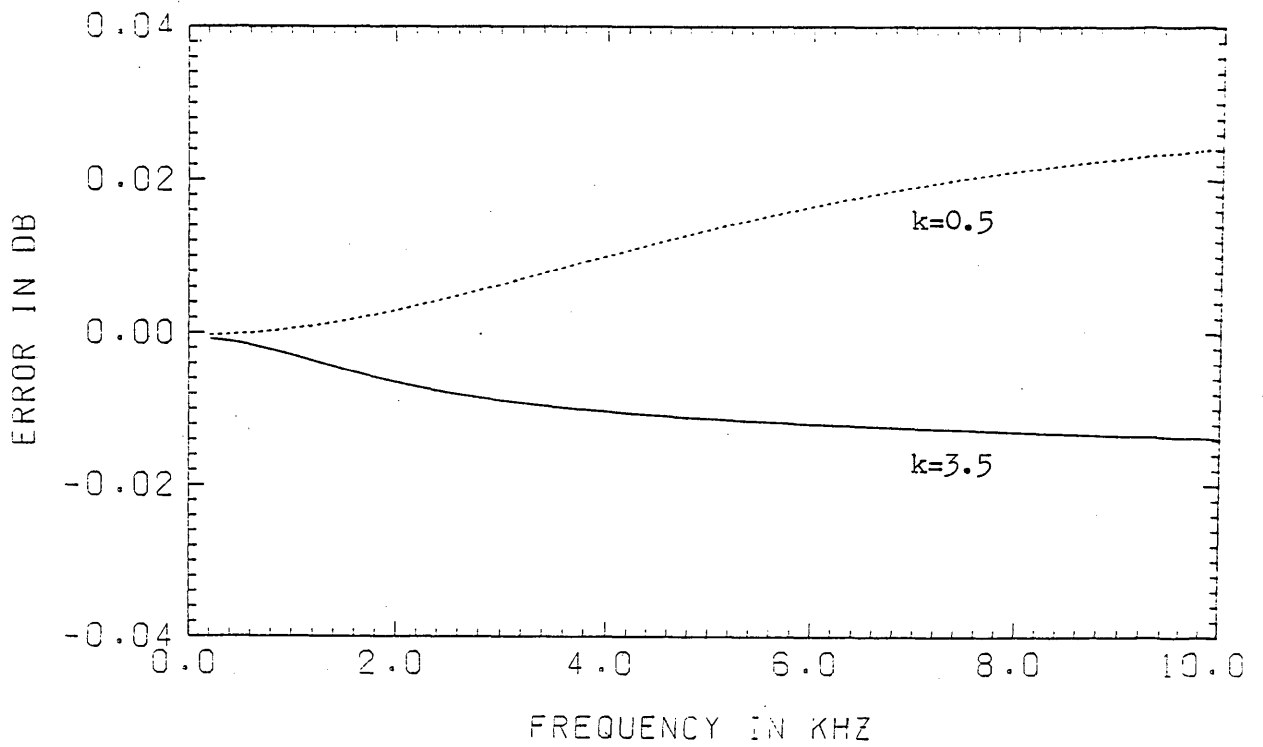


Figure 6.8

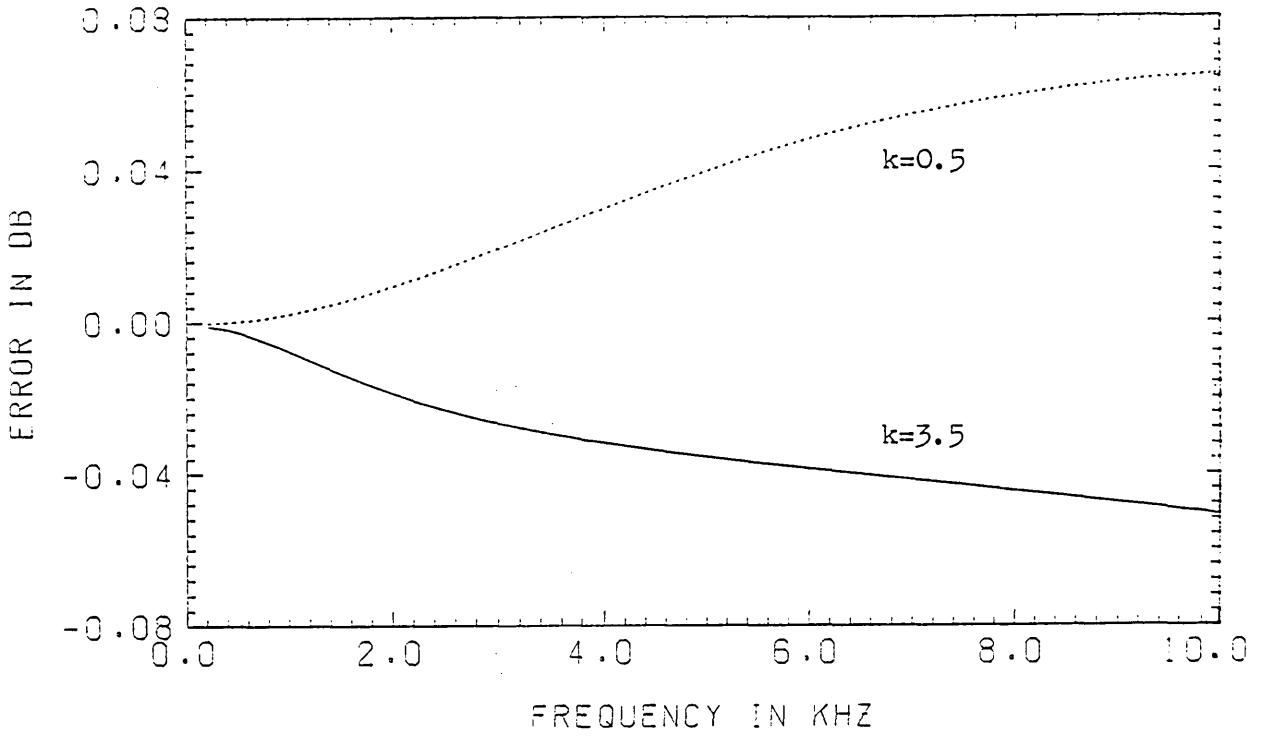


Figure 6.9

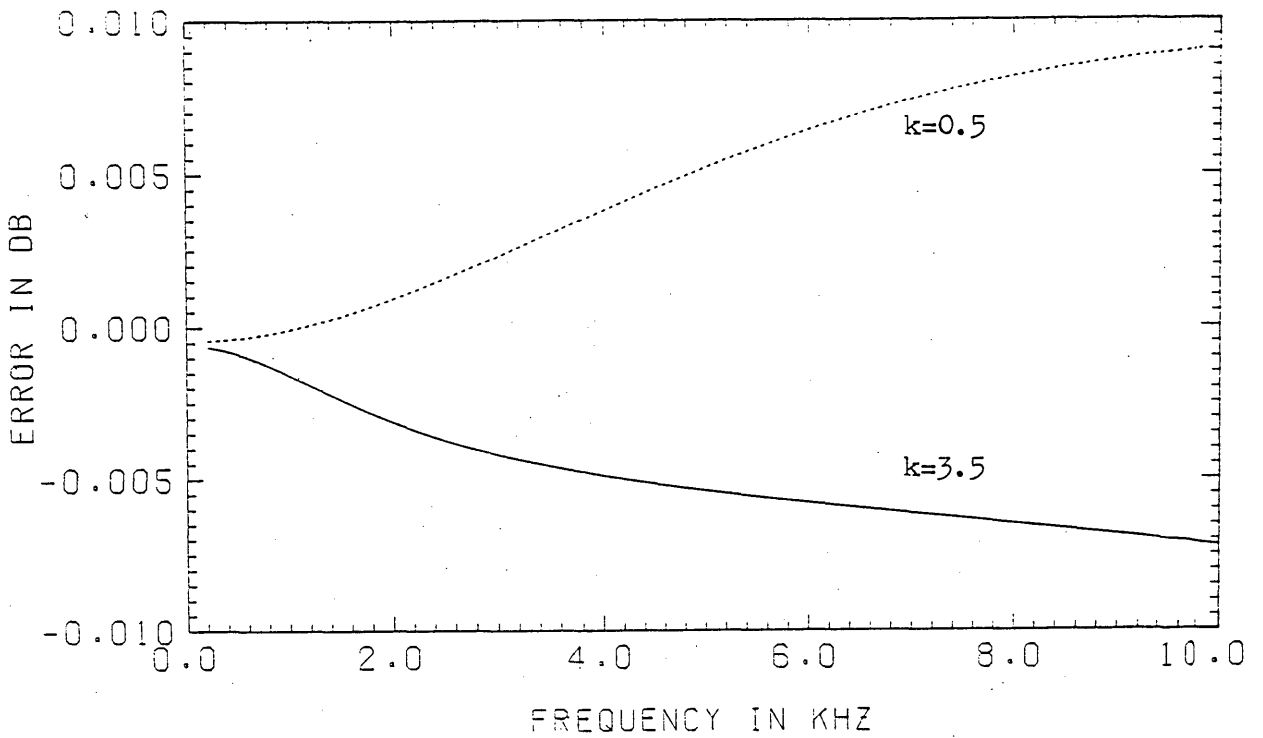


Figure 6.10

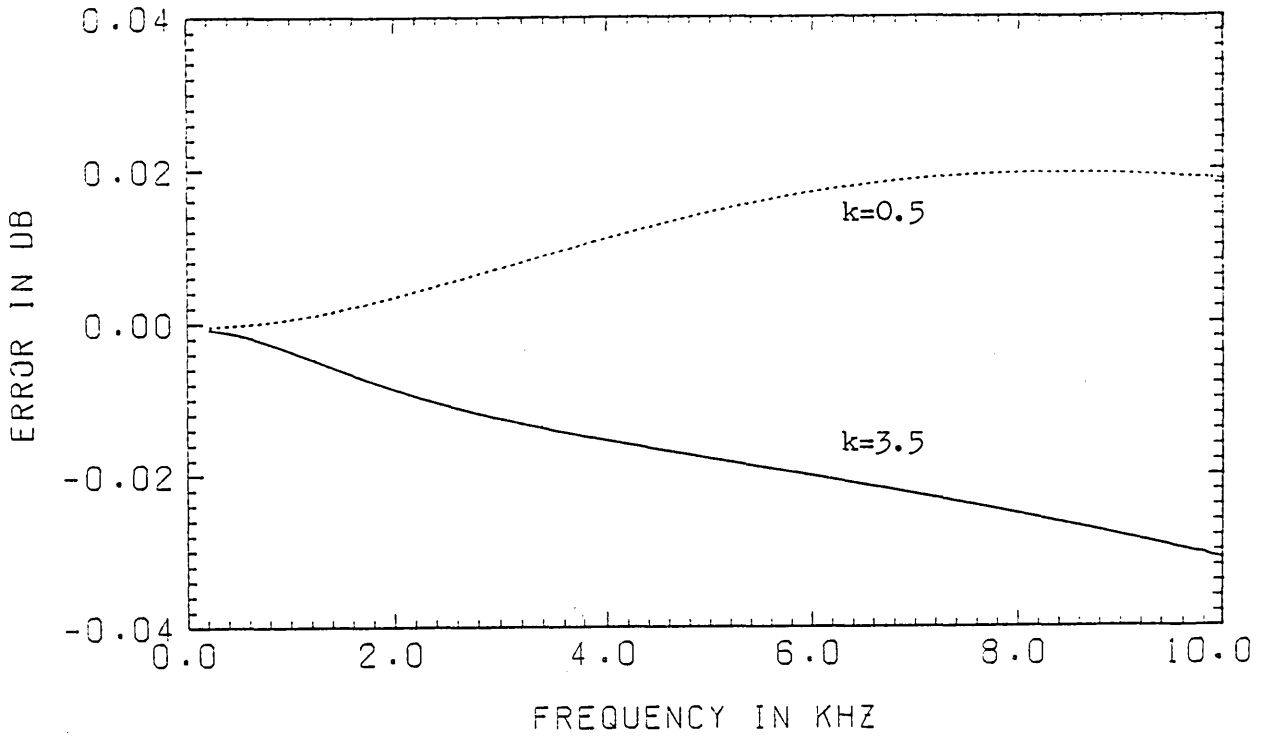


Figure 6.11

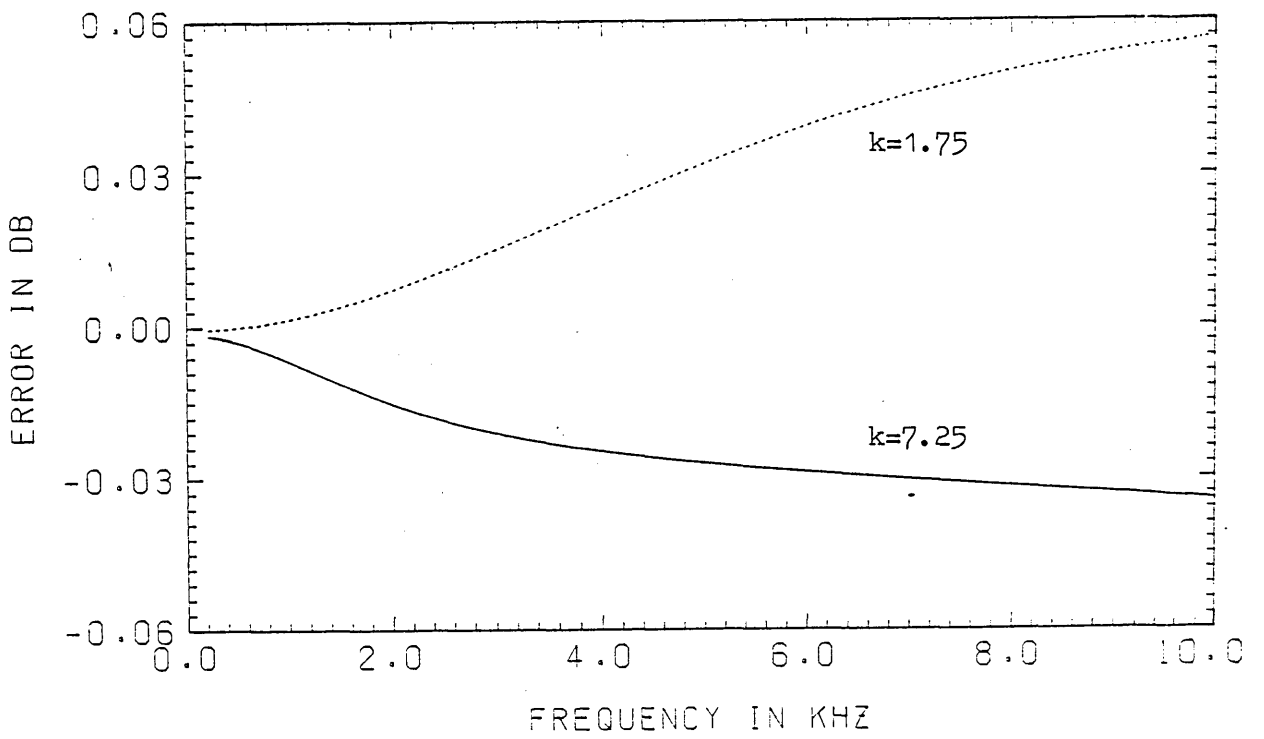


Figure 6.12

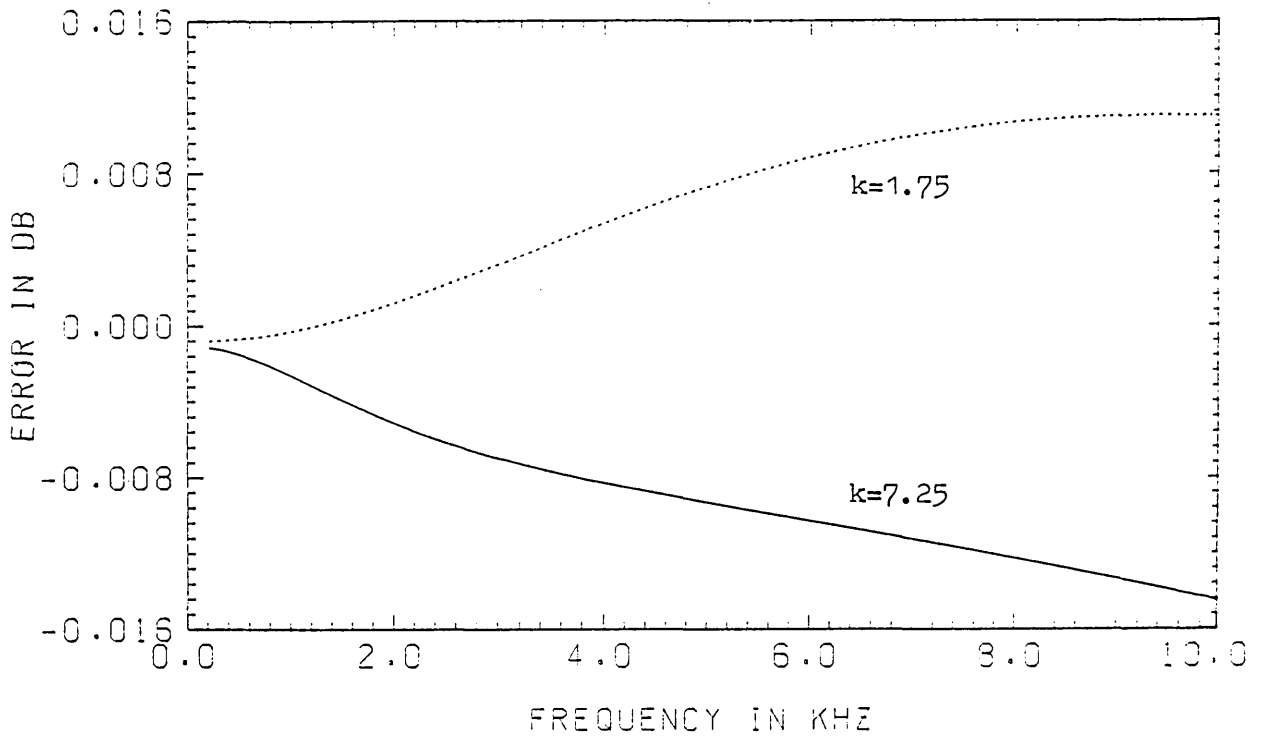


Figure 6.13

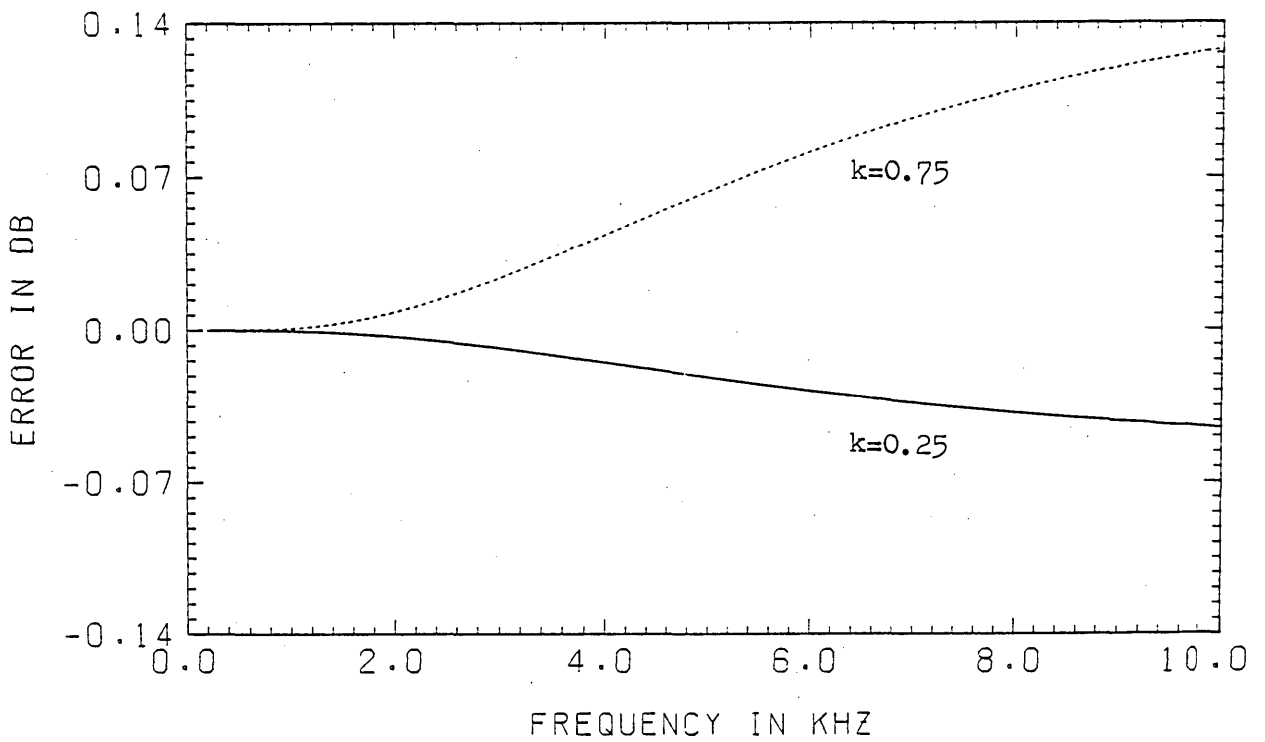


Figure 6.14

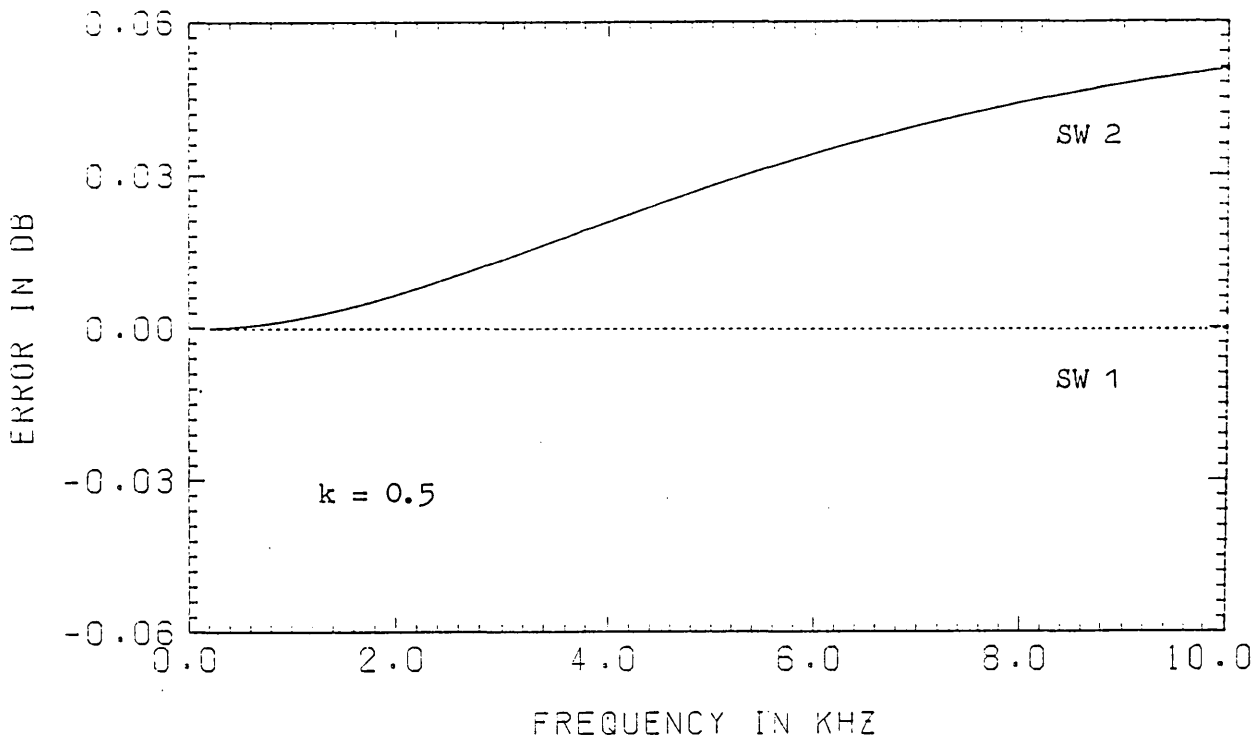


Figure 6.15

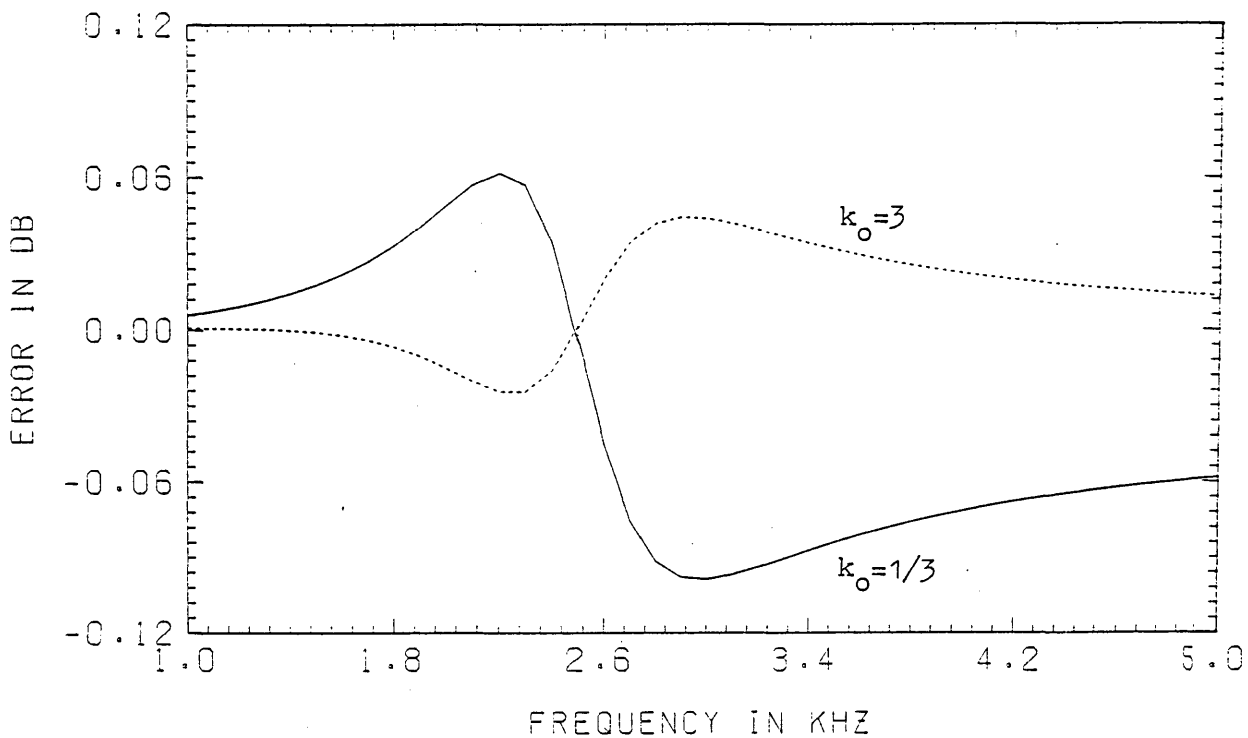


Figure 6.16

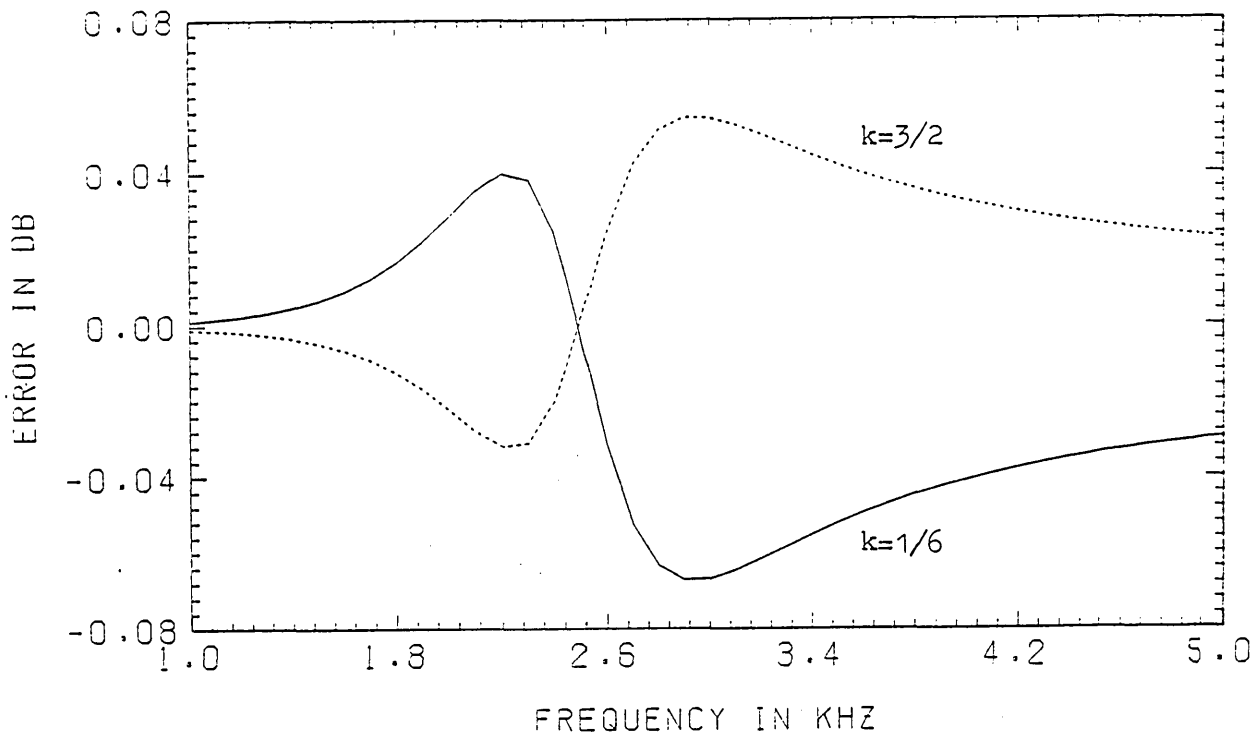


Figure 6.17

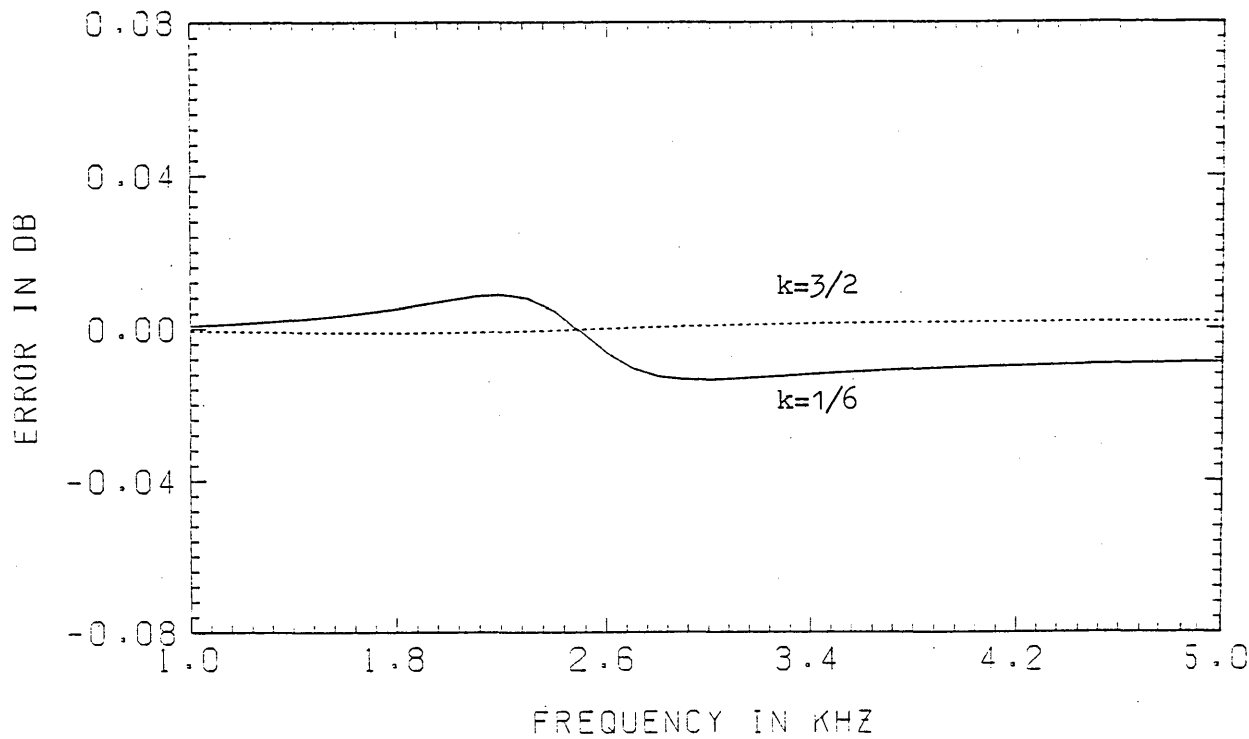


Figure 6.18

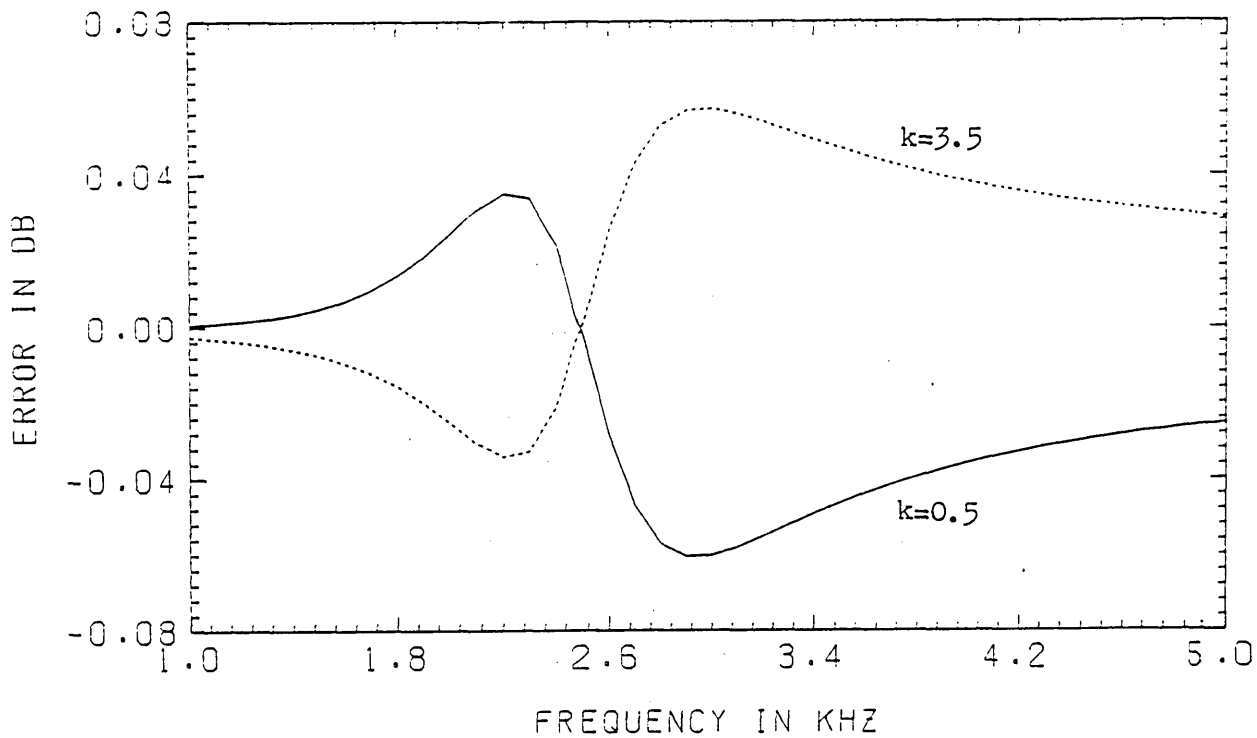


Figure 6.19

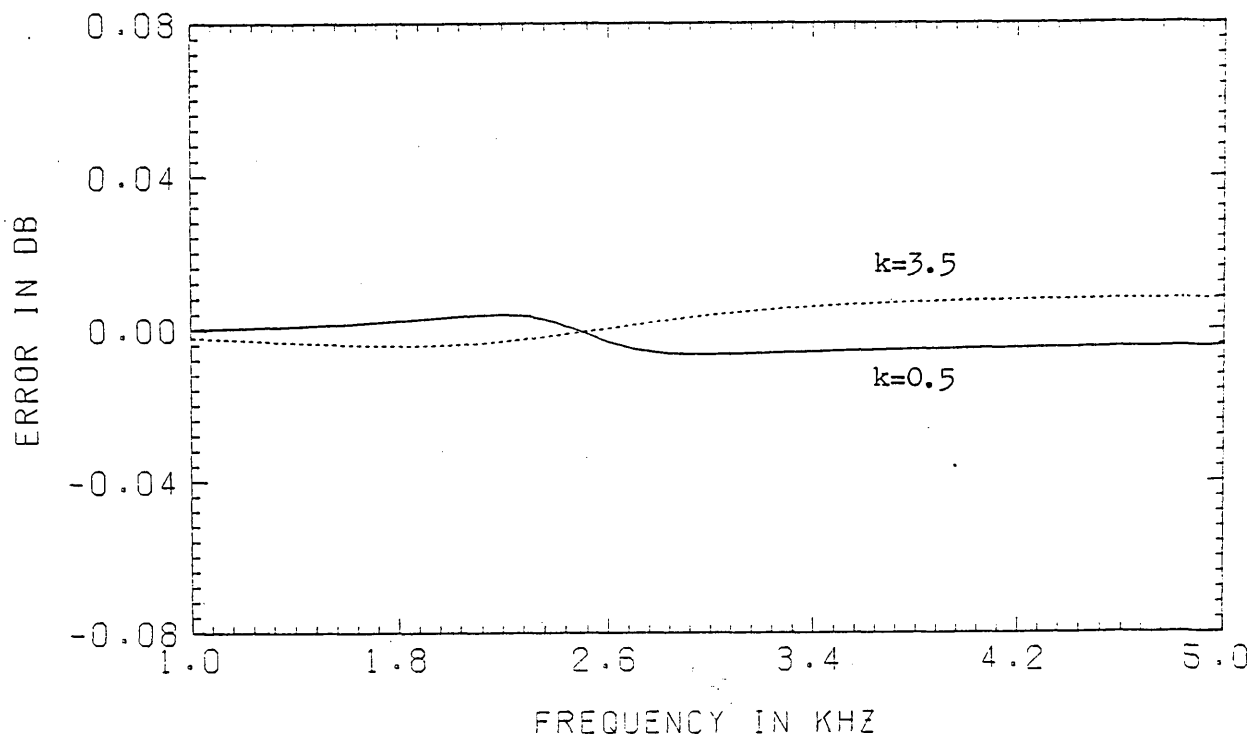


Figure 6.20

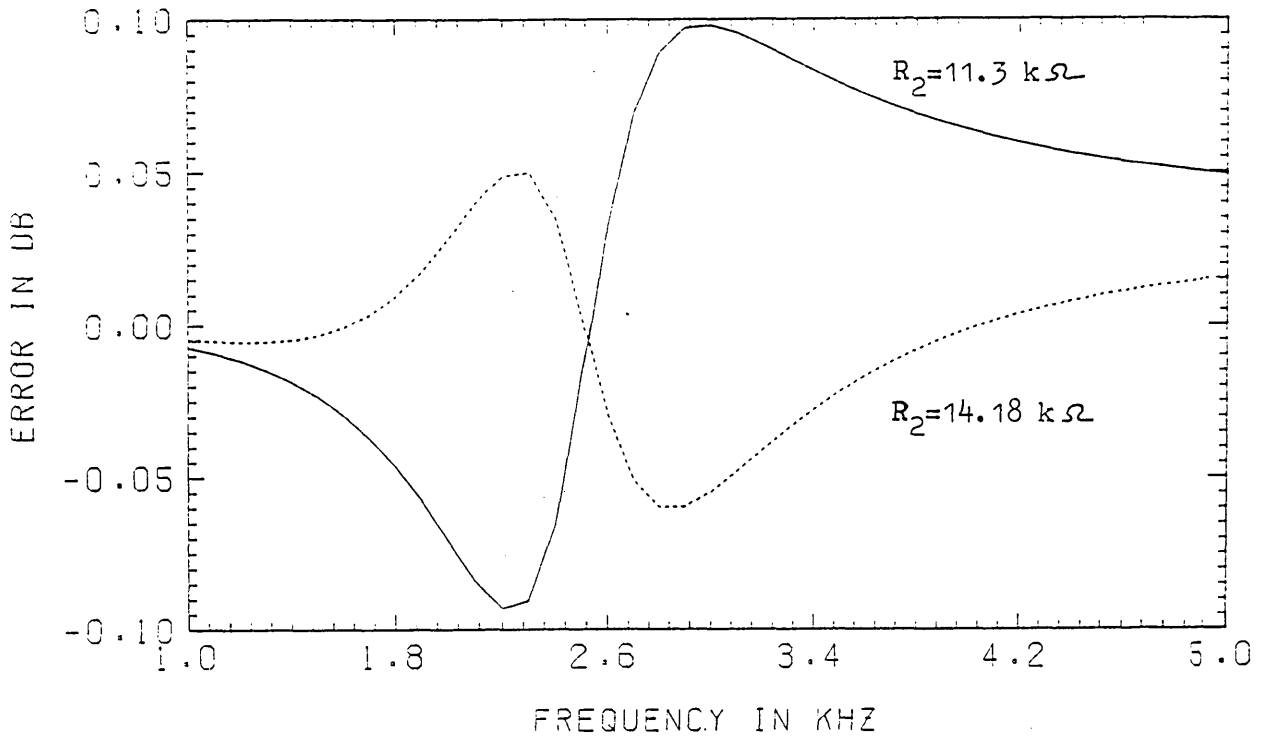


Figure 6.21

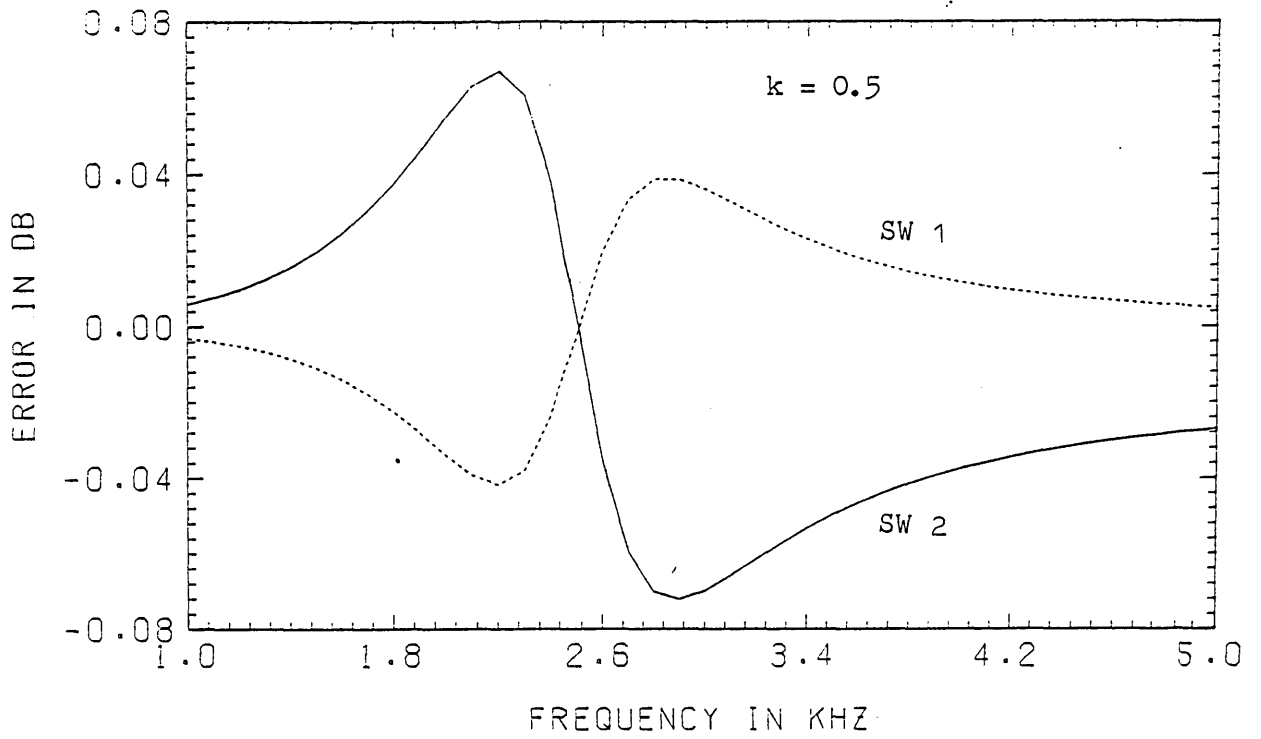
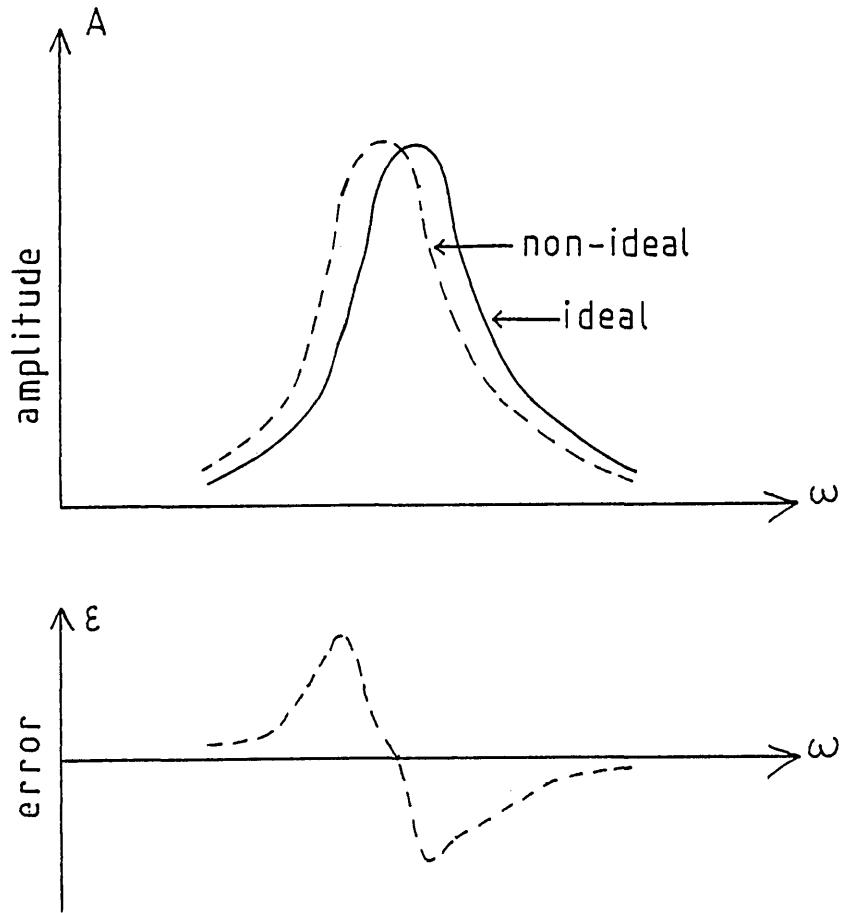


Figure 6.22



$$\epsilon = A(\text{non-ideal}) - A(\text{ideal})$$

Figure 6.23

CHAPTER VII GENERAL CONCLUSIONS AND SUGGESTIONS
FOR FUTURE WORK

The main objective of this work was the design of high-precision active RC Bode-type VE circuits in a form suitable for microelectronic implementation and which lend themselves readily to automatic control. It must be pointed out that none of the VEs we have developed and constructed (with discrete components) have so far been fabricated microelectronically.

Whatever the reason for which an equaliser is used in a communication system, it should be of a very simple structure, easily adjustable and inexpensive. We aimed at structures where the basic VE operation is provided by the use of the following main elements

- a single op-amp.
- a single adjustable resistor.
- a single shaping impedance which may merely consist of a capacitor; but in general it might include several capacitors and op-amps, depending on the required shape of the frequency response.

It is seen from the first chapter that the general transfer function of the structures we are dealing with is required to be of the form

$$T(s) = M \frac{1+\gamma H(s)}{\gamma + H(s)} \quad (1.7)$$

Ideally γ varies within the whole positive range $[0, \infty]$ and it is

related to the adjustable resistor by a positive multiplying constant; the frequency dependent function $H(s)$ can be identified with a normalised driving point impedance function.

In Chapter 3 we introduced the concept of quasi Bode-type VEs; this class of equalisers do not satisfy the transfer function (1.7) itself but only its squared modulus; consequently, their corresponding shaping impedance is restricted to a purely reactive one. Apart from this restriction, they can conceivably be used in applications where phase characteristics are not of paramount importance (e.g. speech).

A new basic structure for Bode-type VEs (Fig. 5.1) has been developed and presented in chapter 5. The capabilities of this structure have been widely investigated; its inherent potential in leading to novel active RC VEs with prescribed requirements on both the variable range of the adjustable resistor and the maximum variable amplitude highlights its flexibility and exhibits its superiority over the existing structures.

At various stages, in this work, we have given some practical examples which have shown that nearly ideal performance characteristics can be obtained with most of the significant number of VEs we have developed. However, as revealed in chapter 6, the responses obtained from the computer-simulated models have shown that the VEs derived from balanced lattice networks (Chapters 3 and 4) are more sensitive to the effects of amplifier imperfections.

One of the major problems, we came across in this work, was the practical realisation of bump equalisers satisfying a biquadratic transfer function of the form given by (4.16a). This, as already pointed out in section 4.3.2, is due to the fact that the requirements for the needed active RC simulated inductor are not fully met by any of the existing circuits. We did however overcome this obstacle - via justified approximations - by adopting the circuit in Fig. 4.11. Nevertheless, it would be of great practical value to develop an alternative single op-amp simulated inductor, easily adjustable and less sensitive to the effects of the amplifier imperfections. Further points that would be significant and of direct interest to be investigated include the following:

- electronic control of the variable element R_v .
- reduction of the phase of quasi Bode VEs.
- independent adjustment of the amplitude and the phase by two variable resistors.
- reduction of the effect of f_T on the loss frequency characteristics of the circuit in Fig. 4.6 and the quasi Bode equaliser developed in Chapter 3.

Salient contributions of original nature contained in this thesis include the following:

- the quasi bump equalisers in Chapter 3.
- the structure of a Bode equaliser in Fig. 4.6 .
- the basic structure in Fig. 5.1.
- the use of transformations by terminal interchange in developing the VEs in Figs. 5.9, 5.10 and 5.11.
- the reduction of the range of the variable element from $[0, \infty]$ to $[0, m]$ (i. e. the circuits in Figs. 5.12 and 5.13).
- the development of a design with a grounded R_v (i.e. the circuit in Fig. 5.14).

REFERENCES

1. BODE, H.W. "Attenuation equalizer", US Patent 2,096,027
Oct. 19, 1937.
2. BODE, H.W. "Variable equalizers", Bell Syst. Tech. J.,
Vol. 17, pp 229-244, April 1938.
3. OSWALD, J. "Sur un nouveau type de correcteur variable",
Cable et Transmission, Vol. 11A, No 3,
pp. 218-236, 1957.
4. HAKIM, S.S. "Bode's variable equaliser", Electron. Technol.
Vol. 38, pp 224-227, June 1961.
5. HAAS, W. "Theory and design of an adjustable equaliser",
Electrical Comm., Vol 40, No 2, pp225-232, 1965.
6. ROLLETT, J.M. and GREAVES, A.J. "An RC-active equaliser
section with independently adjustable group delay
and amplitude", IEE Coll. Digest No 1979/46 of
Colloquium on Electronic Filters, pp. 2/1 - 2/7,
London, May 1979.
7. WILLIAMSON, R. "The Audio Amateur", Vol.3, No 1, pp 3-11,
October 1972.
8. BRGLEZ, F. "Inductorless variable equalizers", IEEE Trans.
on Circuits and Syst., Vol. CAS-22, pp.415-418,
May 1975.
9. BRGLEZ, F. "Minimally active RC variable equalizers",
IEEE Trans. on Circuits and Syst. Vol. CAS-22,
pp. 688-691, August 1975.
10. ORCHARD, H.J. "Active all-pass networks with constant resistance",
IEEE Trans. on Circuit Theory, Vol. CT-20,
pp. 177-179, March 1973.

11. SHIDA, S. and SUZUKI, K. "Variable equalizer with differential amplifiers", IEEE Trans. on Circuits and Syst., Vol. CAS-24, June 1977.
12. TAKASAKI, Y. and al. "Inductorless variable equalizers using feedback and feedforward", IEEE Trans. on Circuits and Syst., Vol. CAS-22, pp 389-394, June 1976.
13. FLEISCHER, P.E. "Active adjustable loss and delay equalizers", IEEE Trans. on Circuits and Syst., Vol CAS-21, pp 527-531, July 1974.
14. THOMAS, L.C. "The biquad: Part I - Some practical considerations", IEEE Trans. on Circuit Theory, Vol. CT-18, pp 350-357, May 1971.
15. THOMAS, L.C. "The biquad: Part II - A multipurpose active filtering System", IEEE Trans. on Circuit Theory, Vol. CT-18, pp 358-361, May 1971.
16. MASUDA, Y. and al. "On the active variable equalizers", Proc. 1974 IEEE Int. Sym. on Circuits and Syst., San Francisco, California, pp 463-467, April 1974.
17. SARAGA, W. "Some new active RC variable equaliser circuits", Proc. 1978 IEEE Int. Sym. on Circuits and Syst., New York, pp. 141-145.
18. SARAGA, W. and ZYOUTE, M. "A microelectronically realisable active RC quasi-Bode-type adjustable bump equaliser", IEE Coll. Digest No: 1979/46 of Colloquium on Electronic Filters, pp. 3/1 - 3/7 , London, May 1979.
19. SINGH, B. Private communication.
20. BHATTACHARYYA, B.B. and al. "A simple inductance simulation scheme and its application in data communication", Proc. IEEE, 65, pp 268-269, 1977.

21. HAIGH, D.G. Private Communication.
22. SINGH, B. "On the design of low-sensitivity active RC filters by simulation of LC filters". Ph.D thesis (in preparation). University of London, 1981.
23. SARAGA, W. and ZYOUTE, M. "A new active RC Bode-type variable equaliser circuit suitable for microelectric realisation", Proc. 1980 IEEE Int. Sym. on Circuits and Syst., Houston, pp. 566-571.
24. RAMSEY, W.T. "Highpass and bandpass filters using a new single amplifier simulated inductor", Proc. IEE on Electronic Circuits and Syst., Vol. 2, No 3 pp. 79-85, May 1978.
25. CHENG, R.H. and LIM, J.T. "Single op-amp networks for shunt arms in ladder filters", Proc. 1977 IEEE Int.Sym. on Circuits and Syst., Phoenix, Arizona pp 313-316.
26. PRESCOTT, A.J. "Loss-compensated active gyrator using differential-input operational amplifiers", Electron. Lett. 2, (7), pp. 283-284, 1966.
27. BERNDT, D.F. and DUTTA ROY, S.C. "Inductor simulation using a single unity gain amplifier", IEEE J. Solid State Circuits, Vol. SC-4, pp 161-162, June 1969.
28. ZYOUTE, M. "A new active RC Bode-type variable equaliser", Proc. IEE on Electronic Circuits and Syst., Vol. 128, No 3, pp.134-137, June 1981.
29. RATHORE, T.S. "Inverse active networks", Electro. Lett., Vol. 13, No 10, pp.303-304, 12th. May 1977.
30. HAIGH, D.G. "Some network transformations by terminal interchange", Proc. 1978 IEEE Int. Sym. on Circuits and Syst., New York, pp.416-421.

31. RATHORE, T.S. and SINGHI, B.M. "Network Transformations",
IEEE Trans. on Circuits and Syst., Vol. CAS-27,
January 1980.
32. DE PIAN, L. "Linear active network theory".
Prentice-Hall International London, 1962.
33. BRUTON, L.T. and LIM, J.T. "High frequency comparison of
GIC-simulated inductance circuits",
Int. J. Circuit Theory and Applications, Vol.2,
pp. 401-404, 1974.
34. HAIGH, D.G. and KUNES, M.A. "A contribution to the optimum
design of active-RC filters using positive impedance
converters", Proc. 1979 IEEE, Int. Sym. on
Circuits and Syst., TOKYO, pp.203-206.
35. GEHER, K. "Theory of network tolerances"
Akadémiai Kiadó, Budapest, 1971.